Sperm glycocalyx is altered during epididymitis as a consequence of bacterial infection

Inaugural Dissertation
submitted to the
Faculty of Medicine
in partial fulfillment of the requirements
for the PhD-Degree
of the Faculties of Veterinary Medicine and Medicine
of the Justus Liebig University Giessen

by
Farhad Khosravi
of
Tehran, Iran

Giessen (2017)

From the Institute of Anatomy and Cell Biology
Director / Chairman: Prof. Dr. Eveline Baumgart-Vogt
Biology of Reproduction Group
Head: Prof. Andreas Meinhardt
of the Faculty of Medicine of the Justus-Liebig-University of Giessen

First Supervisor and Committee Member: Prof. Dr. Andreas Meinhardt
Co-Supervisor: PD Dr. Sebastian Galuska
Co-Supervisor and Committee Member: Prof. Dr. Martin Bergmann
Committee Member and Chairperson: Prof. Dr. Christine Wrenzycki
Committee Member: Prof. Dr. Rüdiger Horstkorte

Date of Doctoral Defense: 25.10.2017

Dedicated to my kind and supportive wife, my dearest friend, and my eternal love:

Negah

Table of Contents

Abbreviations

º	Degree
2-AB	2-aminobenzaminde
Asn	Asparagine
bp	Base pair
BSA	Bovine serum albumin
°C	Degree Celsius
CD	Cluster of differentiation
cDNA	Complementary DNA
CMP	Cytidine monophosphate
Con-A	Concanavalin A
DANA	N-Acetyl-2,3-dehydro-2-deoxyneuraminic acid
DC	Dendritic cells
DC-SIGN	Dendritic Cell-Specific Intercellular adhesion molecule-3-Grabbing Non-integrin
DEFB126	ß-defensin 126
DHB	2,5-dihydrobenzoic acid
dH_2O	Distilled water
DMB	4,5-methylenedioxybenzene
DMSO	Dimethylsulfoxide
DNA	Deoxyribonucleic acid
DNase	Deoxyribonuclease
dNTP	Desoxyribonucleosidtriphosphate
Dol-P	Dolichol phosphate
E. coli	*Escherichia coli*
EDTA	Ethylenediaminetetraacetic acid
e.g.	For example
λem	Emission wavelength
ER	Endoplasmic reticulum
ERK	Extracellular signal-regulated kinase
ESI-MS	Electrospray ionization mass spectrometry
et al.	And others

λex	Extinction wavelength
F	Forward primer
Fuc	Fucose
g	Gram
µg	Microgram
GAG	Glycosaminoglycans
Gal	Galactose
GalNAc	*N*-acetylgalactosamine
GalNAc-T	GalNAc transferase
Galnt	UDP-N-acetyl-alpha-D-galactosamine:polypeptide N-acetylgalactosaminyltransferase
GDP	Guanosine diphosphate
GdS	Glycodelin S
GlcNAc	*N*-acetylglucosamine
GlcNAcT-I	N-acetylglucosaminyltransferase I
GPI	Glycophosphatidylinositol
H	Hydrogen
h	Hour
HCl	Hydrochloric acid
HIV	Human immunodeficiency virus
hlyA	alpha-hemolysin
HPLC	High-performance liquid chromatography
HTF	Human tubal fluid
i.e.	That is
IL	Interleukin
kDa	Kilodalton
KDO	3-Deoxy-D-manno-oct-2-ulosonic acid
kV	Kilovolt
l	Litre
µl	Microlitre
LB medium	Lysogeny broth medium or Luria-Bertani medium
LC	Liquid chromatography
LCMD	laser capture microdissection
LPS	Lipopolysaccharide

µM	Micromolar
µm	Micrometer
MAA	Maackia amurensis agglutinin
MALDI	Matrix-assisted laser desorption/ionization
Man	Mannose
MAPK	Mitogen-activated protein kinase
mbar	Millibar
MEPC	Mouse epididymis proximal caput
mg	Milligram
Mgat 1	Mannosyl (Alpha-1,3-)-Glycoprotein Beta-1,2-N-Acetylglucosaminyltransferase
min	Minute
ml	Millilitre
mM	Millimolar
M-MLV	Moloney Murine Leukemia Virus
MNC	Multinucleated cells
MOI	Multiplicity of infection
MS	Mass spectrometry
MS/MS	Tandem mass spectrometry
m/z	Mass-to-charge ratio
N	Normal (Normality)
Na	Sodium
$NaBH_4$	Sodium borohydride
$NaBH_3CN$	Sodium cyanoborohydride
NaCl	Sodium chloride
NET	Neutrophil extracellular traps
NEU1,3	Neuraminidase 1,3
Neu5Ac	*N*-acetylneuraminic acid
Neu5Gc	*N*-glycolylneuraminic acid
NK cells	Natural killer cells
nm	Nanometer
nM	Nanomolar
No.	Number
O/N	Over night

OD	Optical density
PBS	Phosphate buffered saline
PCR	Polymerase chain reaction
PFA	Paraformaldehyde
PMSF	Phenylmethylsulfonyl fluoride
PNA	Peanut agglutinin
PNGase F	Peptide-N-Glycosidase F
Pofut	Protein O-fucosyltransferases
polySia	Polysialic acid
PSA	Pisum sativum
PTX	Pentraxin-related protein
q.d.	One a day (from the Latin quaque die)
R	Reverse primer
RNA	Ribonucleic acid
RNase	Ribonuclease
ROS	Reactive oxygen species
rpm	Revolutions per minute
RT	Room temperature
RT-PCR	Reverse transcription polymerase chain reaction
S.D.	Standard deviation
S.E.	Standard error
sec	Second
Ser	Serine
Sia	Sialic acid
Siglec	Sialic acid-binding immunoglobulin-type lectin
SLe^x	Sialyl-$Lewis^x$
SNA	Sambucus Nigra
SPE	Solid phase extraction
TAE	Tris-acetate-EDTA buffer
TFA	Trifluoroacetic acid
Th	T helper lymphocyte
Thr	Threonine
TNF	Tumor necrosis factor
TOF	Time-of-flight

U	Unit
UDP	Uridine diphosphate
UPEC	Uropathogenic *Escherichia coli*
UV	Ultraviolet
V	Volt
v	Volume
v/v	Volume per volume
W	Watt
Wbscr17	Williams-Beuren syndrome chromosome region 17
WGA	Wheat germ agglutinin
w/v	Weight per volume
X	Times
yr	years
ZP 1-4	Zona pellucida glycoproteins (1-4)

1 INTRODUCTION

1.1 Sperm production and maturation

The male reproductive system consists of the testes, epididymis, accessory glands, penis, and the excretory ducts [1]. The main function of the testis is spermatogenesis and androgen (e.g. testosterone) production [2]. Spermatogenesis occurs inside the seminiferous tubules where successive mitotic and meiotic divisions of primordial germ cells (spermatogonia) and their derivatives generate haploid spermatids which are subsequently differentiated to spermatozoa (Figure 1) [3]. Necessary growth factors and nutrients for successful spermatogenesis are provided by the Sertoli cells [2]. After meiosis, gene transcription and translation in haploid germ cells is reduced before it completely ceases in elongating spermatids [4]. In the rete testis, spermatozoa are collected from the lumen of the seminiferous epithelium and then transferred to the epididymis [5, 6].

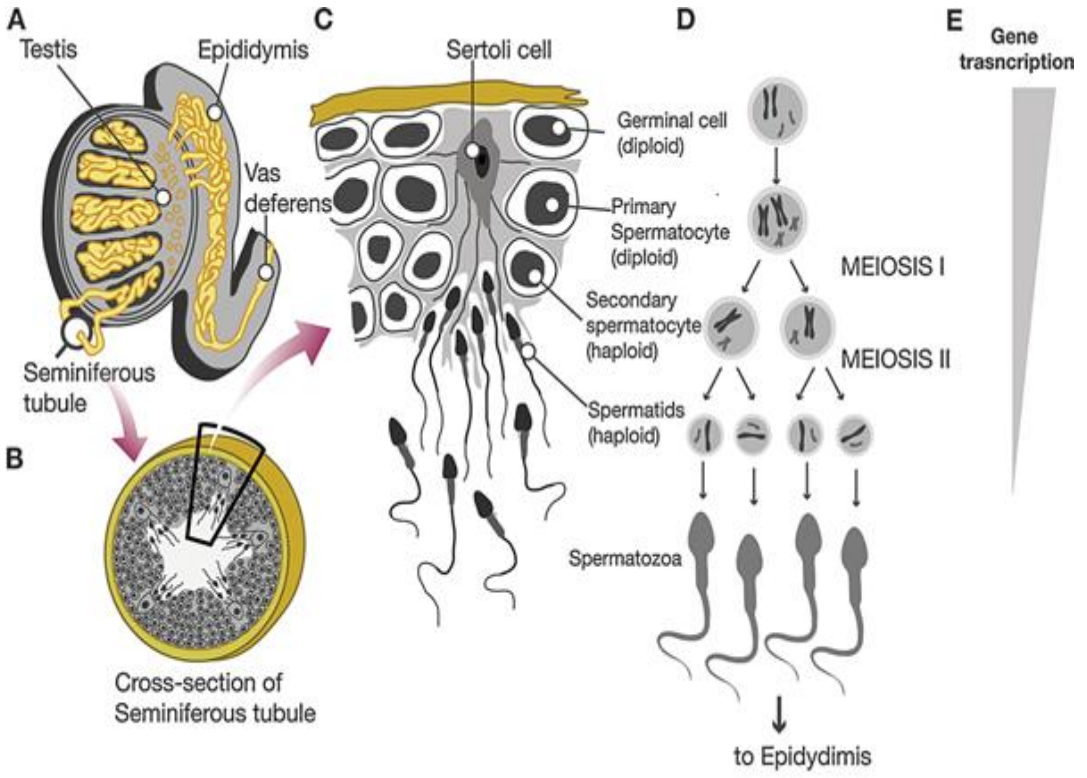

Figure 1. Spermatogenesis occurs in the testis. (**A**, **B**) Spermatozoa are generated inside the seminiferous tubules of the testis. (**C**, **D**) Primary spermatocytes, which are generated from diploid spermatogonia by mitosis, produce haploid sperm following two meiotic divisions. (**E**) Global gene transcription is substantially decreased during spermatogenesis, and finally stopped after production in

the testis and during epididymal maturation of spermatozoa [7]. ()

The testis is connected to the vas deferens through the epididymis. Caput, corpus, and cauda constitute the three regions of the epididymis [8]. Connective tissue septa divide the epididymis into 10 separate segments in both human and mouse [8-10]. The epididymis is lined by epithelial cells which are encompassed by smooth muscle cells and interstitial tissue stroma [8, 11]. Furthermore, immune cells (e.g. lymphocytes and macrophages) are present intraepithelialy and in the interstitium [11]. Spermatozoa acquire their fertilization potential during passage through the epididymis by interaction with epithelial cell secretions [12]. The maturation of spermatozoa further proceeds with the aid of accessory gland (such as the seminal vesicles, prostate gland, and bulbourethral glands) secretions [13].

1.2 Capacitation and acrosome reaction

Since spermatozoa encounter different stimuli (e.g. oestrogen, progesterone) during transit through the female reproductive tract and follicle cell layers (such as cumulus oophorus), membranes of sperm head undergo profound biochemical and physiological alterations. These gradual procedures of sperm modifications are defined as capacitation [14]. Glycoconjugates mainly locate on the cell surface, and they are also entitled as the glycocalyx [15]. The sperm glycocalyx is vulnerable to the different pH in the female genital tract [14] and sugar moieties of the sperm glycocalyx (e.g. sialic acids) can be removed or remodeled during capacitation [16]. Capacitation is considered as a prerequisite for activation of the acrosome reaction. In the female reproductive tract massive changes in the lipid content and the composition of the sperm membrane prepare for a successful acrosome reaction. Such lipid alterations (i.e. in the ratio of cholesterol to phospholipids) not only disrupt membrane stability, but also increase its permeability [14].

Moreover, progesterone and prostaglandins trigger the acrosome reaction via calcium fluxes. The influx of calcium takes place as one of the initiating events in the acrosome reaction [17]. High concentration of calcium in sperm impacts on transportation of other ions such as K^+, Na^+, and H^+. Accordingly, the osmotic pressure of sperm head changes, resulting in enlargement of the acrosome followed by exocytosis. Activation of protein kinases and G-coupled receptors conduct underlying mechanisms for induction of the acrosome reaction [14].

Released enzymes from the acrosome are crucial for facilitating the forward movement of sperm towards the oocyte through the multiple layers of the granulosa cells [14]. Additionally, transferred signals from the zona pellucida promote the acrosome reaction [18].

1.3 Epididymitis

Infectious epididymitis or epididymo-orchitis in men, a frequent entity in urological outpatient settings, is commonly caused by bacteria ascending the genitourinary tract [19]. The majority of patients suffering uropathogenic *Escherichia coli* (UPEC)-caused epididymitis are over 35 years [20]. UPEC are the major pathogen associated with epididymitis [21, 22]. Apart from UPEC, other types of pathogens are also involved in epididymitis such as *Pseudomonas aeruginosa* (in acute patients older than 35 years) as well as *Neisseria gonorrhoeae* and *Chlamydia trachomatis* (in patients younger than 35 years) [22, 23]. Causative bacteria in epididymitis are mainly transmitted sexually. Since these pathogens invade in a retrograde fashion by ascending from the urethra into the epididymis, epididymal inflammations are usually associated with urine infections. Moreover, the risk of UPEC infection in homosexual men is elevated [19].

1.3.1 Symptoms and damage in epididymitis patients

Semen analysis showed that spermatogenesis is impaired in 60% of epididymitis patients [21]. Sperm concentrations and the number of germ cells decreased in these patients [20, 24] and a substantial amount of sperm abnormalities (i.e. azoospermia and oligozoospermia) was reported in the ejaculate of these patients. Furthermore, membrane integrity decreased in infected sperm [25]. Hence, epididymitis patients suffer permanently or transiently from infertility problems. In clinical diagnosis, swelling of the epididymis, especially in the cauda region of these patients, is commonly observed using sonographic examinations [26, 27]. Other symptoms of epididymitis include pain, hydrocele, and sepsis. In a large numbers of epididymitis patients the testis is co-infected (termed epididymo-orchitis) [26].

According to the recommendations of European Association of Urology (EAU), antibiotic therapies may eradicate pathogens within around two weeks [20]. Furthermore, antimicrobial regimes improve semen parameters leading to a rise in the number of normal and a reduction in abnormal forms of spermatozoa. Antibiotics are prescribed up to 84 days in some resistant cases, nevertheless, these *E. coli* pathovars either still persist or cause relapse of infections. Moreover, Lang et al. claimed that in spite of antibiotic regime, sperm

concentration of UPEC infected men remains substantially lower than men infected with commensal *E. coli* [24]. Taken together, it is estimated that in 40% of acute epididymitis patients impairment of fertility persists [20].

1.3.2 Experimental murine model of UPEC-induced epididymitis

This mouse epididymitis model is a useful model to unravel the mechanism how UPEC impairs the normal tissue structures in the host genito-urinary tract. Lang et al. displayed severe clinical manifestations (e.g. swelling, redness, edema) in infected mice comparable to common symptoms in UPEC epididymitis patients. 3 days post UPEC infection bacteria are mainly found the lumen of the epididymis. Moreover, epithelial cells in the epididymis are damaged and devoid of stereocilia. Infection strongly perturbs the integrity of surrounding layers of the cauda (e.g. smooth muscle cells and tight junctions). Concomitant to tissue damage immune cells infiltrate the epididymis postinfection (Figure 2). On the endocrine level, serum testosterone concentrations are substantially diminished in the infected mice. Interestingly, acrosome analysis of sperm in *in vivo* UPEC treated mice revealed that spermatozoa substantially lose their acrosomes [24].

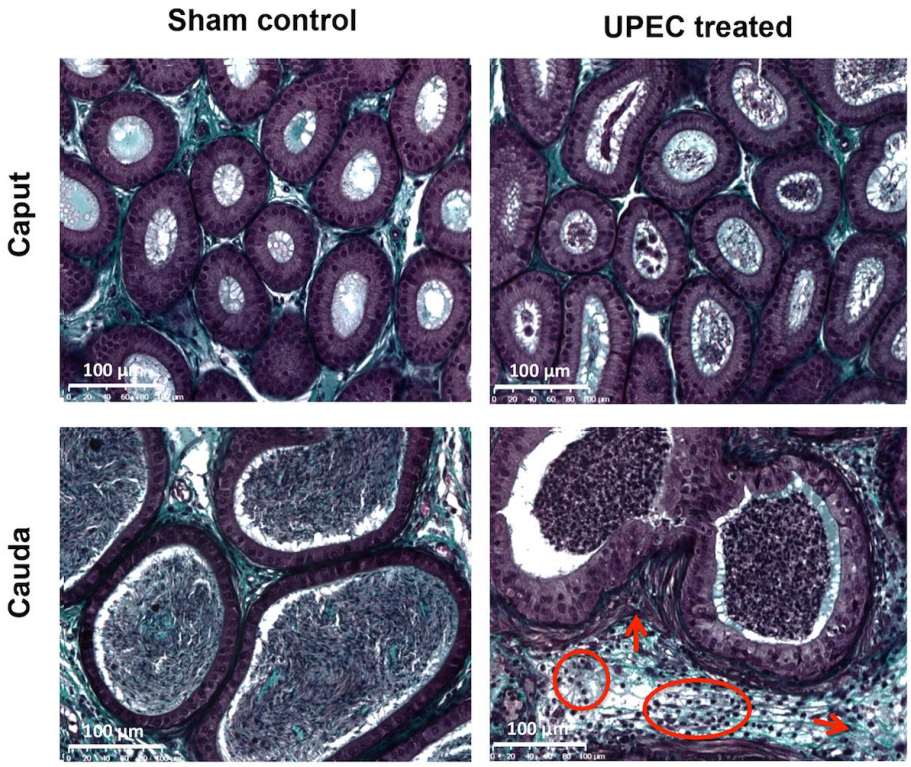

Figure 2. Histopathological alterations following UPEC infection in the cauda epididymis of the experimental model. Masson-Goldner staining of the epididymis sections 3 days after PBS treatment (sham control) and UPEC infection demonstrates that a massive fibrotic remodeling (represented by arrows) i.e. thickening of the smooth muscle cell layer, and collagen accumulation together with interstitial infiltrating leukocytes (indicated by circles) occurs only in the cauda epididymis compared with the caput which remains largely intact [28]. (Copyright © 2016, by the American Society for Biochemistry and Molecular Biology)

Consistent with Lang et al., using the same model Stammler et al. demonstrated that the epididymis segments located in the distal cauda manifested severe defects in histology of epithelial cells and muscle cells [8]. However, as a possible protective mechanism upon the ascending of UPEC, contraction may occur in the epididymal duct. As a result, UPEC ascend is slowed down to move upward from the cauda segments to other regions [8].

1.4 Uropathogenic *Escherichia coli*

UPEC differ from non-pathogenic *E. coli* strains, which also colonize the urinary tract as commensal flora, since UPEC encode genes involved in tissue invasion [29]. UPEC are known to be implicated in 60% of male genito-urinary tract infections [30]. Ascend of these gram-negative opportunistic pathovars to the bladder and kidneys results in cystitis and pyelonephritis, respectively [21]. Furthermore, genito-urinary tract infections are associated with male infertility in up to 10-15% of infertile cases [30].

UPEC modulate inflammatory immune reactions [31, 32]. Controversial studies claim that cytokine production followed by UPEC infection is either elevated in mouse *in vivo* epididymitis model [33, 34] or conversely attenuated in testicular cells and epithelial cells in the bladder [35-37]. Furthermore, neutrophils infiltrate post UPEC infection [21].

As a defense mechanism to eliminate UPEC, antibacterial products such as reactive oxygen species (ROS) are enhanced by leukocytes. Elevated amounts of ROS impair fertility through negative effects on concentration and motility of spermatozoa as well as the ROS-mediated damage of sperm nuclear deoxyribonucleic acid (nDNA) [38, 39]. However, low levels of ROS enhance sperm normal physiological activities e.g. motility, exocytosis of the acrosome, and interactions with the oocyte [40, 41].

1.4.1 UPEC virulence factors

UPEC employ a variety of virulence factors such as adhesins and alpha-hemolysin (hlyA). Adhesins (also termed pili), including P and type 1 fimbria, mediate initial attachments to host

cells [21, 29]. FimH as a member of type 1 fimbria plays an adhesive and invasive role in urinary tract infection via specific binding of the FimH pocket to epithelial cell receptors employing high mannose structures [42]. Moreover, FimH is essential in the formation of biofilm-like structures in bladder intracellular. UPEC evade innate immunity and antibacterial therapies using biofilm structures [43].

UPEC secret hlyA to enhance attachment and colonization of UPEC within the genito-urinary tract [21, 29]. HlyA is a virulence factor and is expressed in at least half of UPEC isolates. Moreover, hlyA as a causative agent is particularly found in acute epididymitis patients [21, 44]. Toxicity of hlyA arises from calcium affinity as well as the formation of pores in the membranes [88, 92-94]. HlyA belongs to the repeat-in-toxin family which contains a binding domain to calcium ions [45]. High levels of hlyA generate pores that trigger cell lysis [21]. HlyA establishes infection via modulations of cell survival and signaling pathways [46]. *In vitro* treatment of sperm with hlyA showed that hlyA impairs fertility via premature induction of the acrosome reaction. In addition, hlyA treated sperm lose the potential of *in vitro* fertilization and formation of blastocyst [24].

Together with these virulence factors, many other agents like capsule K, mannose-resistant adhesins, and the aerobactin system are also involved in the dissemination of UPEC infections [44].

1.5 Glycans

Glycans are defined as arrays of monosaccharides which are covalently linked together with glycosidic bounds (Figure 3). There are different abbreviation systems to demonstrate glycan compositions (Figure 3) [15].

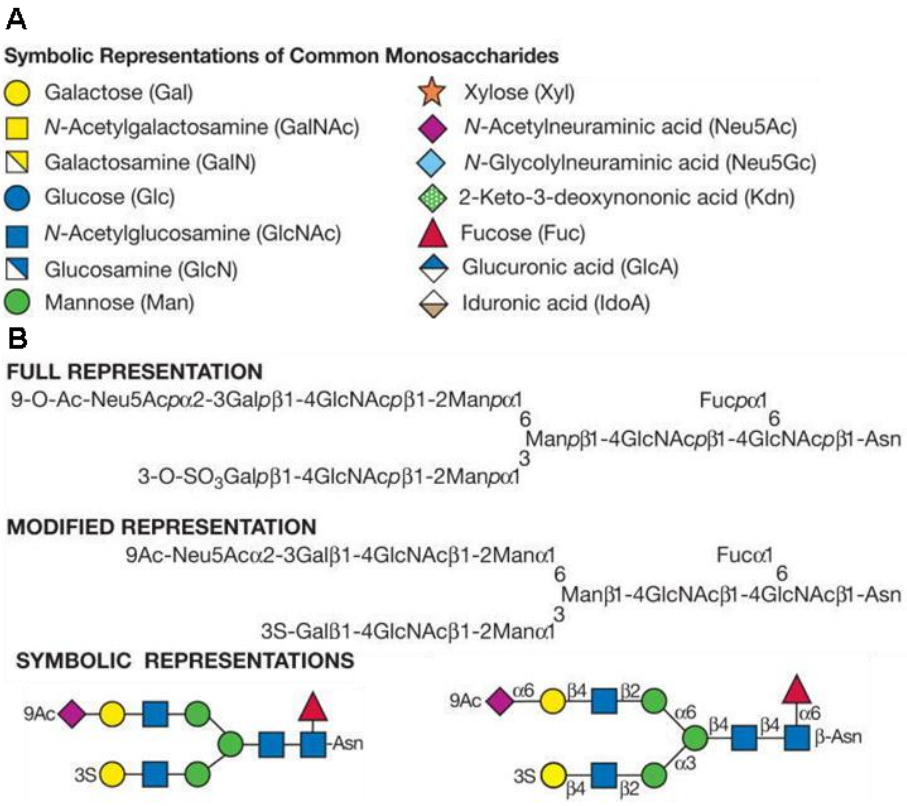

Figure 3. Nomenclature symbols and abbreviations of monosaccharides and glycan structures. (**A**) Common symbols which are used for demonstrating of monosaccharide moieties. (**B**) In order to exhibit glycan structures, several systems (such as full, modified, and symbolic representations) are applied [15]. (Permission from Cold Spring Harbor Laboratory Press)

Glycans can conjugate with lipids and proteins through covalent bonds to form glycolipids and glycoproteins [15]. In eukaryotic cells, predominant forms of glycoconjugates consist of proteoglycans, glycosphingolipids, and glycoproteins (Figure 4) [47]. Glycoproteins occur in three classes, i.e. O-glycans, N-glycans, and O-GlcNAc glycoproteins. In addition to glycoproteins, other types of glycosylated structures exist in living organisms. For instance, in lipid conjugated forms, polysaccharide chains are bound either to ceramide (termed glycosphingolipids) or phosphatidylinositol (defined as glycolipids) which are attached to proteins (together termed glycosylphosphatidylinositol (GPI)). Moreover, hyaluronan is a free form of glycosaminoglycans (GAG). GAGs can also be associated with conjugated forms of proteoglycans (e.g. heparan sulfate, dermatan sulfate, and chondroitin sulfate) (Figure 4) [15, 47].

The mass of glycoconjugates is largely comprised of the glycan part. The high number of glycosylated structures compared to the total number of genes in living organisms implies that glycan biosynthesis is not directly template based (from genome to protein), but is a product

of posttranslational modifications. Among many types of monosaccharides in nature only limited types are expressed in animals. The major types of monosaccharides in animal glycostructures are pentoses, hexoses, deoxyhexoses, hexosamines, uronic acids, and sialic acids. Furthermore, two possible anomeric forms of monosaccharide attachments (α or β) elevate the complexity of glycan structures. The diversity of sugars is further expanded with modifications e.g. acetylation, methylation, phosphorylation, and sulfation in hydroxyl and amino groups. Carbohydrate structures in large extent form the architecture of cells, tissues, and organs. The majority of glycans are secreted or occur on the cell surface. They contribute actively to a variety of related physiological functions such as cell-cell interactions, development, cell signaling, and host-pathogen interactions [15]. Glycans are also essential for fertility through induction of the sperm acrosome reaction and interactions of sperm with the zona pellucida [48, 49].

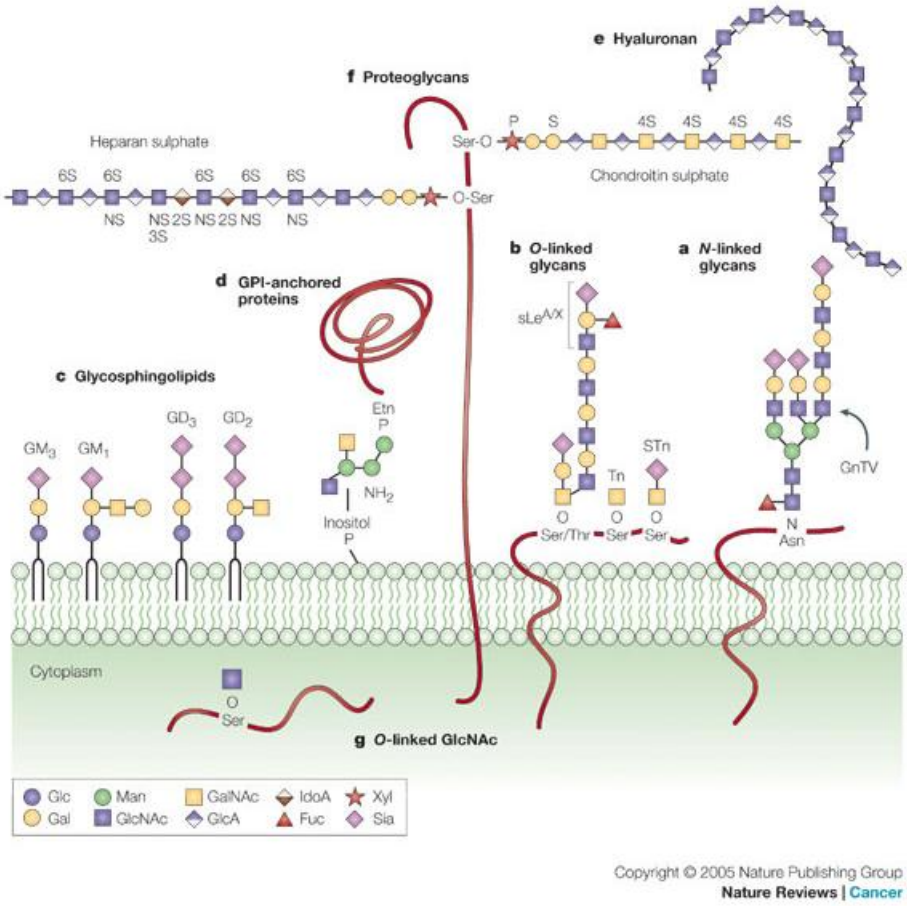

Figure 4. Different types of glycoconjugate structures in eukaryotic cells. N-glycans **(a),** O-glycans **(b)**, and O-GlcNAc glycoproteins **(g)** are three classes of glycoproteins which differ in initiating amino acids and monosaccharides in the attachment site. Glycoconjugated lipids (e.g. glycosphingolipids **(c)** and glycosylphosphatidylinositol (GPI) **(d)**) and proteoglycans **(f)** (e.g. heparan sulfate, dermatan sulfate, and chondroitin sulfate) are other common glycoconjugates in living organisms. In addition to proteoglycans, polysaccharide forms of GAGs are freely found in the

structure of hyaluronan **(e)** in the extracellular matrix [15, 47]. (License number of permission: 4145370715258)

1.5.1 Glycoproteins

The classification of glycoproteins into N- and O-glycans, as two main classes of glycoproteins, is based on the type of amino acids in binding sites including asparagine (Asn) in N-glycans, and serine (Ser) or threonine (Thr) in O-glycans (Figure 4). However, some similar sequences, e.g. *N*-acetyllactosamine disaccharide (Galactose (Gal) β1-4 *N*-acetylglucosamine (GlcNAc) β1), are present in both N- and O-glycans. These sequences are either terminated with fucose (Fuc) or sialic acid, or further extended by the addition of polysialic acid (polySia) chains [15]. The third class of glycoproteins is O-GlcNAc, containing *N*-acetylglucosamine (GlcNAc) which is bound to Ser/Thr in proteins. O-GlcNAcs are located in the cytoplasm and the nucleus (Figure 4) [15, 47].

Microheterogeneity of glycoproteins in individual cells mainly arises from variations in the binding sites of glycans to peptides together with differences in the compositions of attached glycans. Therefore, cell-specific microheterogeneity substantially enhances the variations of glycoproteins [15].

Nucleotides transporting monosaccharides such as uridine diphosphate (UDP)-sugar and guanosine diphosphate (GDP)-sugar are precursors of glycans. Nucleotide-monosaccharides are synthesized in the cytosol or the nucleus. These sugar donors are actively transferred to the endoplasmic reticulum (ER) and the Golgi apparatus which are responsible organelles in the biosynthesis of structural and secreted glycoproteins [50]. Biosynthesis of glycans by means of glycosyltransferases originates primarily in the ER and in the Golgi complex [51, 52]. Secreted glycoproteins are transferred intracellularly or released within vesicles and lysosomes [53]. In addition to structural differences between N- and O-glycans, their biosynthesis and functions are various [14].

Glycans are enzymatically degraded by endoglycosidases and exoglycosidases. Final degradation of glycans occurs in the lysosomes. Cleaved monosaccharides are exported to the cytosol. Therefore, glycans are dynamically recycled in the cells [53].

Evolutionary knowledge of glycans is not well understood. As-yet-known, the composition of glycans is varied both intraspecies and interspecies. Furthermore, recently

evolved species of animals carry more complex compositions of N- and O-glycan. Expression of unusual structures and modification of glycostructures lead to specific physiological functions which play important roles in competitions pertaining to the evolutionary selection pressures, e.g. in host-pathogen interactions [54].

1.5.1.1 N-glycans

In N-glycans, attachments of sugar chains to peptides initiate with the binding of GlcNAc to Asn in a consensus sequence of Asn-X-Ser/Thr. N-glycans are categorized into three classes: high mannose, hybrid, and complex (Figure 5). Nevertheless, a common core structure of five monosaccharides, which consists of 2 GlcNAc and 3 mannose (Man), contributes to all types of N-glycans [15].

Biosynthesis of N-glycans initiates at the cytoplasmic face of the ER. A lipid-like structure (termed dolichol phosphate (Dol-P)) is the precursor of N-glycans. GlcNAc-P is transferred from UDP-GlcNAc to Dol-P. Subsequently, thirteen extra sugars are combined sequentially to Dol-P to generate the N-glycan precursor. During the synthesis of the 14-monosaccharides precursor, an anchored Dol-P (including $Glc_3Man_9GlcNAc_2$) is translocated to the lumen face of the ER membrane, where the oligosaccharide precursor is subsequently bound to Asn. Furthermore, temporary oligomannose structures undergo a required processing in order to reach final form of N-glycans using series of glycosidases and glycosidase transferases in the ER and the Golgi complex [55].

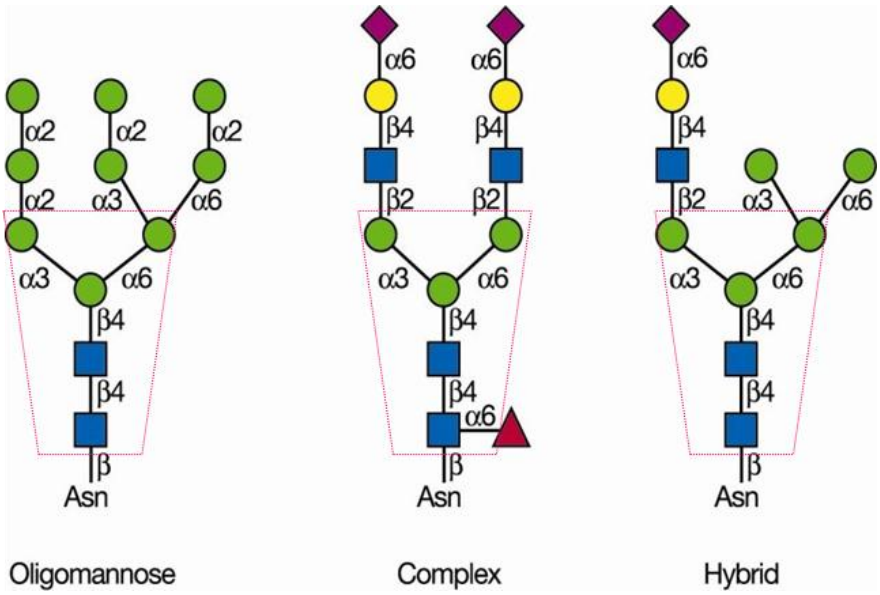

Figure 5. Three major structures of N-glycans. The majority of N-glycans have a common pentasaccharide core sequence, i.e. 2 GlcNAc and 3 Man (red dashed line box). Differences in the type and structure of sugar residues in branches result in classification of N-glycans into oligomannose, complex, and hybrid types [56]. (Permission from Cold Spring Harbor Laboratory Press)

N-glycan mutant murine models cause lethal defects at the embryonic development stage, e.g. deletion in N-acetylglucosaminyltransferase I (*GlcNAcT-I* or Mannosyl (Alpha-1,3-)-glycoprotein beta-1,2-N-acetylglucosaminyltransferase (*Mgat 1*)) as the initiating enzyme in the synthesis of complex-type N-glycans in the Golgi [57, 58]. In addition, the impairment of N-glycan biosynthesis attributes to genetic diseases, e.g. congenital disorders of glycosylation [59]. Taken together, severe consequences, which are associated with defects in N-linked structures in both mouse and human, underpin the physiological importance of N-glycans [57-59].

1.5.1.2 O-glycans

The most common type of O-glycans is so called mucin-type since they are mainly found in mucins. Mucins are high molecular weight glycoproteins, containing numerous O-glycans. Biosynthesis of mucin-type O-glycans is initiated by the attachment of *N*-acetylgalactosamine (GalNAc) to the hydroxyl group of Ser or Thr (Figure 4). Binding of GalNAc to the corresponding amino acid is catalyzed by a GalNAc transferase (GalNAcT). More than 20 types of GalNAcT exist in the Golgi apparatus. GalNAcTs contribute to the synthesis of a variety of mucins in a tissue- and/or cell-specific manner. In contrast to N-glycans, the biosynthesis of O-glycans is simpler, and the structure is less branched. However, O-glycans contain long chains with terminal variations. Mucins are massively detectable in the surface membranes and secretions of many epithelial cells (e.g. in the genitourinary tract), mediating antimicrobial function as a physical and chemical barrier to infection [60]. Other monosaccharides are successively added to initially bound GalNAc in different ways, making up to 8 types of core structures (Table 1) [61].

Table 1. Extension pattern of mucin O-glycans. O-glycans that are initiated by binding of GalNac to Ser/Thr are enlarged by different monosaccharides and linkage types [60]. (Permission from Cold Spring Harbor Laboratory Press)

O-glycan cores	Structure
Tn antigen	GalNAcαSer/Thr
Sialyl-Tn antigen	Siaα2-6GalNAcαSer/Thr

Core 1 or T antigen	Galβ1-3GalNAcαSer/Thr
Core 2	GlcNAcβ1-6(Galβ1-3)GalNAcαSer/Thr
Core 3	GlcNAcβ1-3GalNAcαSer/Thr
Core 4	GlcNAcβ1-6(GlcNAcβ1-3)GalNAcαSer/Thr
Core 5	GalNAcα1-3GalNAcαSer/Thr
Core 6	GlcNAcβ1-6GalNAcαSer/Thr
Core 7	GalNAcα1-6GalNAcαSer/Thr
Core 8	Galα1-3GalNAcαSer/Thr

In addition to O-GalNAC structures, O-fucose and O-glucose modifications of glycans, which are identified as the non-mucin types of O-glycans, are mainly found in epidermal growth factor-like repeats and play a critical role in Notch signaling and embryonic development. O-fucosyltransferases (POFUT), which occur in 2 variants (POFUT1 and 2), and O-glucosyltransferase (POGLUT) initiate the generation of O-fucose and O-glucose glycan structures, respectively. Fuc residues in the structure of epidermal growth factor contribute to Notch signaling [61, 62]. Some studies claimed that Notch signaling is essential for normal spermatogenesis and Leydig cell function [63, 64]. By contrast, Batista et al. revealed that Notch signaling only takes place in Sertoli cells. Furthermore, deletion of Notch1 does not disturb spermatogenesis and fertility competence [65].

O-mannose glycans are another type of O-glycans that are highly present in the brain, and play an active role in the adhesion of neuronal cells [61]. Furthermore, O-mannose compositions contribute to the linkage of the extracellular matrix and cytoskeleton through occurrence in dystroglycan structures [66]. There are two responsible enzymes for priming the synthesis of O-mannose structures termed O-mannosyltransferase 1 and 2 (POMT1 and 2) [61].

1.6 Role of glycans in fertilization

Carbohydrate parts of the zona pellucida (e.g. O-glycans in ZP3) are involved in induction of the acrosome reaction [67, 68]. Subsequently, the cumulus cells and zona pellucida glycocalyx are substantially modulated following the acrosome reaction. The cumulus cells and zona pellucida are surrounded by GAG layers, containing a disaccharide sequence of GlcNAc repeats called hyaluronan [69-71]. Hyaluronidases (e.g. PH20 in pigs) are situated in the sperm acrosome and are activated after release by the acrosome reaction. Hyaluronidases

specifically digest the hyaluronan layer of the egg, resulting in the penetration of sperm through the extracellular matrix of the oocyte in the cumulus [72]. Besides hyaluronidases, β-N-acetylglucosaminidases are released from sperm after the acrosome reaction and cleave outermost GlcNac moieties that are excessively present in hyaluronan structures. Whereas inhibition of β-N-acetylglucosaminidase suppresses fertilization, this enzyme seems to be crucial for sperm passing through surrounding layers of the zona pellucida [73].

1.7 Sialic acids

Sialic acid residues occur mostly at the outermost position of eukaryotic glycoconjugates on the cell surface and glycosylated secretions [74, 75]. However, sialic acids may also bind to internal positions of glycans. In addition to the extensive presence in higher invertebrates and vertebrates, sialic acids are also found in bacteria, which are either pathogens or belong to commensal flora [76].

1.7.1 Sialic acid structure

Sialic acids are a α-keto acids family of nine-carbon backbone amino monosaccharides and include more than 50 members. In mammals, *N*-acetylneuraminic acid (Neu5Ac) and *N*-glycolylneuraminic acid (Neu5Gc) represent the most abundant species among sialic acid members (Figure 6) [77, 78]. During evolution, humans have irreversibly lost the biosynthesis potential for Neu5Gc due to a genetic mutation in Cytidine monophosphate (CMP)-N-acetylneuraminic acid hydroxylase [79, 80]. Unlike other monosaccharides, the nucleotide-sugar precursor of sialic acid is CMP-Sia [50]. Synthesis of sialic acids in eukaryotes occurs in the Golgi apparatus. Moreover, sialyl-transferases mediate attachment of sialic acids to glycan structures. Sialic acids from a position of C-2 are able to bind into C-3 or C-6 of underlying monosaccharide moieties (i.e. Gal or GalNac) [81].

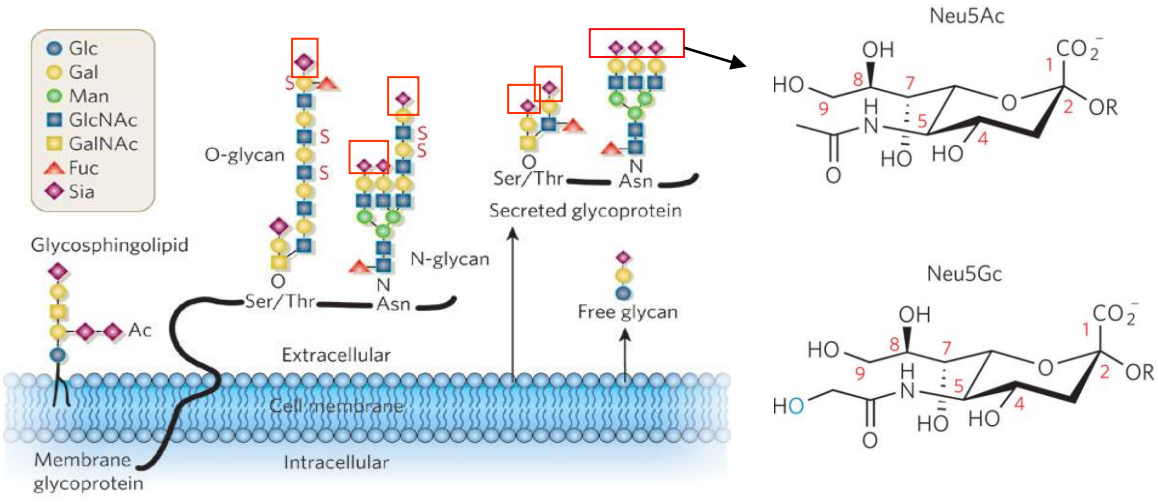

Figure 6. Sialic acid localization and structure. Sialic acids mostly occupy the terminal part of glycostructures (highlighted in red boxes). Neu5Ac and Neu5Gc are two most prevalent types of the sialic acid superfamily in mammals, which differ structurally in one extra oxygen atom bound to C-5 of Neu5Gc (represented in blue)[82]. (License number of permission: 4145330580662)

1.7.2 Physiological and pathological roles of sialic acids

The occurrence of millions of sialic acid moieties, carrying negatively charged carboxylate groups to the largest share of glycoproteins, remarkably elevates the hydrophobicity of the cell surface. As a result, cell-cell interactions are regulated [83, 84]. For instance, sialic acids raise repulsion of cells (e.g. blood cells) to avoid undesired cell interactions [85]. Taken together, electrostatic features and outermost localization enable sialic acids to mediate a wide variety of important biological roles, ranging from immune response to development and many other essential activities, as described in many studies [74-78, 86].

In normal conditions, sialic acids contribute to receptor-ligand interactions. This is the case for Factor H as well as sialic acid-binding immunoglobulin-type lectins (Siglecs), which implicate numerous immunomodulatory functions [85]. In addition, sialic acids play various roles during an ongoing infection [76]. The presence of sialic acid in receptors of several pathogens facilitates the binding of bacteria or viruses to host cell [77, 87-89]. For instance, their binding sites (e.g. *Helicobacter pylori*, *influenza virus A*, and *influenza virus C*) together with toxins from some pathogens (e.g. *Plasmodium falciparum*, *Vibrio cholerae*), all share specific type and linkage of sialic acids [85]. Given sialic acids contribute to the suppression of immune response, some pathogens cover their surface with sialic acids to mislead immune defense [90]. This mimicry approach of pathogens for surviving in hosts is acquired by two main mechanisms. On one hand, several pathogens (such as *Escherichia coli K1*, *Neisseria meningitides B*, Group B *Streptococcus*) are able to generate *de novo* sialic acid [90]. On the other hand, some other pathogens steal sialic acids from host either directly (e.g. *Hemophilus influenzae*) or indirectly with the aid of trans-sialidase and sialyltransferase (e.g. *Trypanosoma cruzi* and *Neisseria gonorrhoeae*, respectively) (Figure 7) [90].

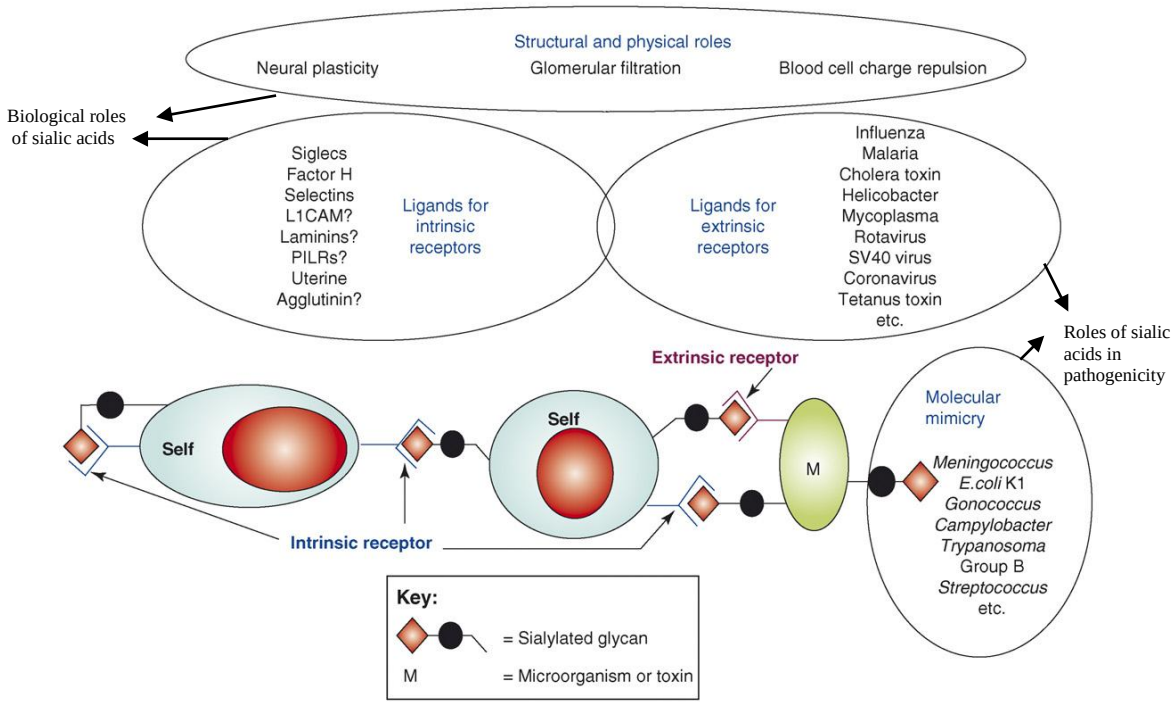

Figure 7. Sialic acids contribution to a variety of physiological and pathological functions. In biological processes, sialic acids widely contribute to binding of intrinsic receptors. Nevertheless, sialic acids mediate roles in pathogenicity since sialic acids can also be recognized by some pathogens as extrinsic receptors. In addition, some pathogens exploit host sialic acids to evade immune response via a mimicry mechanism [85]. (License number of permission: 4140931321525)

1.7.3 Role of sialylated glycans in fertilization

The zona pellucida family are extracellular matrix glycoproteins (i.e. ZP 1-4 in human) that cover the surface of the vertebrate oocytes [91, 92]. Fertilization initiates with the binding of sperm to the zona pellucida. Oligosaccharide parts of the zona pellucida were widely identified in contact sites with sperm receptors [18]. Unlike N-glycans, O-linked glycans of ZP3 play an essential role in the primary attachment of gametes [67, 93]. Moreover, the presence of Gal residues, particularly in O-glycans, is known to be necessary for zona pellucida-sperm interaction [91]. However, mass spectrometry (MS) analysis of the zona pellucida binding sites to human sperm demonstrated the high presence of sialylated capped tetrasaccharide sequences termed Sialyl-Lewis^x (SLe^x). The SLe^x oligosaccharide consists of NeuAcα2-3Galβ1-4(Fucα1-3)GlcNAc and occurs in the zona pellucida inside bi-, tri-, and tetra-antennary structures of both N- and O-glycans (Figure 8) [49].

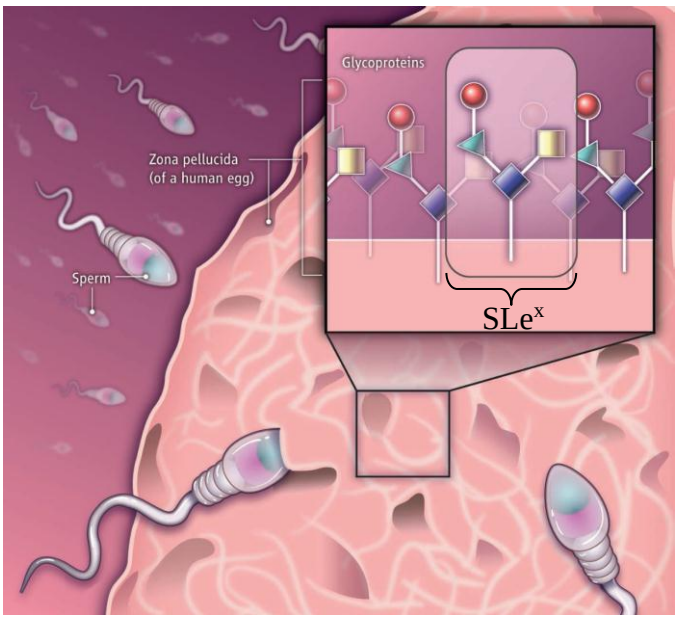

Figure 8. Sperm-zona pellucida attachment is mediated by surface sialic acids. Terminal sialic acids (represented in red circles) in an oligosaccharide array of Sialyl-Lewis^x (SLe^x) in combination with Gal (green triangles), GlcNAc (blue diamonds), and Fuc (yellow boxes) exist in the primary interaction site of sperm-zona pellucida [94]. (Reprinted with permission from AAAS)

In addition to its contribution to the zona pellucida, SLe^x mediates a similar adhesion role during metastasis of cancer cells. Moreover, SLe^x is known to have a role in the accumulation of blood cells (such as platelets or leukocyte) during proinflammatory response [95, 96]. Nevertheless, the concentration of SLe^x in the zona pellucida is approximately double compared with somatic cells [49]. Furthermore, Pang et al. observed the lower rate of fertilization after blocking of SLe^x sequence either using antibodies against sialylated motifs or by applying synthetic sialylated glycoconjugates. In contrast to the SLe^x oligosaccharide, Lewis^x sequence, which is devoid of the terminal sialic acid, failed to manifest any inhibitory effect on the rate of sperm-zona pellucida binding. Thus, these studies indicate that sialic acids in the SLe^x sequences on the extracellular surface of the egg serve as responsible ligands for sperm attachment [49].

1.8 Sperm glycocalyx

Thick layers of glycans capped with millions of sialic acid moieties encompass the sperm surface. Several classes of glycoconjugates such as glycolipids, glycoproteins (both N- and O-glycans), GAGs (e.g. chondroitin and heparan sulfate), and GPI-anchored glycoproteins (e.g. CD52) decorate the sperm surface (Figure 9) [7, 97, 98].

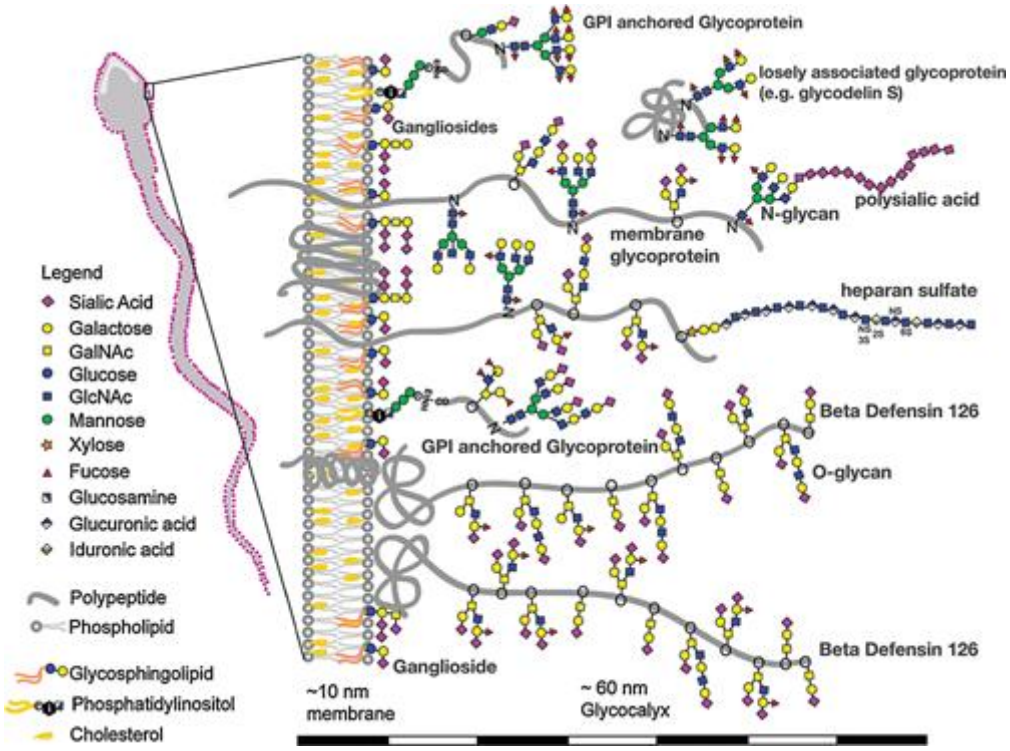

Figure 9. Distribution of different classes of glycostructures on the sperm surface. Glycan structures are mainly conjugated to proteins and lipids (represented in gray). Furthermore, other glycoconjugates are associated with glycosphingolipids and cholesterol (represented in orange and yellow, respectively). Further modifications such as acetylation and/or sulfation may also occur in sperm glycoconjugates [7]. (© 2015 The Authors. Molecular Reproduction and Development published by Wiley Periodicals, Inc)

In comparison to glycoprotein layers of the zona pellucida surrounding the female gamete, the size of the sperm glycocalyx is remarkably thinner (20 to 60 µm in sperm versus 1 to 16 nm in the zona pellucida). On the other hand, more than 50 different glycoconjugates are present in the sperm glycocalyx, while only 3 or 4 glycoproteins constitute the zona pellucida (ZP 1-4). Hence, glycoprotein diversity and surface heterogeneity of glycoconjugate structures in sperm are indeed more complex than the homogeneous structure of the zona pellucida [98].

1.8.1 Biosynthesis of sperm glycoconjugates

The sperm glycocalyx is primarily generated *de novo* during spermatogenesis in the seminiferous tubules using several sets of glycosyltransferases. Biosynthesis of the sperm glycocalyx takes place co- and post-translationally in the ER and Golgi (Figure 10) [7]. In the epididymis, sperm spontaneously is unable to *de novo* biosynthesis of glycans; nevertheless, epididymal maturation mediates a decisive role in the alteration of sperm glycoconjugates [7].

Spermatozoa glycostructures undergo substantial modifications during transmit from the epididymis, where they come in contact with epididymal glycosyltransferases and glycosidases secreted in the lumen [99-102]. Some glycostructures on the sperm surface are only restricted to one specific region of the epididymis (i.e. caput, corpus, or cauda), indicating that glycoconjugates are selectively incorporated into and/or removed from sperm in a region-specific manner [101, 102]. Similarly, the epididymis functions actively in production and incorporation of sialic acids into the sperm membrane during sperm maturation and ejaculation [99].

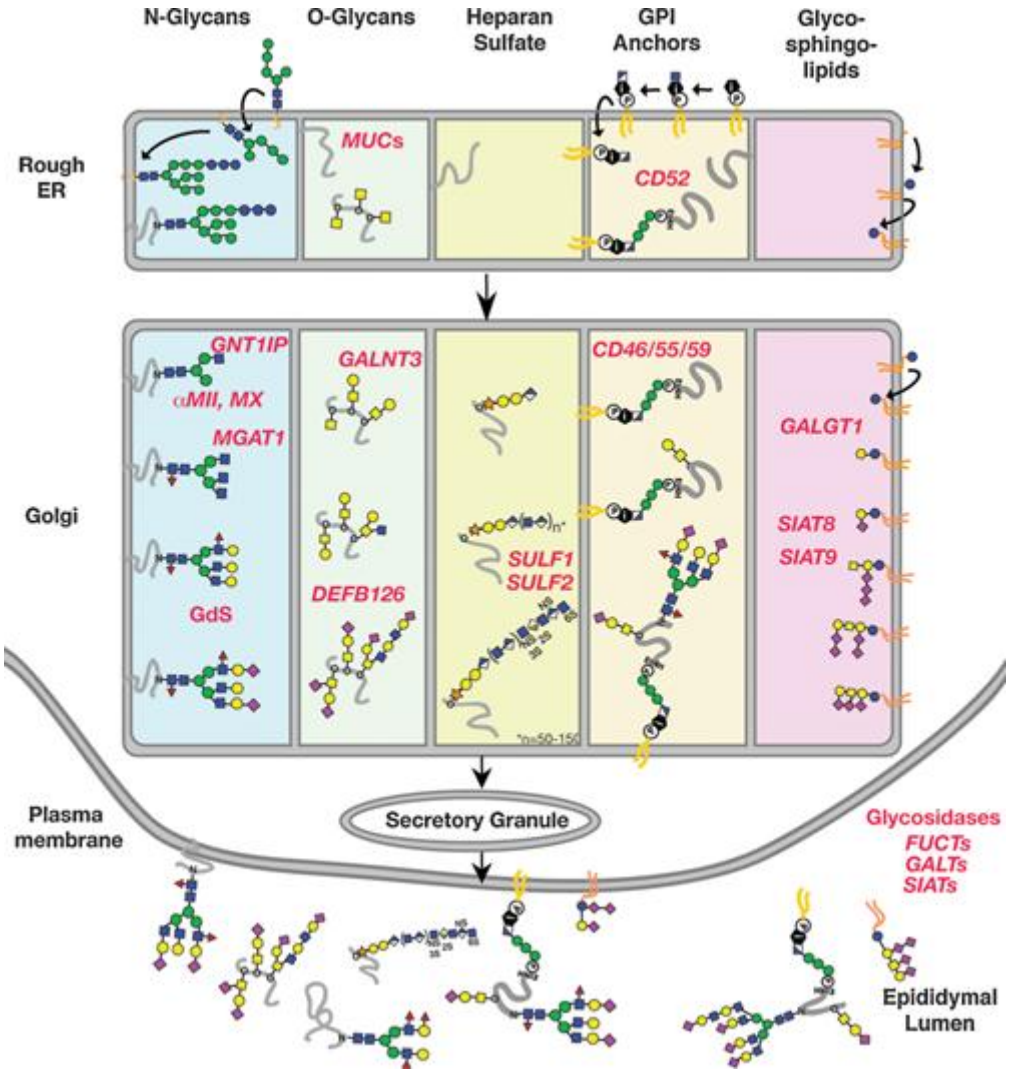

Figure 10. Biosynthesis and alterations of sperm glycoconjugates. ER and Golgi apparatus are the responsible organelles in initiation and elongation of sperm glycoconjugates. Subsequently, generated glycoconjugates are either secreted or translocated onto the surface of sperm membranes. Some alterations in the sperm glycocalyx occur in epididymal lumen due to interaction with glycosidases and glycosyltransferases, e.g. fucosyltransferase (FUCT), galactosyltransferase (GALT), and sialyltransferase (SIAT). Glycoconjugates are abbreviated as follows: GnT1IP (GlcNAcT-I inhibitory protein), GdS (glycodelin S), GALNT3 (N-acetylgalactosaminyltransferase 3), MUC

(mucin), DEFB126 (ß-defensin 126), αMII (alpha-mannosidase II), Mx (alpha-mannosidase IIx), GALGT1 (N-acetylneuraminyl-galactosylglucosylceramide N-acetylgalactosaminyltransferase), SULFF (heparin sulfate 6-O endosulfatase), and SIAT (sialyltransferase) [7]. (© 2015 The Authors. Molecular Reproduction and Development published by Wiley Periodicals, Inc)

1.8.2 Conventional methods to analysis sperm glycocalyx

Classical sugar studies on the sperm glycocalyx are mainly dependent on lectin applications [103, 104]. Additionally, glycoproteomics analysis of sperm glycans using MS applications revealed the presence of several glycan compositions associated with sperm [105].

1.8.2.1 Lectin analysis of sperm carbohydrates

Lectins are carbohydrate-binding proteins with a strong affinity to specific sugar moieties in a lock-and-key manner [106, 107]. Since the majority of lectin studies have been performed on ejaculate samples, the outcome of sperm glycocalyx analysis is biased towards sperm isolation and preparation procedures. For example, different fixation methods affect the outcome of the acrosome staining [108]. Moreover, as a general disadvantage of lectin staining, it is known that various technical conditions and parameters such as alteration in lectin concentration as well as time and temperature of incubation per se may substantially influence the quality of results [109, 110]. However, some lectins, for instance, *Concanavalin A* (Con-A), are able to specifically detect the sperm acrosome in the testis and post-testicular regions. Additionally, since Con-A recognizes the acrosome in a variety of species, it may imply that the binding epitope of Con-A on the sperm acrosome serves as a conserved epitope across various species [111]. *Wheat germ agglutinin* (WGA) lectin binds to sialylated disaccharides, including sialic acid and GlcNac [98]. Intriguingly, based on a lectin profiling study, WGA is able to recognize all different parts of sperm (i.e. acrosome, equatorial segment, post-acrosomal region, midpiece, and tail) with a pronounced fluorescence signal [103]. In addition to Con-A and WGA, other lectins with an exclusive affinity to various monosaccharides (such as *Peanut agglutinin* (PNA), Gal; *Soya bean agglutinin* (SBA), GalNac; *Pisum sativum agglutinin* (PSA), Man; *Ricinus communis agglutinin* (RCA), GalNac; and *Lens Culinaris agglutinin* (LCA), Man) are able to detect specific regions of sperm [103, 104]. Furthermore, analyzing the pattern of sperm sugars using WGA showed that sperm sialic acids are elevated during epididymal passage [98].

Exclusive affinity of Fuc-specific lectins (e.g. *Ulex europaeus agglutinin 1* (UEA-1), *Tetragonobolus* (TPA), *Anguilla anguilla agglutinin* (AAA) and *Lotus tetragonolobus* (LTL)) to the acrosome, but not to plasma membrane, represents the differences in glycan compositions between the acrosome and the sperm membrane [49, 112]. In addition, these fucolectins specifically recognize Lewis^x trisaccharide (i.e. α-L-Fuc-(1-3)-[β-D-Gal-(1-4)]-D-GlcNAc) and Lewis^y tetrasaccharide (i.e. α-Fuc-(1-2)-β-Gal-(1-4)-(α-Fuc-[1-3])-GlcNAc) motifs (Figure 10), proposing the associations of Lewis^x and Lewis^y sequences with the sperm acrosome [105].

1.8.2.2 Glycoproteomics analysis of sperm glycans

Pang et al. in a Matrix-assisted laser desorption/ionization (MALDI)-MS profiling study represented a variety of possible N-glycans on sperm. These identified structures belong to two classes of N-linked glycoproteins: a) the high mannose (also named as oligomannose) structures which carry between 5 to 9 Man, and b) the complex structures which include several types of branched compositions such as bisected bi-antennary, bi-, tri-, and tetra-antennary on sperm. Furthermore, this study demonstrated the association of Fuc moieties in both reducing ends of glycans and antennae of complex N-glycans in the composition of Lewis^x and Lewis^y sequences (Figure 11) [105].

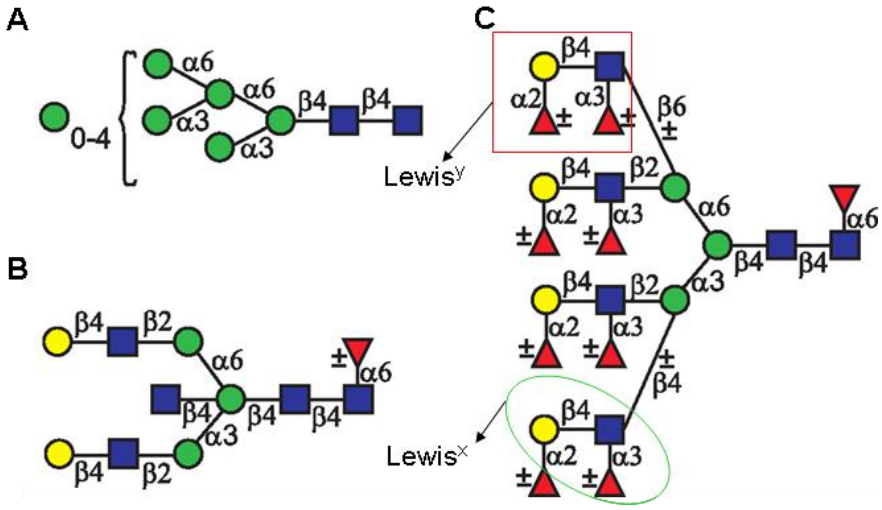

Figure 11. Predominant classes of N-glycans associated with sperm. MALDI-MS analysis of human sperm displayed that spermatozoa comprise two major classes of N-glycans such as (**A**) high mannose as well as different complex structures, including (**B**) bisected bi-antennary structure and (**C**) bi-, tri-, and tetra-antennary structures which may be capped with Fuc moieties in Lewis^x and/or Lewis^y sequences [105]. (Copyright © 2007, by the American Society for Biochemistry and Molecular Biology)

1.8.3 Functional roles of sperm glycans in the female reproductive tract

The epididymis secretes and incorporates CD52 and ß-defensin 126 (DEFB126) into the sperm surface [7]. CD52 is a member of GPI-anchored proteins and carries both N- and O-glycans, which share highly sialylated *N*-acetyllactosamine repeats [7]. These epididymis-mediated modifications in the sperm glycocalyx play essential roles in acquiring the fertilization competence [99-102]. DEFB126, which is a heavily sialylated O-glycan terminated with sialic acids in both α2,3 and α2,6 linkage forms, is one of the well-characterized glycoproteins associated with sperm [7, 113]. During epididymal maturation, DEFB126 is secreted and incorporated into the sperm surface when sperm passes through the distal corpus and cauda regions (Figures 9 and 10) [114, 115]. Importantly, DEFB126 plays essential roles in the protection of sperm against pathogens as well as in sperm penetration through cervical mucus towards the oocyte and subsequent sperm-zona pellucida attachments [115, 116].

PolySia chains (containing α2,8 sialic acid polymers) are attached to N-linked glycoproteins. PolySia is highly expressed and functions during differentiation of stem cells and at the time of neuronal and skeletal muscle development. Moreover, polySia regulates immunity [117, 118]. In human sperm, polySia is located in the postacrosomal region and equatorial ring. In addition, Simon et al. claimed that polySia molecules suppress neutrophil extracellular traps (NET). By this virtue, polySia actively contributes to sperm survival upon female immune response [119].

Lewis sequences in glycan structures mediate immunoregulatory effects [105]. For instance, Glycodelin S (GdS) weakly binds to sperm, but occurs abundantly in seminal plasma. GdS is a non-sialylated N-glycan that bears Lewis^x and Lewis^y sequences [7]. Together with its immunosuppressive role, GdS protect sperm from untimely capacitation [120].

1.9 Aim of the study

A previous study of the group using the murine experimental acute epididymitis model demonstrated premature acrosome reaction as well as drastic structural changes in the spermatozoa and the epididymis, including a significant reduction in sperm concentration, epithelial damage and fibrotic changes, at day 3 post UPEC infection [24]. During invasion several pathogens use cell surface sialic acids for adhesion to host cells [85, 90]. These findings together with Ma et al., which revealed a massive release of sialic acids in a mimicry capacitation condition [16], prompted us to investigate the possible changes in the presence and content of sialylated glycans after UPEC infection in mouse and human spermatozoa. We hypothesize that UPEC or their secreted virulence factors may impair male reproductive potential by putative modifications of the sperm glycocalyx.

To do so, we will analyze the cellular sialylation status of sperm sialic acids in both human patients with a history of acute epididymitis and our well-established mouse epididymitis model compared to healthy controls. Additionally, we aim to investigate the effects of UPEC on the sialic acid levels of epididymal epithelial cells. To this end, we will measure the sialome status of epithelial cells in the cauda region of the mouse model. In agreement with sialic acid quantitative analysis, the morphological status of the acrosomes after infection will be figured out. Along with sialic acid analyses, N-glycan compositions of human sperm will be separately analyzed using LC-MALDI-MS/MS approach. Consequently, we plan to investigate possible alterations in N-glycans following the acrosome reaction.

Taken together, the current study aims to survey whether alterations in sialic acid moieties take place in the sperm glycocalyx as a consequence of UPEC epididymitis. Additionally, we try to collect evidence for introducing the sperm glycocalyx as a diagnostic marker of UPEC induced infertility. Finally, this study may imply some salvaging mechanisms for surviving sperm during infection that may be promising for therapeutic intervention in male infertility caused by UPEC epididymitis.

2 MATERIALS AND METHODS

2.1 Materials

2.1.1 Chemicals

Acetic acid	Merck, Darmstadt, Germany
Acetonitrile	Th. GEYER, Renningen, Germany
Acetone	Merck, Darmstadt, Germany
2-aminobenzaminde (2-AB)	Sigma, Taufkirchen, Germany
Ammonium Bicarbonate	Sigma, Steinheim, Germany
Ammonium formate	Sigma, Taufkirchen, Germany
Bactoagar	Sigma, Steinheim, Germany
Bactotryptophan	Sigma, Steinheim, Germany
Bouin’s solution	Sigma, Steinheim, Germany
Bovine serum albumin (BSA)	Roth, Karlsruhe, Germany
Bromophenol blue sodium salt	Sigma, Steinheim, Germany
Calcium ionophore A23187	Sigma, Taufkirchen, Germany
Dichloromethane	Promochem, Wesel, Germany
2,5-dihydrobenzoic acid (DHB)	Sigma, Taufkirchen, Germany
Dimethyl sulfoxide (DMSO)	Sigma, Taufkirchen, Germany
Dulbecco´s PBS (1X)	PAA, Cölbe, Germany
Eosin	Roth, Karlsruhe, Germany
Ethanol	Fluka Analytical, Hamburg, Germany
Ethidium bromide	Roth, Karlsruhe, Germany
Ethylene diaminetetraacetic acid disodium (EDTA)	Merck, Darmstadt, Germany
Formaldehyde solution 37%	Roth, Karlsruhe, Germany
Formic acid	Sigma, Steinheim, Germany
Glycerol	Merck, Darmstadt, Germany
Human tubal fluid (HTF) medium	Irvine Scientific, Santa Ana, USA
Hydrochloric acid (HCl)	Sigma, Steinheim, Germany
Isopropanol (2-propanol)	Sigma, Steinheim, Germany
2-keto-3-deoxynononic acid (KDN)	Sigma, Taufkirchen, Germany
Mayer’s hematoxylin	Merck, Darmstadt, Germany
β-mercaptoethanol	Sigma, Steinheim, Germany

Methanol	Merck, Darmstadt, Germany
Methyl iodide	Merck, Darmstadt, Germany
4,5-methylenedioxybenzene (DMB)	Dojindo, Kumamoto, Japan
N-Acetyl-2,3-dehydro-2-deoxyneuraminic acid (DANA)	Sigma, Taufkirchen, Germany
N-acetylneuraminic (Neu5Ac)	Sigma, Taufkirchen, Germany
N-glycolylneuraminic (Neu5Gc)	Sigma, Taufkirchen, Germany
Peptide Calibration Standard	Bruker Daltonics, Bremen, Germany
Phenylmethylsulfonyl fluoride (PMSF)	Thermo Scientific, Waltham, USA
PureLink® RNA Mini Kit	Life Technologies, Carlsbad, USA
RPMI 1640	Invitrogen, Darmstadt, Germany
Sodium acetate	Sigma, Steinheim, Germany
Sodium borohydride (NaBH4)	Sigma, Taufkirchen, Germany
Sodium cyanoborohydride ($NaBH_3CN$)	Sigma, Steinheim, Germany
Sodium hydrosulfite	Sigma, Taufkirchen, Germany
Sodium hydroxide (NaOH)	Sigma, Steinheim, Germany
TOPRO®-3	Life Technologies, Carlsbad, USA
Trifluoroacetic acid (TFA)	Promochem, Wesel, Germany
Tris-acetate	Roth, Karlsruhe, Germany
VECTASHIELD® mounting medium	Vector Laboratories, Burlingame, USA

2.1.2 Enzymes

Neuraminidase Vibrio Cholerae	Roche, Mannheim, Germany
N-glycosidase F (PNGase F)	Roche, Mannheim, Germany
Trypsin	Sigma, Steinheim, Germany

2.1.3 Lectins

Maackia amurensis agglutinin (MAA)	Vector Laboratories, Burlingame, USA
Peanut agglutinin (PNA)	Vector Laboratories, Burlingame, USA
Pisum sativum (PSA)	Vector Laboratories, Burlingame, USA
Sambucus Nigra (SNA)	Vector Laboratories, Burlingame, USA

2.1.4 PCR reagents

Deoxyribonuclease (DNase)	Life Technologies, Carlsbad, USA
Desoxyribonukleosidtriphosphate (dNTP)	Promega, Mannheim, Germany
Moloney Murine Leukemia Virus (M-MLV) Reverse Transcriptase	Promega, Mannheim, Germany
Oligo dT	Promega, Mannheim, Germany
Primers	Life Technologies, Carlsbad, USA
RNase inhibitor (RNAsin®)	Promega, Mannheim, Germany
Taq polymerase	Promega, Mannheim, Germany

2.1.5 Equipment

Adhesive Caps	Zeiss, Munich, Germany
Amide column	TOSOH Bioscience, Tokyo, Japan
Autosampler (Midas)	Spark, Emmen, Netherland
Bead homogenizer (TissueLyser)	Qiagen, Hilden, Germany
Blood agar plates	Oxoid, Wesel, Germany
C18 bond Elut LRC	Agilent Technology, Santa Clara, USA
Cell culture CO_2 incubator	Binder, Tuttlingen, Germany
Centrifuge (Hettich Universal 32R)	DJB labcare, Buckinghamshire, UK
Confocal microscope	Leica Microsystems, Wetzlar, Germany
Coverslip	Roth, Karlsruhe, Germany
Electrophoresis system	PEQLAB, Erlangen, Germany
Esquire 3000 ESI-ion trap (IT)-MS	Bruker Daltonics, Bremen, Germany
Fluorescence detector	Jasco, Gross-Umstadt, Germany
Fluorescence detector	Merck-Hitachi Darmstadt, Germany
Gel Jet Imager 2000 documentation system	Intas, Göttingen, Germany
Grease-free slides (SuperFrost)	R. Langenbrinck, Emmendingen, Germany
Heat Block	Medax, Kiel, Germany
HyperSep™ Hypercarb™ SPE Cartridge	Thermo Scientific, Waltham, USA
Laser Capture Microdissection (LCMD)	Zeiss, Munich, Germany
LC system (Smart line)	Knauer, Berlin, Germany
Magnetic stirrer	IKA, Staufen, Germany
Membrane slide	Zeiss, Munich, Germany

Microtome RM2245	Leica Microsystems, Wetzlar, Germany
Microwave oven	Samsung, Schwalbach, Germany
Mini centrifuge (Galaxy 14D)	VWR, Radnor, USA
Mixer Mill MM 300	Retsch, Haan, Germany
NanoDrop ND 2000	Promega, Mannheim, Germany
Neubauer counting chamber	LaborOptik, Marienfeld, Germany
Normal phase column (CHROMABOND®)	Macherey-Nagel, Düren, Germany
Pall Nanosep®10 kDa filters	PALL Life Sciences, Ann Arbor, USA
pH indicator paper (Whatman)	Thermo Fisher, Waltham, USA
pH Meter	Knick, Berlin, Germany
Power supply units	PEQLAB, Erlangen, Germany
Reversed-phase column (Superspher)	Merck-Hitachi, Darmstadt, Germany
RNase-free filter tips	Nerbe plus, Winsen, Germany
SpeedVac	Thermo Fisher, Waltham, USA
Steel target	Bruker Daltonics, Bremen, Germany
Thermocycler	Biozyme, Oldendorf, Germany
Thermo-shaker	Eppendorf, Hamburg, Germany
Thermo-shaker	Peqlab, Erlangen, Germany
Ultraflex I TOF/TOF mass spectrometer	Bruker Daltonics, Bremen, Germany
Ultrasonicator (Ultrasonic bath)	Bandelin, Berlin, Germany
Vacuum manifold (VacMaster™)	Biotage, Uppsala, Sweden
Vortex mixer	Janke & Kunkel, Staufen, Germany
Water purification system	Millipore, Darmstadt, Germany
Weight	Mettler, Greifensee, Switzerland

2.2 Methods

2.2.1 Criteria for selection of sperm donors

All patients and volunteers provided written informed consent for semen analysis. All samples were anonymized. As controls, three healthy males of reproductive age (median: 34 yr; range: 26-44 yr) were recruited during their medical checkup in the outpatient clinic. In addition, ejaculates of three patients (median: 40 yr; range: 19-54 yr) suffering acute unilateral *E. coli*-related epididymitis were analyzed within the first 2 weeks after diagnosis. Patients were part of the Giessen Epididymitis Study (institutional review board no. 100/7, German Clinical Trials Register no. DRKS00003325) and treated according to current guideline recommendations [121]. Out of 22 epididymitis patients providing semen, only the samples of three patients (aged 19, 54, and 47) had a suitable sperm concentration (> 0.5 million/ml) to undergo further analysis. All patients underwent a comprehensive microbiological analysis for classical uropathogens by culture and species-specific PCR analysis to detect *Neisseria gonorrhoeae*, *Mycoplasma genitalium*, *Ureaplasma urealyticum*, and *Chlamydia trachomatis*. Only healthy donors and patients suffering *E. coli* epididymitis were part of the study. Empiric therapy was initiated with levofloxacin 500 mg q.d. orally for 10 days. Sexually active men were asked to provide a semen sample 14 days after first presentation.

2.2.2 Isolation of human sperm

Semen samples were collected by masturbation into a sterile container. Ejaculates were liquefied and then semen analysis was performed according to World Health Organization (WHO 2010) recommendations [122]. Parameters such as pH, volume, concentration, viability and motility were recorded and subsequently assessed. For motility assay, the proportion of immotile and progressive motile spermatozoa in semen was defined under a light microscope by the average movement status of 100 spermatozoa in two consecutive counting experiments. To estimate the vitality of spermatozoa, 10 µl of ejaculate and 10 µl of eosin were mixed for 30 sec, and then the ratio of live (unstained) to dead (red head) spermatozoa was evaluated following two times random counting processes under a light microscope. To select motile sperm, the swim-up procedure was applied [123]. One ml of fresh semen sample was placed in a sterile centrifuge tube, and 1 ml of prewarmed (37°C) human tubal fluid (HTF) medium was layered over it. The tube was inclined at an angle of 45º and incubated for 1 h at 37°C. After incubation, 1 ml of upper medium containing highly

motile sperm was removed, diluted with 2 ml of HTF medium and centrifuged at 500 × g for 5 min. Following spin down, the supernatant was discarded and pellets of all ejaculate aliquots containing highly motile spermatozoa were pooled in one tube. Motile spermatozoa were diluted in 0.5 ml of HTF medium and counted using a Neubauer counting chamber under a light microscope. To prove the success of the swim-up procedure, the motility of spermatozoa was assessed following swim-up and compared to sperm motility in semen. The diluted fraction of spermatozoa was centrifuged (700 × g, 10 min). Finally, the obtained sperm pellet was washed and centrifuged twice with Dulbecco's phosphate-buffered saline (PBS) medium (pH 7.4) at 700 × g for 10 min.

2.2.3 Bacterial strains and propagation

The UPEC strain CFT073 used in our study (NCBI Reference Sequence: NC_004431.1, GenBank: AE014075.1) was kindly provided by Prof. Chakraborty from the Institute of Medical Microbiology, Justus Liebig University of Giessen. Propagation of UPEC was performed by overnight (O/N) cultivation of the bacteria on a blood agar plate and then inoculation in lysogeny broth (LB) medium. Subsequently, bacteria growing in an exponential phase (OD_{600}=0.5–1.0) were acquired following incubation at 37°C on a shaker, as previously described [35]. The concentration of bacteria was calculated using standard growth curves [35, 124]. Following centrifugation at 4,500 × g for 8 min at RT, bacteria were washed by PBS. Next, the pellet containing *E. coli* was diluted in 10 ml of PBS and RPMI 1640 and then used for *in vivo* and *in vitro* experiments, respectively.

LB medium (pH 7.4)

0.5% (w/v)	Yeast extract
1% (w/v)	Bactotryptophan
1 M	Sodium chloride (NaCl)

LB-Agar

1.5%	Bactoagar in LB medium

2.2.4 *In vitro* infection of human sperm with UPEC

Isolated spermatozoa after swim-up procedure (~ 7.5×10^6) were mixed with 5×10^5 UPEC (multiplicity of infection (MOI) ~ 0.07) for 3 h at 37°C and 5% CO_2. The pellet (700 × g, 10 min) was collected after two washing steps using PBS (pH 7.4).

2.2.5 Mouse experimental epididymitis model

Adult inbred C57BL/6J mice (10-week-old) were purchased from Charles River Laboratories (Sulzfeld, Germany). All animal studies were performed according to a German protocol for the care and use of laboratory animals approved by the Animal Ethics Committee of the Regierungspraesidium Giessen (permit no. GI 18/17–No. 124/2012). Mice were euthanized by CO_2 inhalation. All attempts were made to diminish suffering.

To induce epididymitis, 5-10 µl of PBS suspension containing between 4-8 × 10^4 bacteria were injected bilaterally close to the epididymis into the vas deferens, which was previously ligated to prevent retrograde ascend of the bacteria [125, 126]. For sham controls, an equal volume of PBS alone was injected into the vas deference of control animals. An ascend of UPEC from the injection site to the epididymis was previously demonstrated [24]. Three days post-infection, mice were sacrificed and the epididymides were removed. The epididymides from one side were snap frozen in liquid nitrogen after cryo-embedding in optimum cutting temperature (OCT) media for lectin staining, whilst the epididymides from the contralateral side were immediately fixed in Bouin's solution and embedded in paraffin. Subsequently, sections were utilized for histological staining and LCMD.

2.2.6 Lectin fluorescence staining

After swim-up freshly prepared human spermatozoa (approximately 50,000 sperm diluted in 10 µl PBS) were smeared onto clean grease-free SuperFrost slides and air-dried. Serial cryosections (8 µm) were prepared from frozen mouse epididymides. Human spermatozoa and mouse epididymis sections were fixed with 2% paraformaldehyde for 30 min. Two % paraformaldehyde fixative was prepared by diluting 37% formaldehyde solution in PBS. The mouse epididymis caput epithelial cell line (MEPC5) was kindly provided by Dr. Vera Michel (Institute of Anatomy and Cell Biology, JLU, Giessen). Cells were grown on glass coverslips and fixed in acetone. After fixation sections were washed using PBS and blocked with 0.1% bovine serum albumin (BSA) in PBS for 1 h at room temperature (RT). To investigate the presence of specific monosaccharides and linkages in sperm and the epididymis, FITC-conjugated lectins (including PNA, PSA, *Maackia amurensis agglutinin* (MAA), and *Sambucus Nigra* (SNA)) were used at a final concentration of 10 µg/ml in PBS containing 0.1 % BSA and incubated for 30 min in a moisture chamber. All FITC-labeled lectins were purchased from Vector Laboratories (Burlingame, USA). Subsequently, slides were washed

three times with PBS. For visualization of nuclei, slides were incubated with TOPRO®-3 (dilution 1:1,000; 1 min). To preserve the fluorescence signal during prolonged storage, 25 µl of VECTASHIELD® mounting medium was dispensed onto the section and then dispersed using a coverslip. Coverslips were sealed to the slide using a transparent nail polish. Images were acquired using a laser scanning confocal microscope. Excitation filters were set to 488 nm to detect FITC (lectins-bound glycostructures) and 633 nm to visualize nuclei with Topro®-3.

2.2.7 Laser capture microdissection

Paraffin embedded murine epididymides were sectioned (5 µm) using a microtome (RM2245) and mounted on membrane slides for LCMD. As previously described, sections were sequentially deparaffinized, rehydrated, stained with Mayer's hematoxylin, washed, dehydrated and air-dried (Table 2) [127]. Tissue areas were collected using a 20 × objective and dissected in Robo-Laser pressure catapulting (LPC)-mode. To calculate the number of dissected cells, stained nuclei by Mayer's hematoxylin were counted. Isolated area from tissue was collected in an adhesive cap. Thereafter, the adhesive caps were cut and transferred into glass vials for sialic acid analysis [127, 128].

Table 2. Preparation steps for epididymis sections prior to LCMD. Sections were deparaffinized, rehydrated, stained, and dehydrated as described below.

Steps	Solution	Incubation time
Deparaffinization and rehydration	100% xylene	5 min
	100% xylene	5 min
	100% ethanol	5 min
	100% ethanol	5 min
	95% ethanol	5 min
	70% ethanol	5 min
	dH_20	5 min
Nuclear staining	Mayer's hematoxylin	30 sec
Washing	Running tab water	15 min
Dehydration	70% ethanol	5 min
	100% ethanol	5 min
	100% ethanol	5 min

2.2.8 Release and DMB-labeling of sialic acids

Washed spermatozoa obtained after swim-up as well as collected tissue samples were subjected to sonication (10 min) and hydrolyzed in 500 µl of 2 N acetic acid for 90 min at 80 °C, transferred into glass vials, and dried. Fluorescent labeling of sialic acids was performed using 80 µl of 4,5-methylenedioxybenzene (DMB)-reaction buffer for 2 h at 55°C, as already described [129-132]. Labeling was terminated by adding 20 µl of 0.2 M sodium hydroxide (NaOH) [127, 133, 134]. To calculate the amount of Neu5Ac a four-point calibration line was generated using different concentrations of Neu5Ac (i.e. 0.005, 0.01, 0.05, and 0.10 nM).

Acetic acid (2 N)

4.5 ml	Glacial acetic acid
40 ml	dH_2O

DMB-reaction buffer

1 M	β-mercaptoethanol
9 mM	Sodium hydrosulfite
20 mM	Trifluoroacetic acid (TFA)
2.7 mM	DMB

NaOH (0.2 M)

0.8 g	NaOH
100 ml	dH_2O

2.2.9 HPLC and online HPLC-ESI-MS of DMB-labeled samples

DMB-labeled sialic acids from spermatozoa and epithelial cells were separated for quantification by a reversed-phase column (Superspher 100 C-18e-RP, 250 × 4 mm) at 40°C using an Ultimate LC system, which was directly coupled with an Esquire 3000 ESI-ion trap (IT)-MS [127, 134]. Fluorescently-labeled sialic acids were separated by applying mobile phases (A and B) containing acetonitrile / methanol / water/ TFA (4:4:92:0.1) (v/v) (A) and acetonitrile/ methanol/ water/ TFA (45:45:10:0.1) (v/v) (B). The LC method consisted of a linear gradient from 0% to 15% (B) in 30 min (Table 3). The flow rate was 250 µl/min over 60 min. The fluorescence detection settings for extinction (λex) and emission (λem) wavelengths were 372 nm and 456 nm, respectively. Typical ESI source conditions were: spray voltage 1.4 kV, capillary temperature of 250°C, end plate offset of −500 V, and capillary exit of 140 V [127]. Series of samples were injected sequentially using an Autosampler (Midas™) equipped with a sample cooling system.

Table 3. HPLC gradient program for separation of DMB-labeled samples. Followed by fluorescent labeling of spermatozoa and epithelial cells, sialic acids were analyzed using a 55 min gradient program.

Time	A%	B%
0	100	0
25	95	5
30	85	15
35	0	100
40	0	100
55	100	0

2.2.10 *In vitro* enzymatic desialylation

To induce a mimicry desialylation, spermatozoa after swim-up were incubated with 5 mU/ml sialidase (Neuraminidase Vibrio Cholerae) in HTF medium for 3 h at 37°C and 5% CO_2. Spermatozoa were washed two times using PBS (700 × g, 10 min) and collected in a pellet following centrifugation.

Enzymatic desialylation of epididymis frozen sections was performed in a humidified chamber following incubation with 5 mU/ml of sialidase in a sialidase buffer for 1 h at 37°C. Afterward, slides were placed at RT and washed three times with PBS for 5 min each [135].

Sialidase buffer (pH 5)
0.1 M Sodium acetate
0.15 M Sodium chloride

2.2.11 Inhibition of sperm sialidase

Desialylation of sperm was inhibited by adding 1 mM N-Acetyl-2,3-dehydro-2-deoxyneuraminic acid (DANA), which is a specific endogenous neuraminidase inhibitor, to HTF medium for 3 h at 37°C and 5% CO_2. After treatment, spermatozoa were collected by centrifugation (700 × g, 10 min) after two washing steps using PBS.

2.2.12 Induction of acrosome reaction

The acrosome reaction was induced following incubation of spermatozoa for 1 h at 37°C and 5% CO_2 in HTF medium supplemented with 10 µM calcium ionophore A23187 solution dissolved in dimethyl sulfoxide (DMSO) [104]. Following treatment, the suspension was centrifuged (700 × g, 10 min). After centrifugation, the pellet of spermatozoa was resuspended in PBS buffer (pH 7.4) and washed twice (700 × g, 10 min each).

2.2.13 Isolation of human sperm N-glycans

To quantify and profile sperm N-glycans, glycoproteins of spermatozoa were digested to glycopeptides. Next, N-glycans were isolated, hydrolyzed, fluorescently labeled and analyzed using LC-MS applications.

2.2.13.1 Protein digestion

Swim-up sperm samples were washed using PBS and the pellet was resuspended in 50 mM ammonium bicarbonate (pH 8.5). Subsequently, ultrasonication of sperm sample for 10 min was performed. Afterward, 1 µl of trypsin solution was added and incubated O/N at 37°C. Tryptic digestion of sperm glycoproteins to glycopeptides was terminated following incubation with 20 µl PMSF solution (containing 100 mM PMSF in isopropanol) for 2 h at RT. Inhibition process of trypsin was continued by shaking on a heat block for 10 min at 100°C.

Trypsin solution

1 mg	Trypsin (from bovine pancreas)
1 ml	Hydrochloric acid (HCl) (0.001 M)

2.2.13.2 N-glycan digestion and purification

After heating, sperm glycopeptides were cooled down at RT for 10 min. Subsequently, N-glycans were liberated from peptides in a process which was initiated via applying 20 units of N-glycosidase F (PNGase F) O/N at 37°C. Afterward, released glycans were collected from sperm suspension using a solid phase extraction (SPE) by C18 cartridges. Before running through, C18 cartridges were washed and primed via successive administration of 2 ml methanol, 2 ml TFA 0.1%, 2 ml 40% acetonitrile, TFA 0.1%, 2 ml 80% acetonitrile, TFA

0.1%, 2 ml TFA 0.1%, and 10 ml water. Thereafter, sperm sample was applied onto C18 cartridge. To release adsorbed N-glycans from C18 cartridge, 4 ml of TFA 0.1% was added and eluted fraction was collected in a glass vial. Released N-glycans were condensed to 0.5 ml volume using a vacuum centrifuge termed as SpeedVac concentrator [136].

To increase the purity of N-glycans, 10 kDa molecular weight cutoff filters (Pall Nanosep® centrifugal device) were used. Prior to administration of samples, pre-condition steps of 10 kDa filters were performed by adding ethanol/ water (50:50) (v/v) followed by centrifugation at 13,000 rpm for 5 min and the filtrate was discarded. Subsequently, the fraction of N-glycans obtained from SpeedVac was applied on the filter and centrifuged at 13,000 rpm for 5 min. Next, 100 µl ethanol/ water solution (50:50) (v/v) was added and centrifuged twice at 13,000 rpm for 10 min each. Finally, all filtrates were collected and N-glycans were condensed by drying of the liquid phase via SpeedVac [137].

To initiate hydrolysis of liberated glycosylamines to related reducing monosaccharides, 200 µl of 1% formic acid was added to dried N-glycan sample. Followed by ultrasonication, the sample was dried using SpeedVac [137].

2.2.13.3 Desalting of N-glycans

Sodium (Na) ions may disturb LC-MS analysis of sperm. Therefore, Na^+ ions were removed using a Hypercarb cartridge (HyperSep™ Hypercarb™ SPE). To force the liquid through the Hypercarb cartridge membrane, the cartridge was placed on a vacuum manifold (VacMaster™). Before elution of N-glycans, pre-condition steps were performed via successive administration of dH_2O and acetonitrile/ 0.1% TFA solutions [136].

Precondition steps of Hypercarb cartridges:

2 ml	dH_2O
2 ml	40% acetonitrile/ 0.1% TFA
2 ml	80% acetonitrile/ 0.1% TFA
10 ml	dH_2O

Dried N-glycans were resuspended in 500 µl dH_2O and dissolved with the aid of an ultrasonicator. Subsequently, sperm N-glycan solution and 4 ml of dH_2O/ 0.1% TFA solution were added to the primed cartridge. As a result, the liquid phase containing salts leaves the cartridge, but N-glycans bind to the filter. Finally, N-glycans were released in four steps from

the Hypercarb cartridge using consecutive administration of acetonitrile/ 0.1% TFA solutions as follows:

Elution steps for releasing of desalted N-glycans from Hypercarb:

500 µl	20% acetonitrile/ 0.1% TFA
500 µl	40% acetonitrile/ 0.1% TFA
500 µl	60% acetonitrile/ 0.1% TFA
500 µl	80% acetonitrile/ 0.1% TFA

Following elution steps, obtained fractions containing desalted N-glycans were pulled down in a glass vial and then reduced to dryness via SpeedVac [136].

2.2.14 Fluorescent labeling of N-glycans

Fluorescent labeling of sperm N-glycans with 2-aminobenzaminde (2-AB) was performed by administration of a 2-AB/ sodium cyanoborohydride ($NaBH_3CN$) reagent to the dried glycans. To prepare this reagent, 63 mg of $NaBH_3CN$ was dissolved in 1 ml DMSO/ acetic acid (77:23) (v/v) mixture containing 48 mg/mL 2-AB. Intense shaking was applied using an ultrasonicator and then 50 µl of 2-AB/ $NaBH_3CN$ reagent was added to sperm N-glycans. After ultrasonication, the vial was placed in a heating block at 65°C for 3 h and later was cooled down for 5 min at RT. Subsequently, 90 µl dH_2O and 900 µl acetonitrile were added to 2-AB-labeled glycans and mixed by an ultrasonicator. Unbound 2-AB was removed using a normal phase column (CHROMABOND® SiOH). Before loading the sample, pre-conditioning of the column was performed via consecutive aspiration of 1 ml of dH_2O (4X) and 1 ml of 95% acetonitrile (4X). After pre-conditioning, the sample was loaded into normal phase and the column was eluted 10 times with 1 ml of 95% acetonitrile. Finally, in order to separate the labeled N-glycans from the column, 1 ml of dH_2O (2X) was introduced to the column and flow through collected. The 2-AB-labeled fraction of N-glycans was reduced to dryness using a SpeedVac.

2.2.15 HPLC profiling of 2-AB-labeled N-glycans

2-AB-labeled N-glycans were separated and quantified under normal phase condition by an Amide column (TSKgel Amide-80) at 40°C using an Ultimate LC. Applied mobile phases (A and B) consisted of acetonitrile/ ammonium formate (50 mM, pH 4.5). The flow rate was 1

ml/min over 70 min. To record 2-AB fluorescent signal, HPLC detector was adjusted to λex = 330 nm and λem = 420 nm under gain of 1,000.

Dried 2-AB-labeled glycans were dissolved in 20 µl of 50 mM ammonium formate (pH 4.5) and then 80 µl acetonitrile under ultrasonication. Subsequently, 10% of the mixture was injected using an autosampler and N-glycans were separated in HPLC via a linear gradient program from 20% to 100% (B) in 55 min (Table 4).

Table 4. HPLC gradient program for separation of 2-AB-labeled samples. Following 2-AB labeling, sperm N-glycans were separated within 55 min using a 70 min gradient program.

Time	%A	%B
0	80	20
50	0	100
55	0	100
56	80	20
70	80	20

Applied mobile phases

A 80% acetonitrile/ 20% ammonium formate (50 mM, pH 4.5)
B 20% acetonitrile/ 80% ammonium formate (50 mM, pH 4.5)

2.2.16 Enzymatic desialylation of the N-glycan fractions

Collected HPLC fractions, containing 2-AB-labeled N-glycans of human spermatozoa in glass vials, were reduced to dryness in a SpeedVac and dissolved in 20 µl sodium acetate buffer (50 mM, pH 5) by 3 min ultrasonication. Five mU/ml sialidase (Neuraminidase) were added to the glass vial and incubated for 15 h at 37°C. After incubation, the sample was dried and dissolved two times with 50 µl methanol followed by evaporation in a SpeedVac [138]. Desialylated N-glycans and untreated control samples were mixed with 10 µl ammonium formate (50 mM, pH 4.5) and 30 µl acetonitrile. Following 3 min ultrasonication, 50% of the sample was injected into the HPLC column. Desialylated and control samples were separated using HPLC via the same linear gradient program that was designed for the analysis of 2-AB-labeled samples (Table 4) from 20% to 100% (B) in 55 min under a gain of 1,000.

2.2.17 Permethylation of N-glycans

Dried sperm N-glycans were dissolved via an ultrasonicator in 500 µl of reduction buffer inside a screw-capped glass vial. After dissolving, the cap of glass vial was loosely closed and stored O/N in darkness at RT. In order to terminate the reduction, a few drops of acetic acid were added to the cooled down vial, placed on an ice container, until pH decreased to five. Appropriate pH was controlled either using a pH indicator paper or visually since the generation of bubbles in reaction with acetic acid in pH 5 were totally ceased. The liquid phase was evaporated in a SpeedVac. The condensed sample was subjected to 500 µl methanol thrice followed by strong agitation using an ultrasonicator and evaporation under a nitrogen stream. Possible salt contamination was removed using a Hypercarb cartridge, as previously described (in 2.2.13.3). To proceed the permethylation of desalted and lyophilized N-glycans, 300 µl DMSO was added to the vial. In addition to DMSO, a tiny amount (a spatula tip) of smashed NaOH under a stream of argon was introduced to the vial. Subsequently, the contents of the glass vial were mixed using a vortex for 5 min followed by spinning down at 2,500 × g for 1 min. Fifty µl of methyl iodide was introduced to the mixture. After 5 min vortexing, the sample vial was shaken for 40 min at RT. Subsequently, the vial was cooled down (using an ice bath) in order to prepare the required temperature for incubation with 1 ml 10% acetic acid together with 1 ml of dichloromethane. To extract permethylated glycans into the organic phase, samples were vortexed (5 min) and spun down (2,500 × g, 1 min). The water phase removed. 1 ml 10% acetic acid was mixed with the organic layer using 5 min vortex. After 1 min centrifugation (2,500 × g), the water layer was discarded. The organic layer was washed using 1 ml dH_2O four times, spun down (2,500 × g for 1 min each). After every centrifugation step, the water phase was discarded. Separation of organic phase from the remaining water was further continued after 30 min incubation of the glass vial at -20°C. The organic phase containing permethylated glycans of sperm was conveyed to another vial and dried using a nitrogen stream [136].

Reduction buffer

10 mg	$NaBH_4$
1 ml	NaOH (0.01 M)

2.2.18 MALDI-TOF-MS

To identify N-glycan structures of sperm, permethylated N-glycans were analyzed via matrix-assisted laser desorption/ionization time-of-flight (MALDI-TOF). For MALDI-TOF-MS analysis, the sample was mixed with the matrix solution. The matrix contains crystallized molecules which adsorb the energy of laser and conduct it to sample. Subsequently, the matrix triggers desorption of the analyte molecules. 2,5-dihydrobenzoic acid (DHB) was chosen as a common matrix for glycan analysis with more resistance upon contaminants. To prepare DHB solution, 20 mg DHB was dissolved in 1 ml of methanol/ water at a ratio of 70:30 (v/v) [105]. Permethylated N-glycans were dissolved in 15 µl of 50% methanol followed by ultrasonication. Next, a mixture of 1 µl of sample and 1 µl of DHB solution was made and applied to a stainless steel target. The sample and the matrix were mixed via pipetting and later air dried. N-glycan masses were analyzed using an Ultraflex I TOF/TOF mass spectrometer supplied with a nitrogen laser and a LIFT-MS/MS (tandem mass spectrometry) facilities. The spectrometer was operated in positive-ion reflector mode for detection of permethylated glycans. To control the MALDI-TOF instrument, FlexControl 2.4 software was utilized. Flex Analysis software 3.0 processed the raw data and analyzed the acquired MS and MS/MS spectra. All described software were purchased from Bruker Daltonics (Bremen, Germany). The setting was calibrated externally using a standard peptide. To acquire sum spectra, 200-400 single spectra were accumulated for parent ion signal and fragments. In order to identify the N-glycans, GlycoWorkbench software was applied to match MS and MS/MS data with possible glycan structure available at the glycan databases as well as to draw glycan compositions used in the annotation of MS and MS/MS spectra.

2.2.19 Analysis of gene expression by RT-PCR

Reverse transcription polymerase chain reaction (RT-PCR) copies defined sequences from a cDNA and can be used to determine if expression of specific genes occur in a tissue or cell. Therefore, expression levels of different O-glycan synthesis genes were investigated in the mouse epididymis using RT-PCR. To do so, ribonucleic acid (RNA) was isolated from tissue, quantified, reverse transcribed to complementary DNA (cDNA), amplified by PCR, and visualized using electrophoresis separation.

2.2.19.1 RNA isolation

RNA was isolated from ≤ 5 mg mouse epididymis tissue using PureLink® RNA Mini Kit according to the manufacturer's protocol. To avoid RNase contamination, RNase-free filter tips and tubes were utilized in the entire process of RNA isolation. Prior to lysis, 1% β-mercaptoethanol was added to the lysis buffer (containing guanidinium isothiocyanate). The epididymis was homogenized and lyzed for 3 min in 300 µl of the lysis buffer together with metal beads using a homogenizer (TissueLyser). The supernatant was transferred to a new vial and an equal volume of 70% ethanol was added and vortexed shortly. The lysed sample was applied to a spin cartridge and centrifuged (12,000 × g, 15 sec, RT). The flow-through was discarded and again the same amount of 70% ethanol was added to the cartridge followed by centrifugation (12,000 × g, 15 sec, RT). 700 µl of wash buffer I was administered to the spin cartridge. After spin down (12,000 × g, 15 sec, RT), the flow-through was discarded. The cartridge was inserted into a new collection tube and 500 µl of wash buffer II was added to the cartridge followed by centrifugation (12,000 × g, 15 sec, RT). The addition of wash buffer II and centrifugation was repeated. In order to dry the membrane containing bound RNA, the cartridge was spun down at 12,000 × g for 2 min. A recovery tube was inserted instead of the collection tube and then 50 µl of RNase-free water layered in the center of the cartridge followed by 1 min incubation at RT. To release RNA from the membrane of the cartridge, the cartridge was centrifuged at 12,000 × g for 2 min at RT. RNA concentration was measured using a NanoDrop. Finally, RNA samples were stored at -80°C.

To eliminate possible DNA contamination, isolated RNA was incubated with Deoxyribonuclease I (DNase I). For this purpose, 1 µg of RNA was mixed with 1 µl of DNase I (1 U/µl), 1 µl of reaction buffer, and DEPC-treated water to 10 µl. The mixture was incubated for 15 min at RT. Next, DNase was inactivated by administration of 1 µl EDTA (25 mM) to the tube followed by 10 min heating at 65°C. Absence of DNA contamination in RNA sample after digestion with DNase was proved by PCR for β-actin (as a housekeeping gene) using RNA sample as template.

2.2.19.2 cDNA synthesis

Isolated RNA was reverse transcribed to complementary DNA (cDNA) by *Moloney Murine Leukemia Virus* (M-MLV) reverse transcriptase. RNA was incubated with 2 µl oligo dT in a total volume of 21 µl and denatured at 70°C for 10 min. Thereafter, the denatured

RNA vial was kept on ice. The reverse transcription master mix was prepared (Table 5) and heated for 2 min at 42°C. RNA degradation was avoided using a RNase inhibitor (RNAsin®) in the master mix. To synthesize cDNA, the master mix was added to the denatured RNA vial and incubated for 75 min at 42°C followed by 15 min at 70°C. Finally, cDNA samples were stored at -20°C.

Table 5. cDNA synthesis master mix. Reverse transcription of denatured RNA was performed using a combination of the following materials.

Material	Volume (µl)
RT buffer 5x	8
dNTP	2
RNAsin 40 U/ µl	1
dH_2O	4
M-MLV	1

2.2.19.3 PCR

The quality of synthesized cDNA was checked via performing PCR for β-actin. First, a master mix was prepared (Table 6), containing β-actin primers (forward primer (F): ATGGTGGGTATGGGTCAGAA and reverse primer (R): GGGTCATCTTTTCACGGTTG). Afterward, DNA was amplified using a thermocycler with described conditions (Table 7).

Table 6. List of PCR components. PCR master mix was prepared using the following materials:

Material	Volume (µl)
H_2O	16.75
Taq buffer (5x)	5
$MgCl_2$	1
dNTP (10 Mm)	0.5
Primer mix	0.5
cDNA	1
Taq polymerase	0.25

Table 7. PCR program for β-actin. β-actin PCR was performed using a thermocycler according to outlined program.

Cycle	Temperature	Time
1	94°C	4 min
25	94°C	30 sec
	60°C	30 sec
	72°C	30 sec
1	72°C	10 min

To identify the expression of O-glycan synthesis genes in the epididymis, PCR was performed on four types of initiating enzymes in the synthesis of O-glycans, including N-acetylgalactosaminyltransferases (Galt), N-acetylgalactosaminyltransferases-like (Galtl), protein O-fucosyltransferases (Pofut) and protein O-mannosyltransferases (Pomt), using 21 pairs of primers (Table 8). Selected primers were designed via the "Primer-BLAST" tool at http://www.ncbi.nlm.nih.gov/tools/primer-blast/. All applied primers were purchased from Life Technologies (Invitrogen).

Table 8. List of PCR primers. Primers that were used in PCR to investigate the expression of the initiating enzymes in the biosynthesis of O-glycans. Williams-Beuren syndrome chromosome region 17 (*Wbscr17*) gene is also known by other names: *Galnt16*, *Galnt20*, *Galntl3*, *GalNAcT17*, and *GalNAc-T5L*.

Gene	Primer Sequences (5′→ 3′)	PubMed Accession No.	Product length (bp)
Galnt1	F: GACTCGCCGAGGCTTTACTC R: AGTCATAGCCCCAAAGTGGC	NM_013814.3	112
Galntl1	F: TCGACGTCATCAGCTTGGAC R: GGTTTAGTGGGGTCAGTCCG	NM_001081421.1	139
Galnt2	F: ACTTCGCGGATGGAGTTGTT R: CGAACGGTCCACCACAGTAA	NM_139272.2	125
Galntl2	F: TGGCCGTGGACAGACATTAC R: ACTCGAGAGCAGGGAAGGAT	NM_030166.3	139
Galnt3	F: CCGAGACGCTCACGTTCTTA R: CTCACCACGGCAGTGTAGTT	NM_015736.2	100
Galnt4	F: ACCCTACGGGGGCTAATCTT R: CCGTCTTTGGGGCAGTTTTG	NM_015737.4	169
Galntl4	F: ATGCCCACGTGGAGTTCAAT R: TTTAGGTAGCGGCACCACAG	NM_173739.3	178
Galnt5	F: CCAGTCATGGCAGGTGGATT R: CCACTCTGGAACAGGGGATG	NM_172855.3	163

Galntl5	F: TACTGCGAGTGGTTCACGTC R: CCTTAATTCCACGCGCTCAC	NM_026449.3	113
Galnt6	F: CGTCGGGAAACCCACGAG R: CTCTCTGGATCCAATCCGG	NM_001161767.1	139
Galnt7	F: CTTGATGCCCACTGTGAGG R: ACCACCCCCTTGGGGTATAA	NM_144731.4	141
Galnt10	F: TTTCCCCAGCGTGAGGATTC R: ACACGATGGTCTTCCGGTTC	NM_134189.2	182
Galnt11	F: CCTGGAGCGCCGCTATC R: CAGAACTGTCCAGGTAGCAGA	NM_144908.3	143
Galnt12	F: CTACTACCACCGCAATCCCC R: CTCTGGCACGTGCAATTCTG	NM_172693.3	139
Galnt13	F: TATCCGGACTCCCAGATCCC R: ATCCAGGCACAAGTCGTCAG	NM_173030.2	198
Galnt14	F: TTCCGAGTGTGGATGTGTGG R: AAAAGGCCGAGCTGCATAGT	NM_027864.2	189
Wbscr17	F: CTTCGTGAATGAGGCCCTGT R: GGGTAGCGTTTGTGGACGTA	NM_145218.3	159
Pofut1	F: ATTTGCGAAGCTGCTGAACC R: GGAGGGTGCCAGATTTTCCA	NM_080463.3	178
Pofut2	F: GTCGCGCCTGTCCTCTTAAA R: TGCTGGCTCCTAAACTCGTC	NM_030262.3	167
Pomt1	F: TGACTGGCCTGGGACTACTT R: AAATGGTGGCCCACTGTCAT	NM_145145.1	140
Pomt2	F: TGCTCACATCTGTTGGGATGA R: GCTGTGGTGCTCGTATCTGT	NM_153415.3	184

1.25% agarose gel was made in Tris-acetate- EDTA (TAE) buffer supplemented with 2-4 drops (based on the size of gel) of 0.5% ethidium bromide solution (as a fluorescent tag for DNA staining). Amplified PCR products mixed with a loading buffer were loaded into wells of agarose gel and separated using an electrophoresis system at 100 V for 30 min. Finally, separated PCR products were visualized under UV light and photographed using a gel documentation system.

TAE buffer
40 mM Tris-acetate
1 mM EDTA (pH 8)

Loading buffer (6x)
0.25% (w/v) Bromophenol blue
30% Glycerol

2.2.20 Statistical analysis

HPLC data were analyzed by utilizing two tailed-paired Student *t*-test. P-values ≤ 0.05 were considered statistically significant. All indicated values are means ± S.E. from at least three independent experiments. The sample size was estimated using a post hoc G*Power analysis.

3 RESULTS

3.1 Premature acrosome reaction in the mouse epididymitis model

In order to elucidate if the UPEC-induced acrosome reaction leads to an activation of endogenous sialidases initiating a subsequent desialylation of spermatozoa, the established mouse epididymitis model was utilized [126]. Lectin fluorescence staining of frozen cauda sections from mouse epididymides by FITC-PNA, a lectin with affinity to Gal-β(1-3)-GalNAc. FITC-PNA is commonly used to detect the acrosome in sperm. Staining revealed that a substantial number of spermatozoa have prematurely lost their acrosomes in the epididymitis mouse model three days post UPEC infection compared to untreated and PBS sham controls (Figure 12). Premature acrosome reaction in the majority of spermatozoa in the lumen of the epididymis following UPEC infection (Figure 12) is in accordance with previous findings [24]. In contrast, in untreated and sham controls, the acrosomes were intact in most spermatozoa.

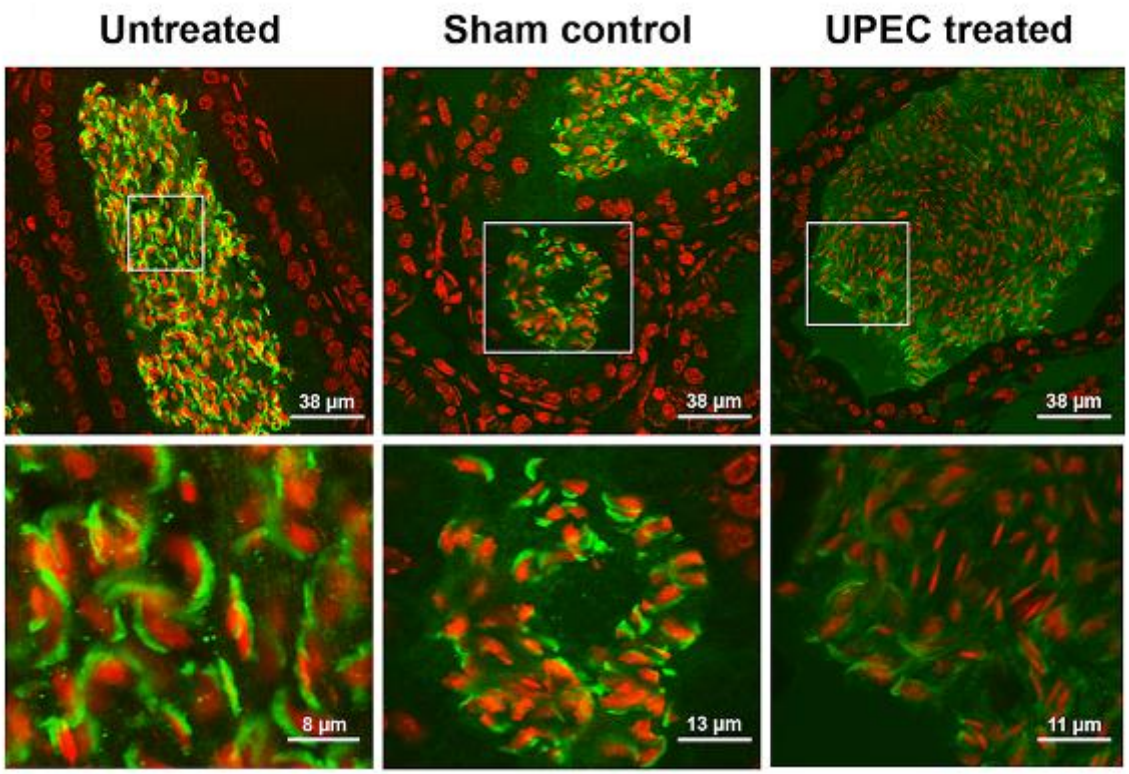

Figure 12. UPEC-caused premature acrosome reaction in epididymal spermatozoa. Acrosomes were stained with PNA-FITC lectin (green) and nuclei were counterstained using TO-PRO-3 (red) in cauda epididymides from mice 3 days post-UPEC treatment, PBS sham controls, and untreated controls. Inserts in the first row were magnified digitally and are shown in the second row [28]. (Copyright © 2016, by the American Society for Biochemistry and Molecular Biology)

3.2 Presence of both α2,3- and α2,6-linked sialic acids in epididymal sperm and epithelial cells

To gain a first insight into the sialylation status of epididymal spermatozoa and epithelial cells, α2,3- and α2,6-linked sialic acid residues were visualized on epididymal sections using FITC-conjugated MAA (Figure 13) and SNA (Figure 14) lectins, respectively. As control, sections were labeled after *in vitro* sialidase treatment. A reduced fluorescence signal in sialidase treated sections confirmed the specific occurrence of Neu5Ac residues in both types of α2,3- and α2,6-linked sialic acids in caudal spermatozoa, epithelial cells, and epididymal fluid.

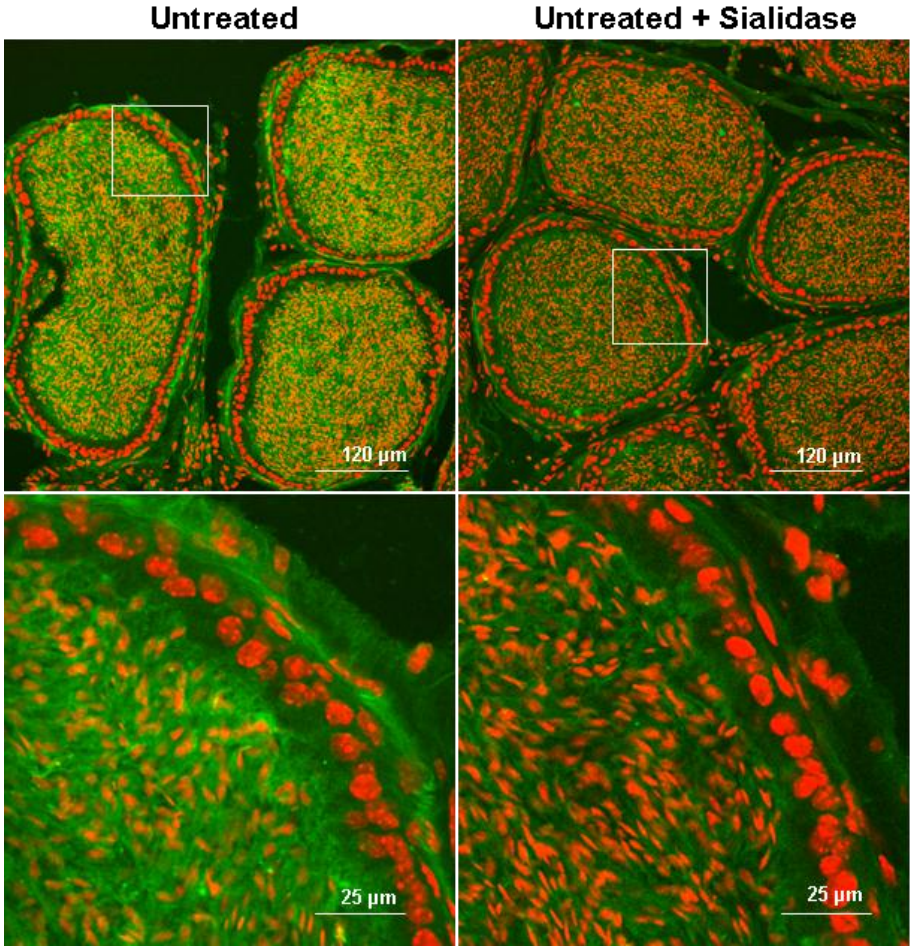

Figure 13. **Presence of α2,3-linked sialic acid residues in caudal spermatozoa and epididymal epithelial cells.** α 2,3-linked sialic acid residues were visualized by MAA-FITC lectin (green) in sections from the epididymis of control mouse prior and following *in vitro* sialidase treatment. Nuclei were counterstained with TO-PRO-3 (red). In contrast to untreated control, sialidase-treated sections showed a weaker and diffused signal of sialic acid labeling in spermatozoa, epithelial cells, and luminal fluid. Images in the lower row were magnified digitally from the frames in the upper row.

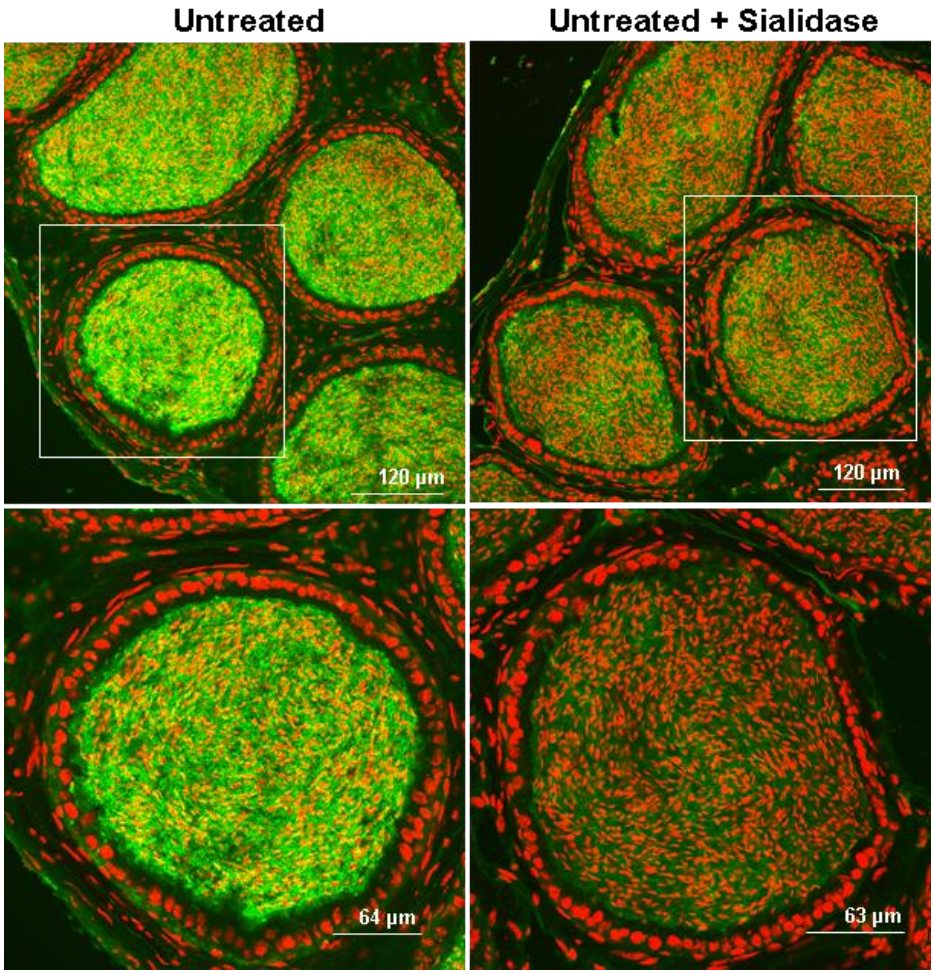

Figure 14. Presence of α2,6-linked sialic acid residues in caudal spermatozoa and epithelial cells. α 2,6-linked sialic acid residues were visualized by SNA-FITC lectin (green) in sections from the epididymis of control mouse (untreated) prior and following *in vitro* sialidase treatment (untreated + sialidase). Nuclei were counterstained with TO-PRO-3 (red). In contrast to untreated, sialidase-treated sections showed a weaker and diffused signal of sialic acid labeling in spermatozoa and luminal fluid. Images in the lower row were magnified digitally.

To confirm the presence of sialic acids in epithelial cells of the epididymis, a mouse epididymis proximal caput (MEPC5) cell line was stained with SNA and MAA (Figure 15). Consistent with the observed affinity of epididymis sections to sialic acid-specific lectins (Figures 13 and 14), MEPC5 cell staining also demonstrated the substantial presence of both α2,3- and α2,6-linked sialic acid residues (Figure 15).

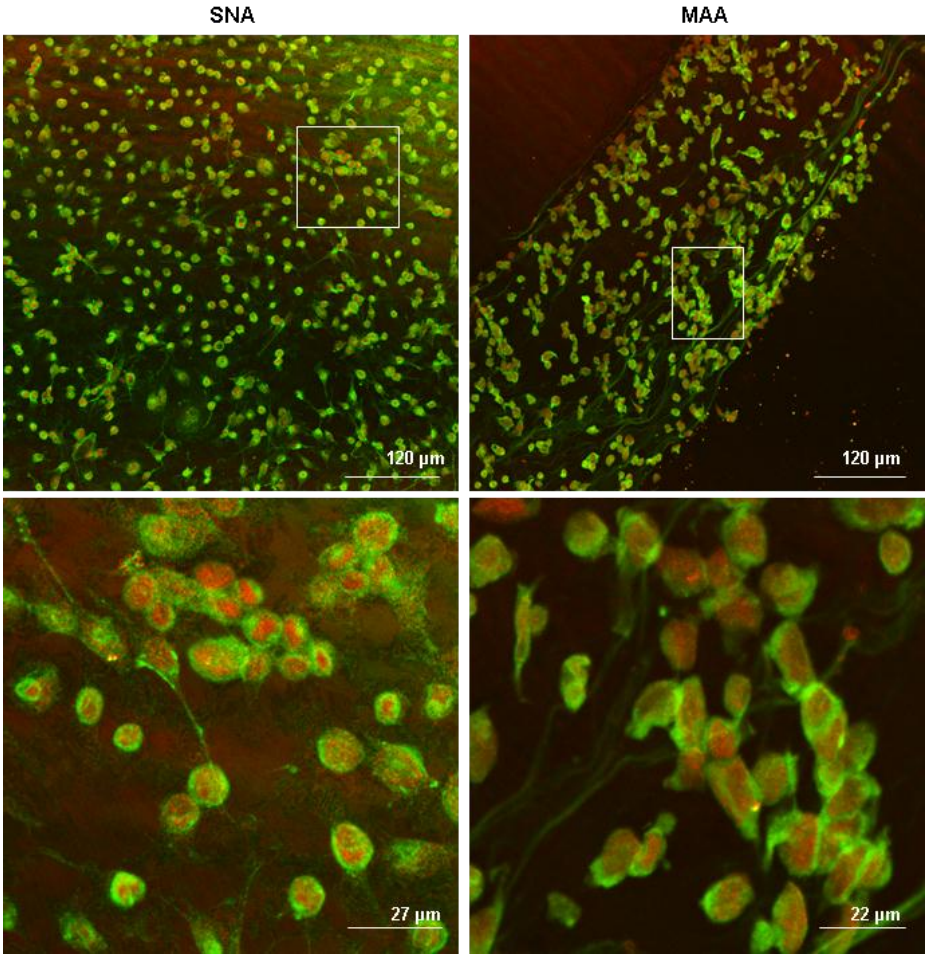

Figure 15. Association of both α2,3- and α2,6-linked sialic acid residues with epidydimal epithelial cells. The cells of the MEPC5 cell line from mouse proximal caput were acetone fixed. Then α2,6- and α2,3-linked sialic acids were visualized using SNA and MAA lectins, respectively (green). Nuclei were counterstained with TO-PRO-3 (red). Images were acquired using a confocal microscope and frames in the upper row were magnified in the lower row digitally.

3.3 Redecoration of α2,6-linked sialic acids of sperm in the mouse epididymitis model

To elucidate the status of α2,6-linked sialylation after UPEC infection, FITC-conjugated SNA lectin was employed on epididymal sections (Figure 16). Fluorescence microscopy revealed a diffusely distributed and weaker SNA labeling in spermatozoa of UPEC infected mice, whilst in untreated and sham controls prominent staining of α2,6-linked sialic acid residues was evident in the acrosome and sperm tail (Figure 16). The reduced SNA staining in UPEC treated mice suggested that Neu5Ac residues were cleaved during infection.

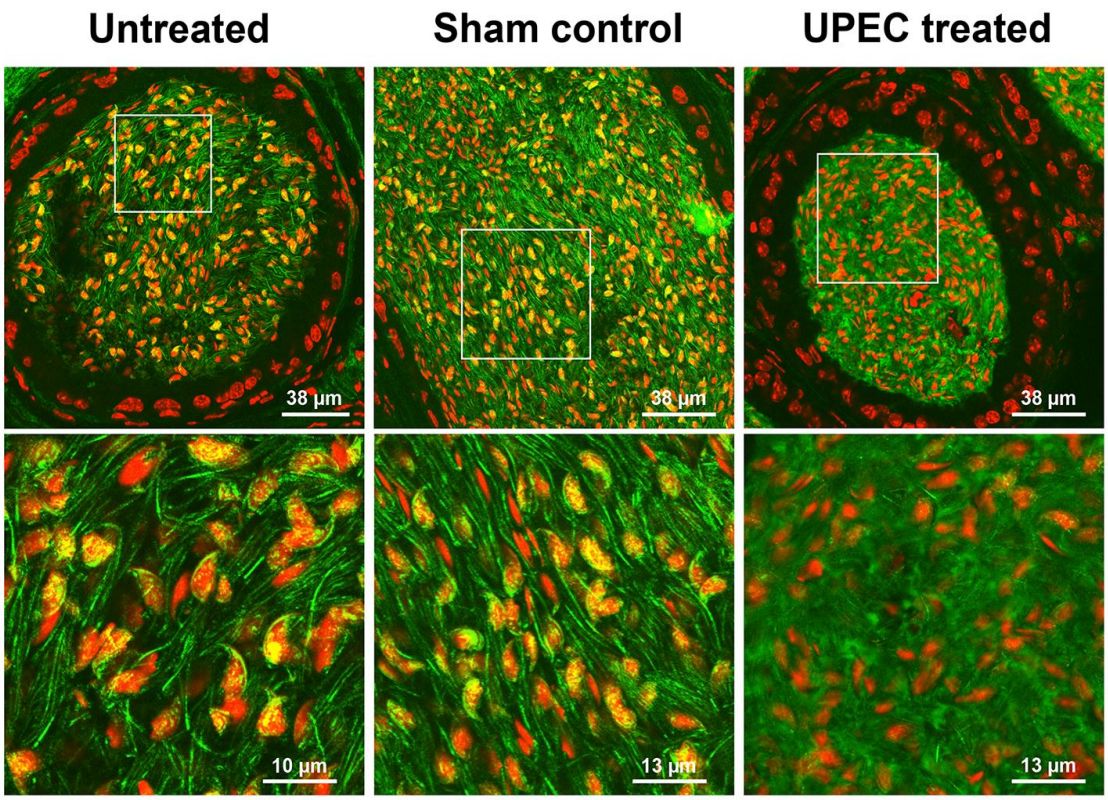

Figure 16. Decreased content of α2,6-linked sialic acid in caudal spermatozoa after UPEC epididymitis. α2,6-linked sialic acid residues were visualized by SNA-FITC lectin (green) and nuclei were counterstained with TO-PRO-3 (red) in sections from the mouse epididymis 3 days post UPEC infection, PBS sham control and untreated control. In contrast to untreated and sham controls, in UPEC infection a more diffuse sialic acid labeling is evident. Images in the lower row were magnified digitally from the frames seen in the upper row [28]. (Copyright © 2016, by the American Society for Biochemistry and Molecular Biology)

3.4 No evident alterations in α2,3-linked sialic acids of sperm in the mouse epididymitis model

SNA prevalently binds α2,6-linked sialic acid residues. However, α2,3-linked sialic acid residues may also be detected by this lectin, although to a lesser degree. Therefore, to clarify the status of α2,3-linked sialic acids in sperm and epithelial cells, cauda epididymal sections from 3 days UPEC treated, untreated and sham control mice were stained using FITC-conjugated MAA lectin. Unlike α2,6-linked sialic acids (Figure 16), the presence of α2,3-linked sialic acids in sperm and epithelial cells failed to be altered substantially after UPEC infection (Figure 17).

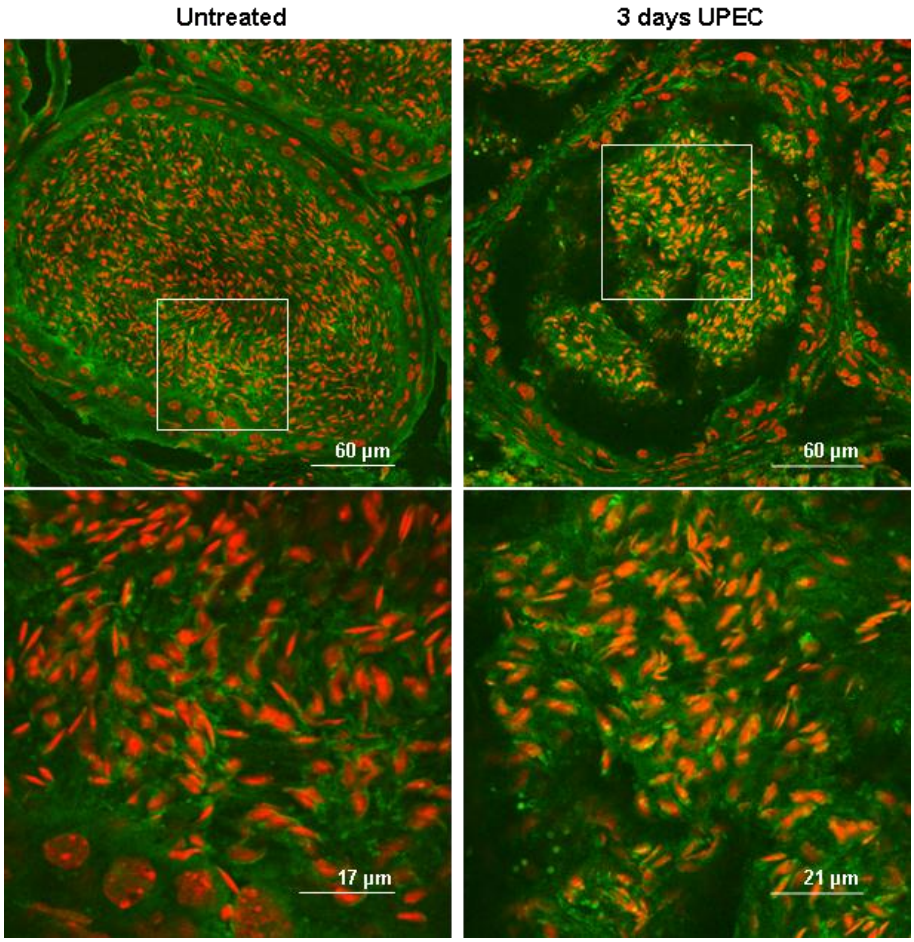

Figure 17. Unchanged presence of α2,3-linked sialic acids in caudal spermatozoa after UPEC epididymitis. α2,3-linked sialic acid residues were visualized by MAA-FITC lectin (green) and nuclei were counterstained with TO-PRO-3 (red) in sections from the mouse epididymis 3 days post UPEC infection and from untreated control. Untreated and UPEC infection staining showed a similar pattern of α2,3-linked sialic acid labeling and no evident differences in fluorescence signal were observed. Images in the lower row were magnified digitally from the frames above.

3.5 Reduction of sialic acid content in epididymal sperm in the mouse epididymitis model

Since qualitative as well as quantitative lectin analysis of sialic acids are often misleading and SNA lectin visualizes only a fraction of sialic acid residues on glycoconjugates, a recently developed combination of LCMD and DMB-HPLC-ESI-MS analysis was applied (Figure 18) [127]. Starting from murine paraffin embedded tissue samples, epididymal spermatozoa were isolated via LCMD after nuclear staining using Mayer's hematoxylin (Figure 18A, B). Thereafter, sialic acids were released under acidic conditions, fluorescently labeled and subjected to a HPLC-ESI-MS system. The obtained chromatograms showed smaller peaks of DMB-labeled Neu5Ac in infected material (Figure 18C). The respective DMB-Neu5Ac mass

at m/z 448 $[M + Na]^+$ in the ESI-MS spectrum verified the presence of DMB-Neu5Ac during the corresponding retention time of a DMB-Neu5Ac standard (Figure 18C). Calculation of corresponding peak areas demonstrated a significant reduction of Neu5Ac (~ 19%) in spermatozoa in UPEC epididymitis (Figure 18D).

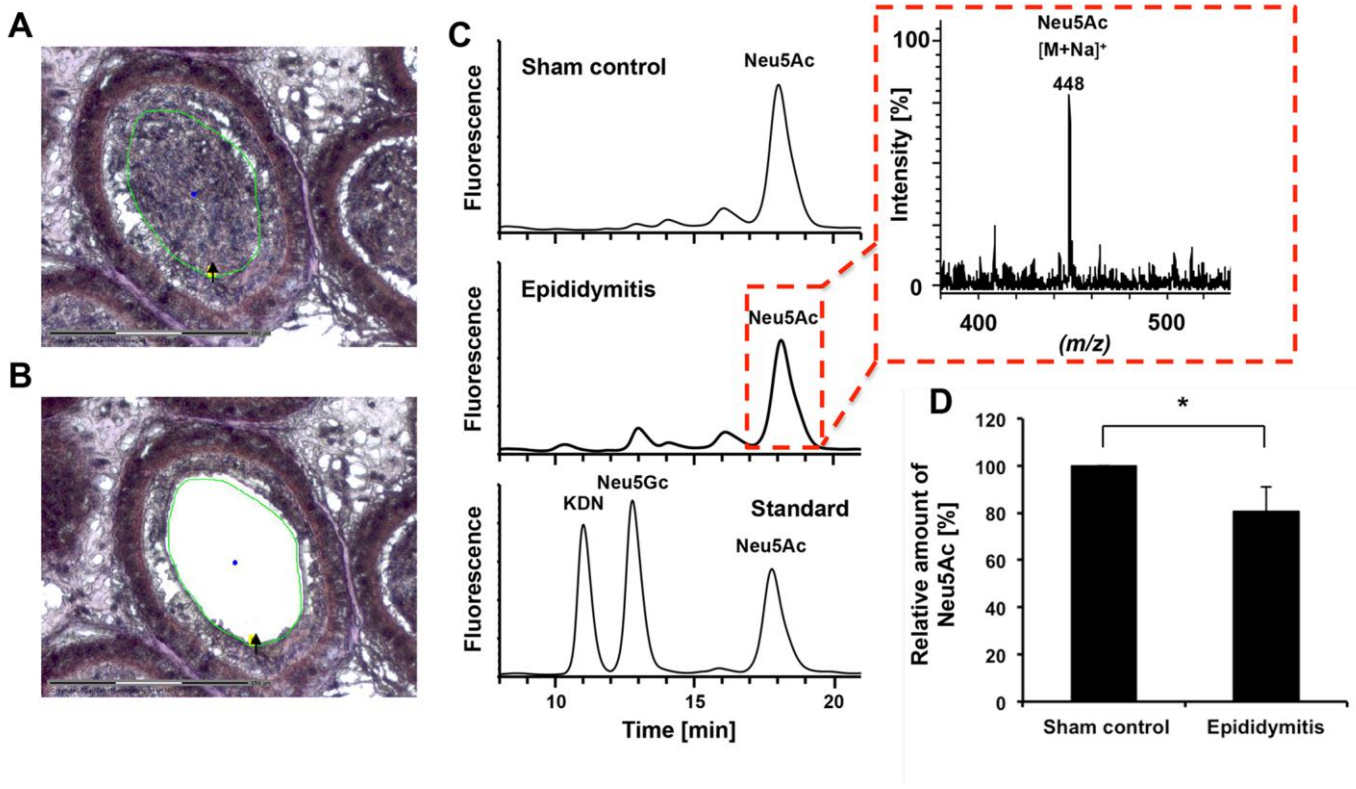

Figure 18. Desialylation of epididymal spermatozoa following UPEC infection. (**A**) Spermatozoa from the epididymal lumen were isolated by laser microdissection from hematoxylin stained paraffin embedded tissue sections. Excised area is indicated by the black arrow and green circle. Scale bar = 150 µm. (**B**) Same section after excision of luminal content. (**C**) Obtained spermatozoa were subsequently used for sialic acid quantification. After hydrolysis and fluorescent labeling, DMB-sialic acid residues were separated using RP-HPLC. A set of sialic acid standards was used for the generation of a calibration line and to control the retention times. ESI-MS spectra were recorded during the HPLC runs to verify the presence of different sialic acid species as shown exemplary for Neu5Ac in UPEC treated and PBS sham control epididymides. (**D**) The amounts of Neu5Ac and the respective standard deviations (S.D.) were calculated from four epididymides obtained from PBS sham control and UPEC injected mice, respectively (n= 4 animals). Given mean values were set to 100% for sham control. The statistical evaluation was performed using Student's *t*-test (unequal variances, two tailed). Significance levels are classified as follows *****, $p \leq 0.05$. KDN= 2-keto-3-deoxynononic acid, Neu5Ac=*N*-acetylneuraminic acid, Neu5Gc=*N*-glycolylneuraminic acid [28].

3.6 Sialic acid loss in epididymal epithelial cells in the mouse epididymitis model

Release of sialic acids from the spermatozoa to the luminal fluid following UPEC infection could be enzymatically mediated by soluble sialidases, a hypothesis supported by an

observation of Ma et al. [16], who described that the sialidases NEU1 and NEU3 are released from the cell surface of spermatozoa after proteolytic activation. Consequently, soluble neuraminidases would be also able to affect the cell surface of surrounding cells. To test this hypothesis, the sialylation status of epididymal epithelial cells − whose apical surface borders to the luminal fluid − was analyzed using the above mentioned combined LCMD/DMB-HPLC-ESI-MS strategy (Figure 19). In support, epididymal epithelial cells showed a reduction of sialic acid residues (~ 49%) 3 days post infection with UPEC compared to sham (Figure 19C, D). Reduction of Neu5Ac from epithelial cells is substantially stronger in comparison to spermatozoa (Figure 18).

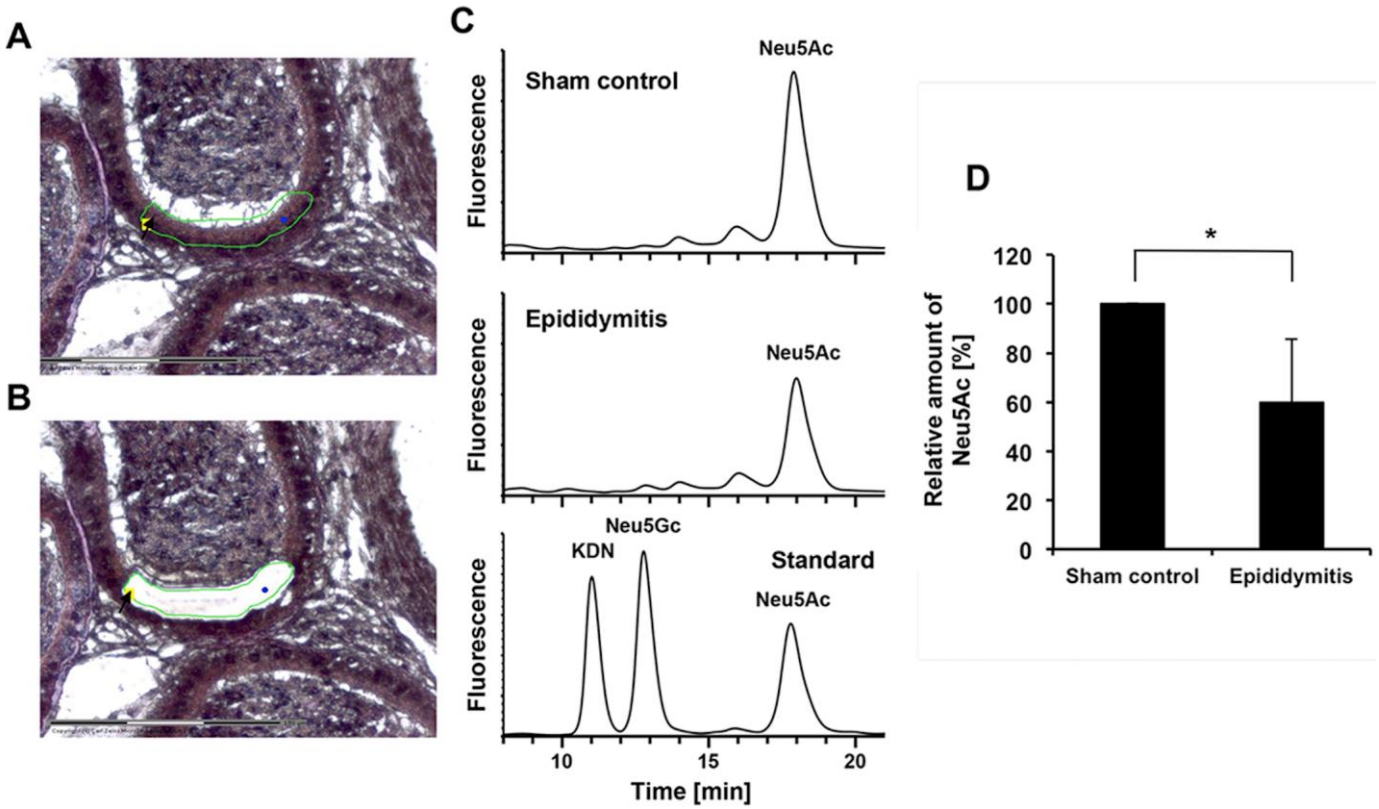

Figure 19. Reduction of sialic acid content in epithelial cells in UPEC epididymitis. (**A**) Epithelial cells were isolated from paraffin embedded mouse epididymis by laser microdissection. Excised area is indicated by the black arrow and green line. (**B**) Same section after excision of epithelium. Scale bar = 150 µm. (**C**) DMB-labeled sialic acid residues of the isolated cells were separated using RP-HPLC. A set of sialic acid standards was used for quantification and to control the retention times. ESI-MS spectrum was recorded during the HPLC runs (data not shown). (**D**) The amounts of Neu5Ac and the respective S.D. of 5 different controls and infected mice (one epididymis from five animals each). Given mean values were set to 100% for sham control. Significance levels are classified as follows *****, $p \leq 0.05$. KDN= 2-keto-3-deoxynononic acid, Neu5Ac=*N*-acetylneuraminic acid, Neu5Gc=*N*-glycolylneuraminic acid [28]. (Copyright © 2016, by the American Society for Biochemistry and Molecular Biology)

Thus, the obtained results demonstrate that the sialylation status of epididymal spermatozoa in the lumen as well as that of the lumen lining epithelial cells decrease in the epididymis after bacterial infection.

3.7 Presence of KDO in UPEC

Whereas in UPEC treated samples a peak for DMB-Neu5Gc was apparent in the HPLC-chromatogram, in sham control hardly any signal was detectable. However, no mass corresponding to DMB-Neu5Gc was obtained by ESI-MS in untreated as well as infected mice (data not shown). Due to the fact that DMB reacts with all α-keto acids, possible contamination in infected mice by α-keto acids originating from the pathogen was examined by separate analysis of bacteria only. In UPEC, the presence of DMB-labeled 3-Deoxy-D-manno-oct-2-ulosonic acid (KDO) − a well-known bacterial α-keto acid [77] − was measurable as a prominent peak at the retention time of DMB-Neu5Gc (Figure 20). In addition, KDO-related monoisotopic pseudomolecular masses of DMB-KDO at *m/z* 337 ($[M + H]^+ - H_2O$), 355 ($[M + H]^+$), and 377 ($[M + Na]^+$) were monitored in the ESI-MS spectrum at this particular time. Thus, in UPEC treated mice bacterial KDO was obviously recorded at the retention time of DMB-Neu5Gc (Figure 20).

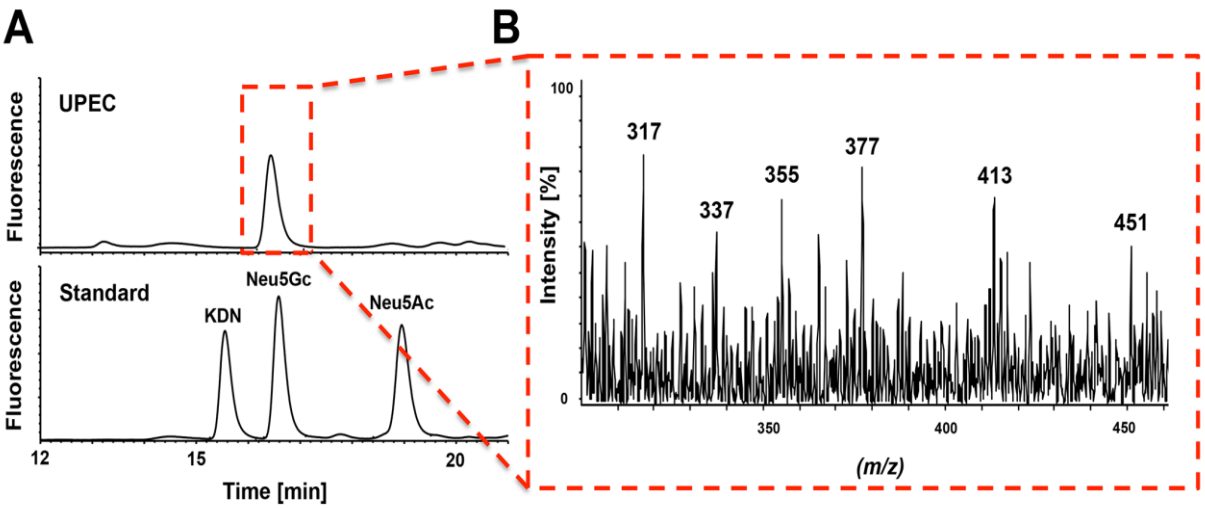

Figure 20. Analysis of α-keto acids in UPEC. (**A**) Sialic acid standards and UPEC samples were hydrolyzed and α-keto acids were fluorescently labeled with DMB for HPLC separation. (**B**) ESI-MS spectrum recorded during the elution time of the peak is highlighted by the red dotted frame. KDN= 2-keto-3-deoxynononic acid [28]. (Copyright © 2016, by the American Society for Biochemistry and Molecular Biology)

3.8 Hyposialylation of spermatozoa after chemical induction of acrosome reaction

To investigate the correlation of the acrosome reaction, a process which untimely occurs in epididymitis, with sperm hyposialylation, acrosomal exocytosis in human sperm was artificially induced using a calcium ionophore chemical (A23187). The obtained HPLC chromatograms showed an attenuated fluorescence intensity of DMB-labeled Neu5Ac in ionophore treated spermatozoa compared to untreated controls (Figure 21A), indicating a significant reduction in sperm sialic acids after induction of the acrosome reaction (Figure 21B).

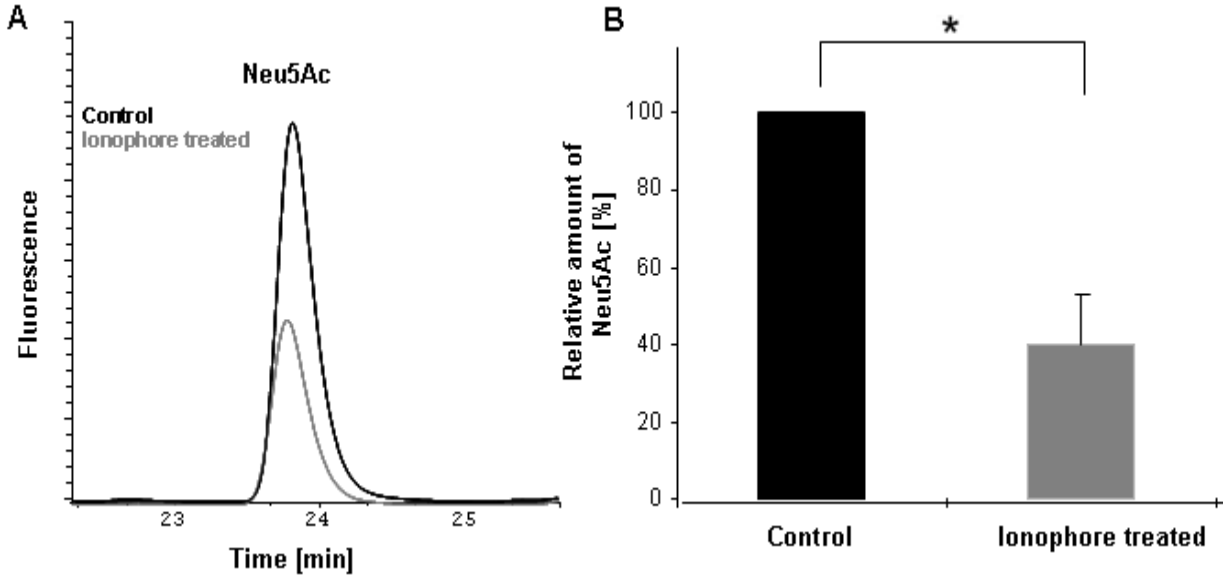

Figure 21. Reduced amounts of sialic acids after acrosome reaction in human sperm. Human spermatozoa from swim-up ejaculates of healthy individuals were acrosomally reacted using the ionophore A23187. **(A**) After hydrolysis and fluorescence labeling, DMB-sialic acid residues were isolated by RP-HPLC. **(B)** The amount of Neu5Ac was compared between untreated and ionophore-treated portions. Given mean values were set to 100% for untreated control sperm. The statistical evaluation was performed using Student's *t*-test (unequal variances, two tailed). *, $p \leq 0.05$; n=3.

3.9 Premature acrosome reaction in human sperm caused by UPEC infection

In order to investigate if UPEC can also induce hyposialylation in human spermatozoa, motile spermatozoa of healthy donors collected after swim-up were subsequently infected with UPEC. PSA-FITC lectin staining detected a substantially higher number of completely or partially acrosome reacted spermatozoa in UPEC treated spermatozoa (Figure 22).

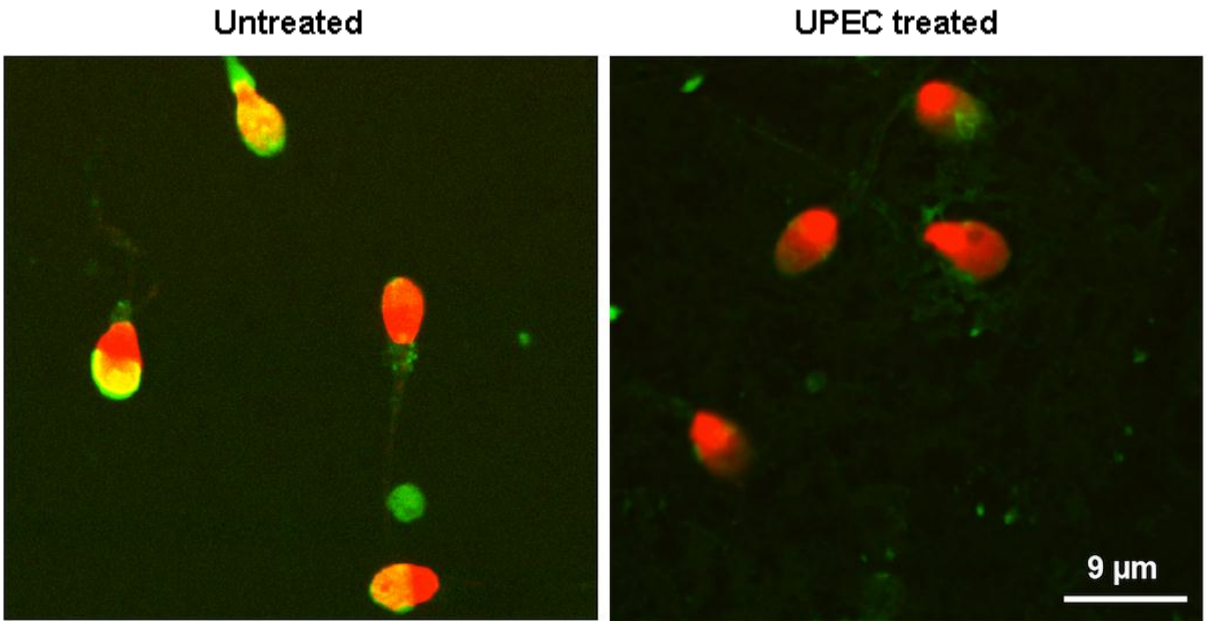

Figure 22. Increased acrosome reaction in human spermatozoa after UPEC infection *in vitro*. Following swim-up, spermatozoa were incubated with UPEC. The acrosomes were labeled by PSA-FITC lectin (green) and nuclei were counterstained with TO-PRO-3 (red). Presence of the acrosome was compared to untreated control [28]. (Copyright © 2016 by the American Society for Biochemistry and Molecular Biology)

3.10 Sperm desialylation as a consequence of UPEC infection

In order to investigate if UPEC can also induce hyposialylation in human spermatozoa, motile spermatozoa of healthy donors collected after swim-up were subsequently infected with UPEC for 3 h, and the sialylation status was quantified by HPLC (Figure 23). DMB-HPLC analysis demonstrated a significant reduction in the amount of Neu5Ac following UPEC infection compared to untreated control. As a positive control, neuraminidase was added for 3 h. Accordingly, hyposialylation of sperm (both in presence and absence of UPEC) after incubation with neuraminidase increased substantially compared to controls devoid of neuraminidase (Figure 23).

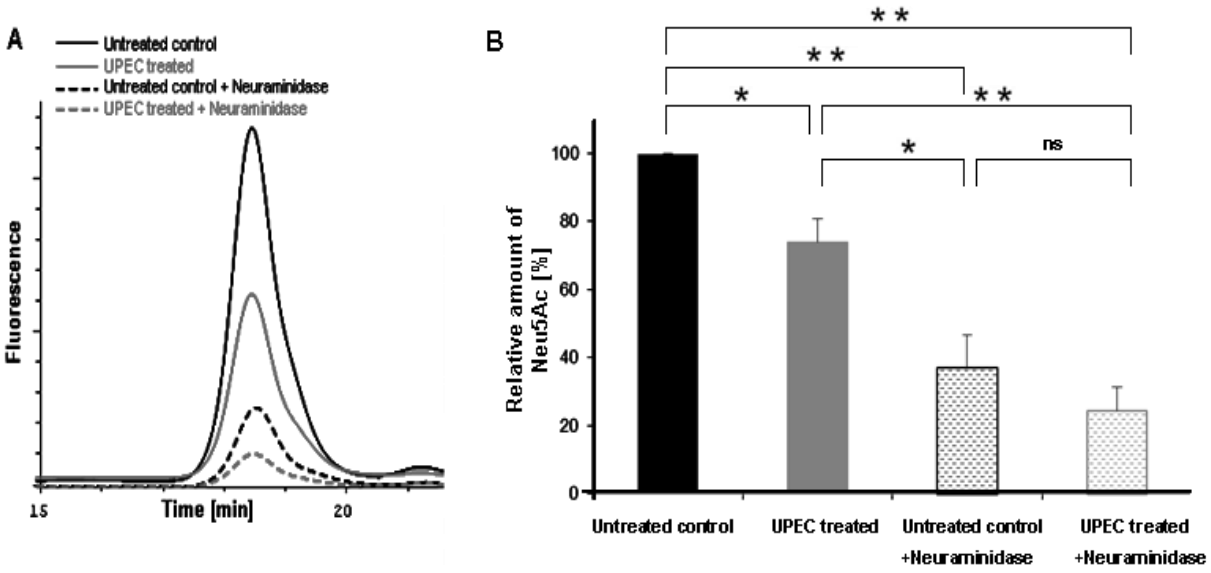

Figure 23. **Decreased content of human sperm sialic acid after UPEC treatment.** Human spermatozoa from swim-up ejaculates of healthy donors were treated with UPEC for 3 h *in vitro* and then for 3 h with neuraminidase. (**A**) After hydrolysis and fluorescence labeling DMB-sialic acid residues were isolated by RP-HPLC. (**B**) The amount of Neu5Ac was compared between untreated and UPEC and/or neuraminidase-treated portions. Given mean values were set to 100% for untreated control. The statistical evaluation was performed using Student's t-test (unequal variances, two tailed). Significance levels are classified as follows: *, $p \leq 0.05$, **, $p \leq 0.01$, ns, not significant (n:3).

3.11 Counteracting of sperm *in vitro* desialylation with sialidase inhibitors

To examine if the investigated hyposialylation of spermatozoa is mostly the consequence of a general loss of glycoconjugates (e.g. due to the degradation of the glycoprotein backbone) or alternatively the activation of neuraminidases during the acrosome reaction, motile human spermatozoa were treated with UPEC in the presence of the sialidase inhibitor DANA (Figure 24). Here, co-incubation of DANA with UPEC prevented hyposialylation of human spermatozoa completely (Figure 24). Consequently, the decreased sialylation values are based on the enzymatic activity of released endogenous sialidases. A bacterial sialidase activity could be excluded by *in silico* analysis of the UPEC genome.

Consequently, the decreased sialylation status in infected spermatozoa is likely based on the enzymatic activity of released sialidases.

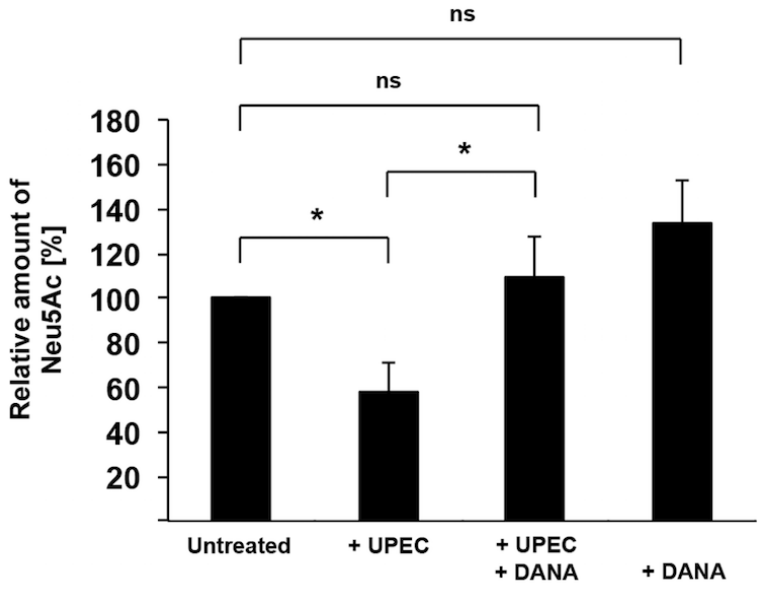

Figure 24. Counteraction of UPEC dependent desialylation of human spermatozoa by a sialidase inhibitor *in vitro*. Spermatozoa from healthy donors prepared by swim-up were incubated with UPEC for 3 hours and the amount of Neu5Ac was compared with untreated samples using the DMB-HPLC approach as shown in figure 18. In parallel, UPEC treated as well as untreated spermatozoa were co-incubated with the sialidase inhibitor DANA. Given mean values were set to 100% for untreated controls. Significance levels are classified as follows: *, $p \leq 0.05$; ns, not significant. n=3.

3.12 Acrosome malformation in epididymitis patients

In addition, semen samples of patients suffering *E. coli* epididymitis were included in our study. For this purpose, spermatozoa were obtained by swim-up from ejaculates of men 14 days after diagnosis and treatment of *E. coli* based unilateral epididymitis. The analyzed samples showed malformation (in sperm head), and the acrosomes are mainly reacted (partially or completely, visualized by PSA-FITC staining) in epididymitis patients compared to intact acrosomes of healthy controls (Figure 25).

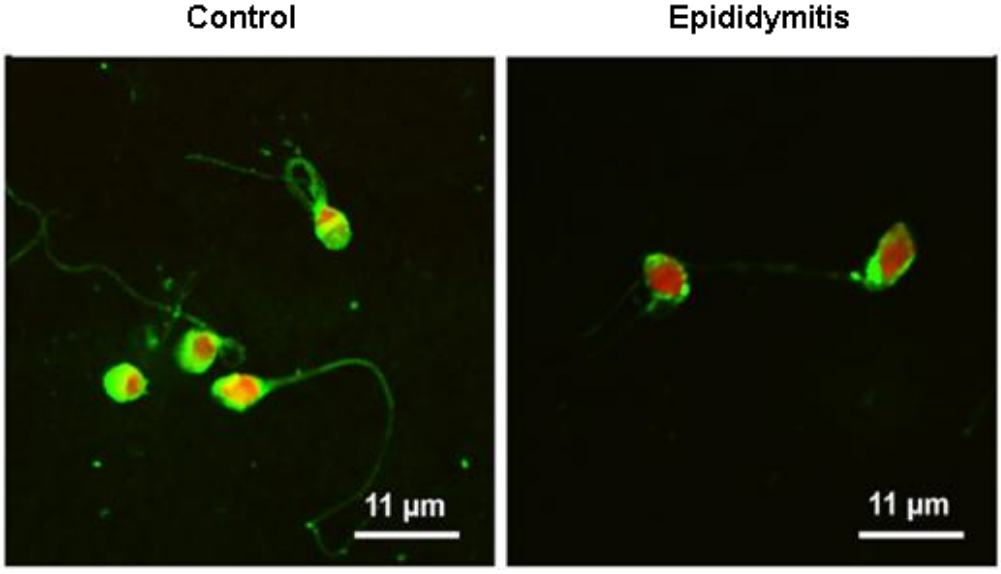

Figure 25. Impaired acrosome integrity in spermatozoa of epididymitis patients. Acrosomes of swim-up spermatozoa obtained from healthy men (control) and patients 14 days after diagnosis and treatment of acute epididymitis were visualized by PSA-FITC lectin (green). Nuclei were counterstained with TO-PRO-3 (red) [28]. (Copyright © 2016 by the American Society for Biochemistry and Molecular Biology)

3.13 Hyposialylation in sperm of men with a recent history of epididymitis

Patients suffering *E. coli* epididymitis showed much lower levels of Neu5Ac (~ 75% reduction) than healthy control spermatozoa (Figure 26). Thus, in agreement with the determined loss of sialic acid residues in the mouse epididymitis model and in the *in vitro* experiments, spermatozoa of epididymitis patients are also hyposialylated.

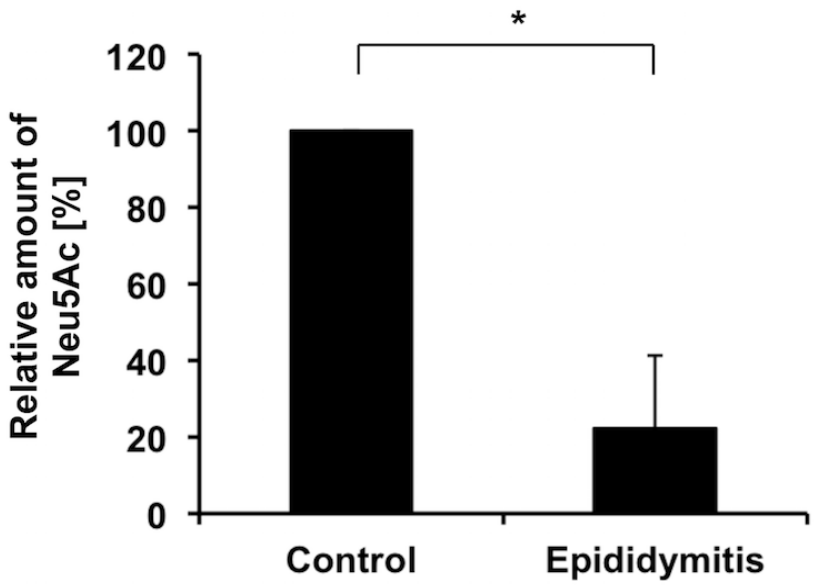

Figure 26. Reduced levels of Neu5Ac in patients with a history of acute epididymitis. Sialic acid residues of isolated spermatozoa from these patient groups (n=3) were released and fluorescently labeled with DMB for quantification. The statistical evaluation was performed using Student's t-test (unequal variances, two tailed). Given mean values were set to 100% for all sham controls. Significance levels are classified as follows: *, $p \leq 0.05$; ns, not significant [28]. (Copyright © 2016 by the American Society for Biochemistry and Molecular Biology)

3.14 Contribution of sialylated N-glycans to the sperm glycocalyx

To identify the presence of sialic acids in the structure of sperm N-glycans, N-glycans were isolated from human sperm glycoproteins, fluorescently labeled with 2-AB, and separated with HPLC. In parallel, N-glycan isolation and 2-AB labeling efficiency were controlled using standard glycoproteins (e.g. fetuin) (Figure 27).

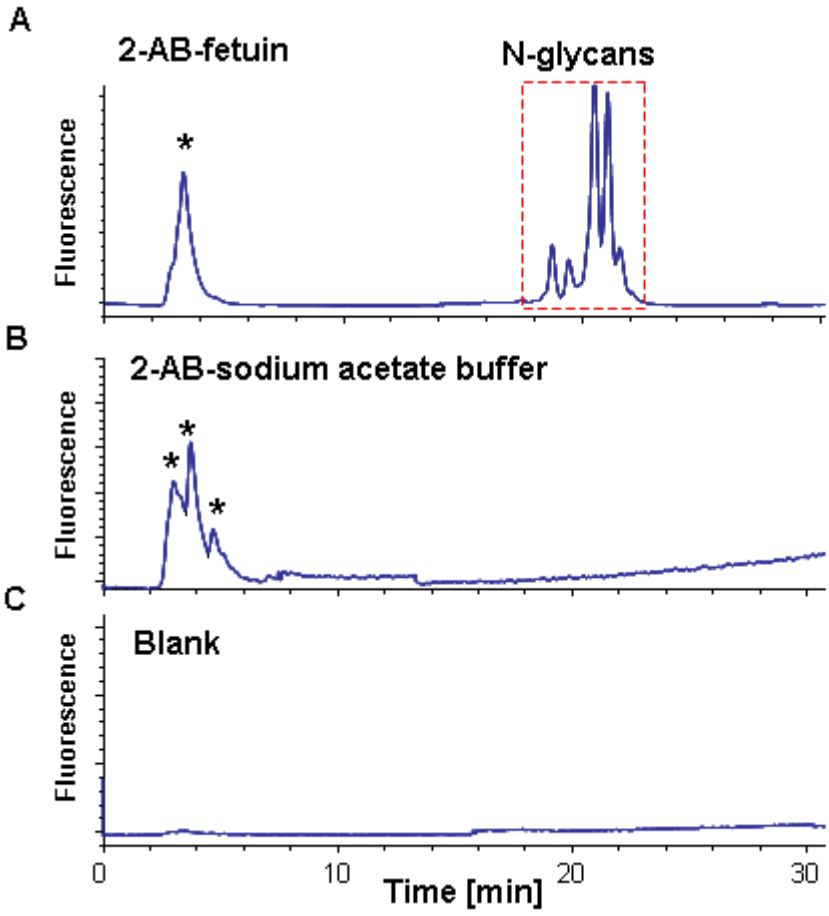

Figure 27. Establishment of a HPLC method for N-glycan profiling. To analyze N-glycans, samples were digested, hydrolyzed, conjugated with 2-AB and injected to HPLC. For this purpose, (**A**) fetuin as a standard glycoprotein (carrying N-glycans) was used as a positive control of the system. The red dotted box demonstrates different N-glycan structures of fetuin. (**B**) To exclude 2-AB-related peaks from fractions containing N-glycan, 2-AB was added to sodium acetate buffer and then injected to HPLC. (**C**) To control the purity of HPLC, a blank run was applied. (*) indicates chemical peaks, including unbound 2-AB, which was eluted in the beginning and excluded from N-glycan analysis.

To separate N-glycans of human spermatozoa, 2-AB-labeled samples were applied to the HPLC system (Figure 28A). The putative contribution of sialic acid to the N-glycan compositions of each HPLC fraction was investigated using sialidase treatment of the

collected fraction. After enzymatic desialylation, these fractions were reinjected to HPLC, resulting in detection of 2-3 digested peaks with lower intensities (Figure 28C) from each sialylated N-glycan fraction (Figure 28A). Thus, the presence of several sialic acids in the structure of corresponding N-glycans could be inferred. In contrast to sialylated N-glycans, spermatozoa also contained neutral N-glycans (Figure 28A) including non-sialylated structures. Their corresponding chromatograms after the sialidase incubation and reinjection remained consistent in retention time, number, and intensity (Figure 28B).

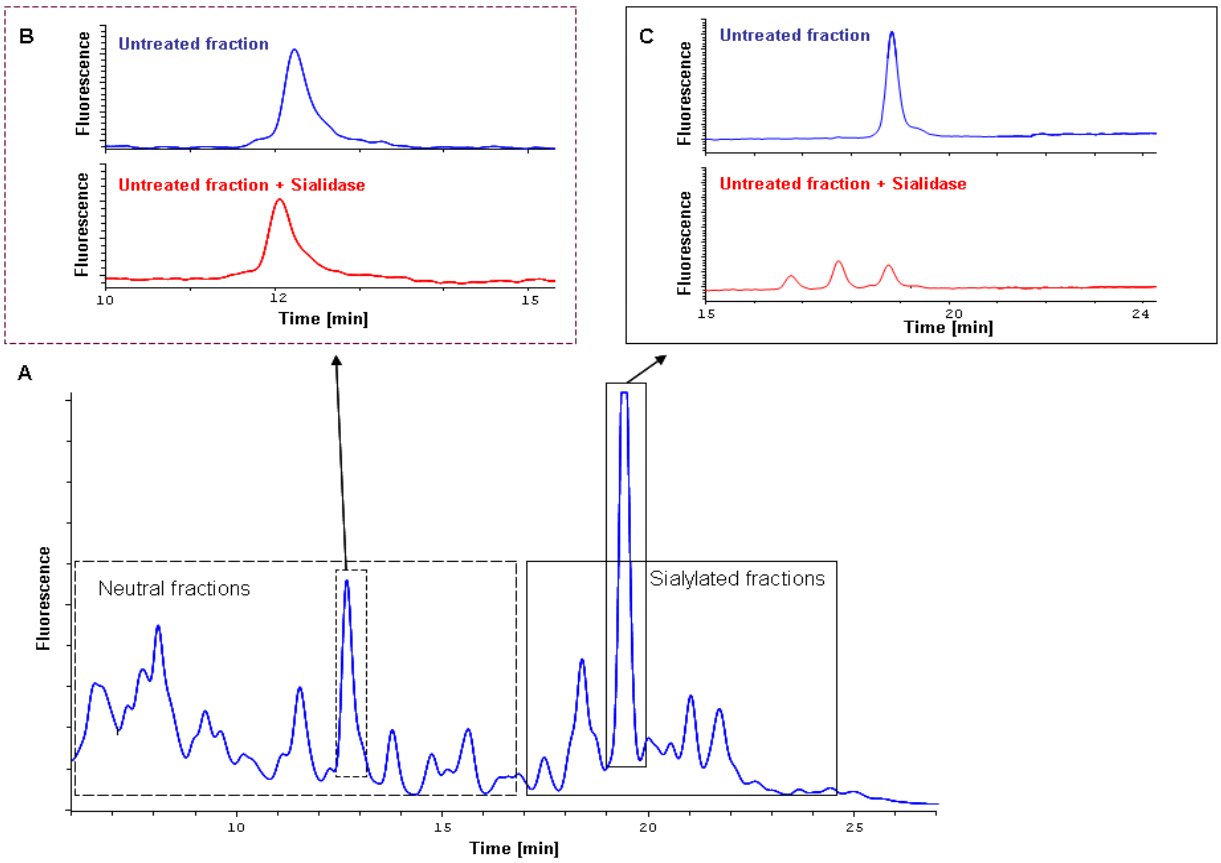

Figure 28. Detection of sialylated and non-sialylated N-glycans in human spermatozoa. (**A**) Spermatozoa after swim-up from healthy donors were subjected to N-glycan isolation and 2-AB fluorescence conjugation followed by HPLC analysis. Eluted fractions were collected and incubated with 5 mU/ml sialidase for 15 h. (**B**) Fractions highlighted by dashed box carry neutral non-sialylated N-glycans as sialidase treatment failed to alter retention time, intensity, and number of detected peaks after HPLC. (**C**) Fractions highlighted by the solid box contain sialylated N-glycans as shown by the occurrence of three lower intensities fractions recorded in different retention time after sialidase treatment.

3.15 N-glycan profiling of human spermatozoa

Detection of sialic acids in the structure of sperm N-glycans based on our HPLC analysis prompted us to characterize rigorously the compositions of sperm N-glycans. For this purpose, 2-AB- labeled N-glycans of sperm from healthy donors were sequenced following permethylation using a MALDI-TOF/TOF mass spectrometer in a positive mode (Figure 29).

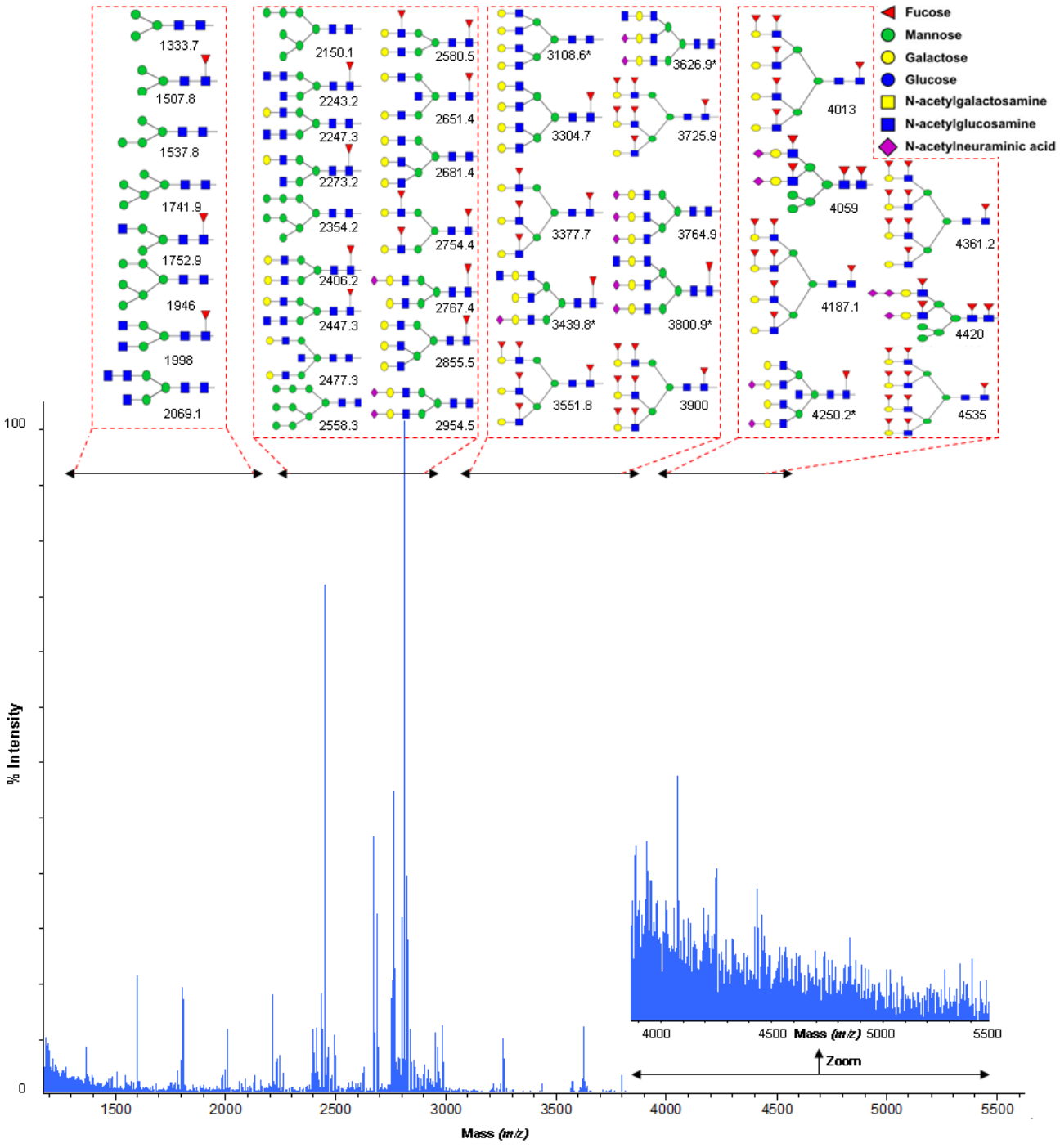

Figure 29. MALDI-TOF profiling of N-glycan structures in spermatozoa. Following swim-up from healthy donors, N-glycans of spermatozoa were isolated (including trypsin and N-glycosidase digestion), processed (such as 2-AB labeling, purification, and permethylation), and then analyzed by MS. Annotated compositions are according to the molecular mass of positive ion mode of acquired spectrum. The proposed compositions are mainly sodiated ($[M + Na]^+$). However, four protonated ($[M + H]^+$) compositions were also registered, and superscripted by a star symbol (*). The intensity was normalized to 100% based on the most abundant peak (at *m/z* 2954). Insert shows a magnification (50 times) of low signal intensity at *m/z* range from 3900 to 5500 of the spectrum.

3.15.1 Substantial presence of sialylated N-glycan compositions in human sperm

According to the MALDI-TOF MS profiling of permethylated derivatives of sperm N-glycans in a positive ion mode, the highest intensity signal at *m/z* 2954 $[M + Na]^+$ was consistent with a biantennary structure capped with two sialic acid residues (Figure 30A, B). This biantennary composition was verified using a MALDI-TOF/TOF fragmentation analysis (Figure 30C). In addition, acquired fragment ions (at *m/z* 2490 and 1912) from MS/MS of the precursor peak (at *m/z* 2954) provided evidence, which let us suggest the occurrence of sialic acids in the antennae of this biantennary N-glycan composition (Figure 30C).

Employing the MALDI-TOF MS profiling strategy, ten possible sialylated N–glycan structures were characterized in association with sperm in both complex and hybrid classes of N-glycans, terminating with 1-3 sialic acid residues attached to Gal moieties (Figure 31). The sialylated complex class of sperm glycans consists of three subclasses, including two biantennary (at *m/z* 2954, and 2967), four triantennary (at *m/z* 3440, 3765, 3627, and 3801), and one tetraantennary (at *m/z* 4250) structures (Figure 30). In addition to complex structure, acquired ions at *m/z* 4059, 4420, and 4435 were consistent with three hybrid structures (Figure 31).

Two sialylated hybrid compositions (at *m/z* 4059 and 4220) carry SLe^x antennae, a critical sialylated tetrasaccharide in physiological functions. In addition to the SLe^x, the presence of core Fuc in attachment to GlcNac was detected in six out of ten sialylated N-glycans (at *m/z* 2967, 3439, 3800, 4435, 4059, and 4420 (Figure 31).

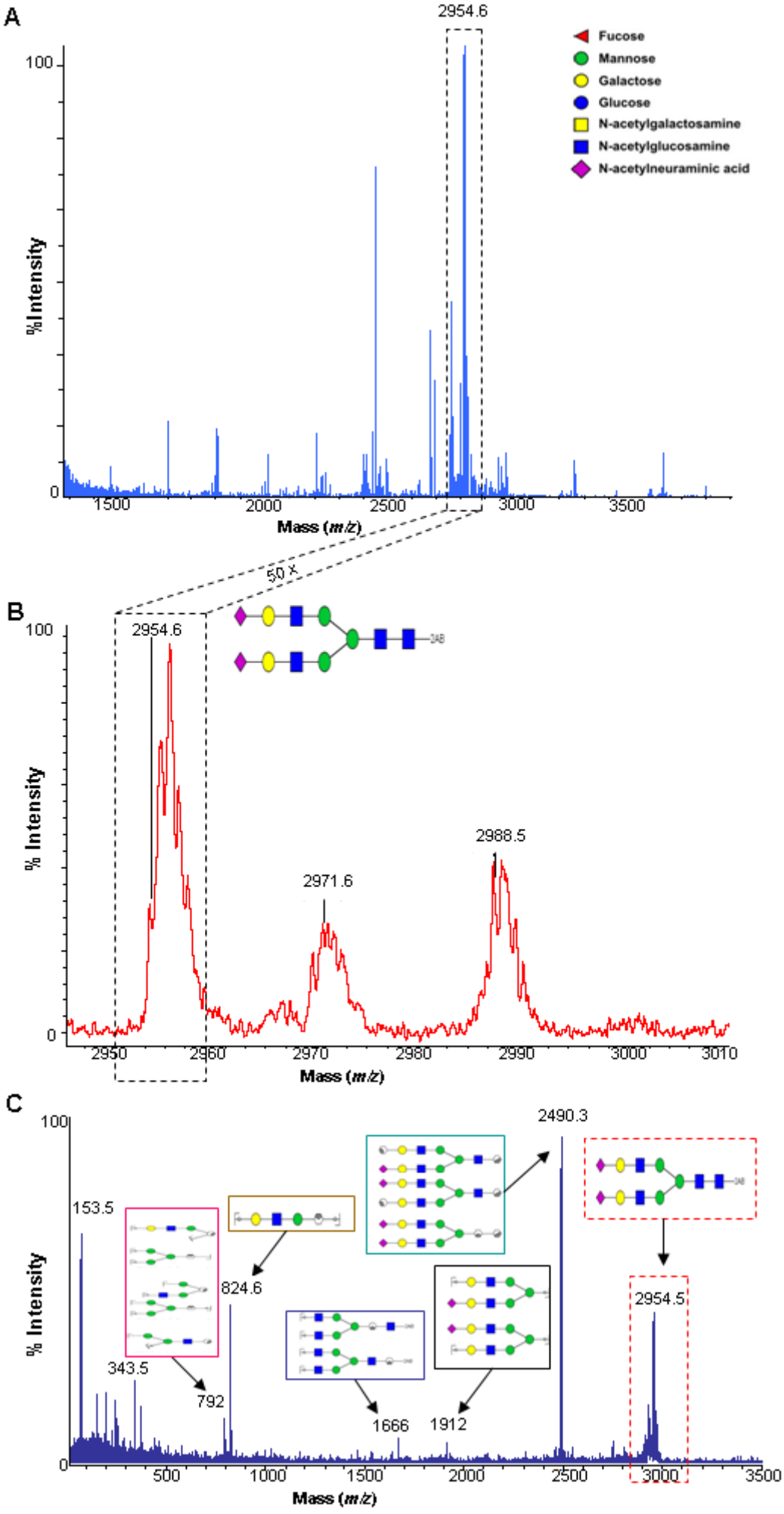
A
2954.6
Fucose
Mannose
Galactose
Glucose
N-acetylgalactosamine
N-acetylglucosamine
N-acetylneuraminic acid
100
0
%Intensity
1500
2000
2500
3000
3500
Mass (m/z)
50 x
B
100
2954.6
2971.6
2988.5
% Intensity
0
2950
2960
2970
2980
2990
3000
3010
Mass (m/z)
C
100
153.5
824.6
343.5
792
1666
1912
2490.3
2954.5
% Intensity
0
500
1000
1500
2000
2500
3000
3500
Mass (m/z)

Figure 30. Identification of sialic acid compositions in a disialylated biantennary structure associated with human spermatozoa. (**A**) MS profiling of permethylated 2-AB-labeled N-glycans demonstrated a dominant presence of a signal at *m/z* 2954. (**B**) The MS spectrum was magnified (50 times). The peak at *m/z* 2954 was highlighted by a black dashed box and its corresponding disialylated bicentenary composition was annotated according to a positive ion mode ($[M + Na]^+$). (**C**) MS/MS sequencing of *m/z* 2954 (red dashed line box) generated fragment ions at *m/z* 2490 (green solid line box), 1912 (black solid line box), 1666 (blue solid line box), 824 (brown solid line box) and 792 (pink solid line box) which were consistent with the precursor ion assigned sialylated biantennary composition in Figure 30B.

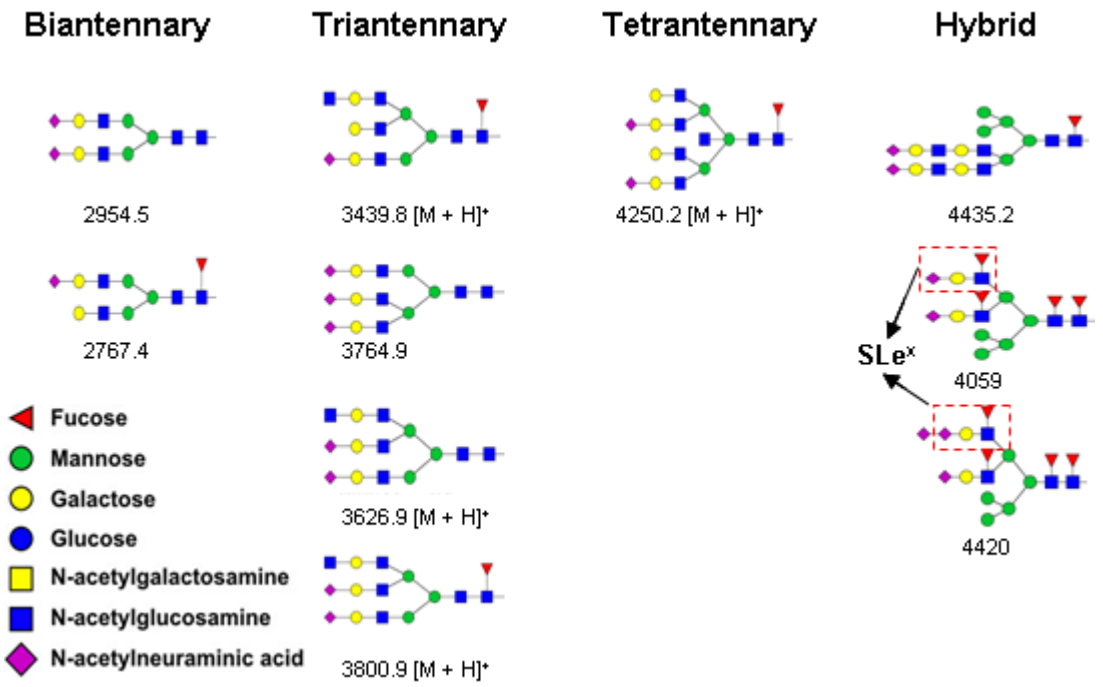

Figure 31. Identification of sialylated N-glycans in association with human spermatozoa. Data analysis of MALDI-TOF/TOF sequencing (Figure 29) revealed the presence of nine sialylated structures. Silalyl-Lewis^x (SLe^x) antennae capped two of the sialylated N-glycan structures (highlighted by red dashed boxes). The majority of the adducts have acquired an additional Na ion ($[M + Na]^+$) in the spectrometer, but some of the exceptional adducts, which obtained H cation instead of Na ion were denoted by $[M + H]^+$.

3.15.2 Non-sialylated N-glycan compositions of human sperm

Rigorous MALDI-TOF MS sequencing of associated N-glycans with human sperm revealed (Figure 29) that, apart from sialylated structures (Figure 31), several neutral compositions occurred in the N-glycome. Characterized non-sialylated structures were categorized into two major classes of N-glycans: oligomannose and complex. Oligomannose compositions carry between three to nine Man residues in attachment to two GlcNac (at *m/z* 1334, 1508, 1538, 1742, 1946, 2150, 2354, 2558) (Figure 32A). In addition to oligomannose structures, complex N-glycan were detected in four subclasses, i.e. biantennary (at *m/z* 1753, 1998, 2069, 2202, 2243, 2273, 2406, 2447, and 2580) (Figure 32B), bisected biantennary (at

m/z 2477, and 2651) (Figure 32B), triantennary (at m/z 2681, 2855, 3304, 3377, 3552, 3726, 3900) (Figure 32C), and tetraantennary (at m/z 3109, 4013, 4361, 4535, and 4187) (Figure 32D). The majority of identified tri- and tetraantennary compositions carried Lewis^x or Lewis^y in the outermost position of N-glycans (Figure 32D).

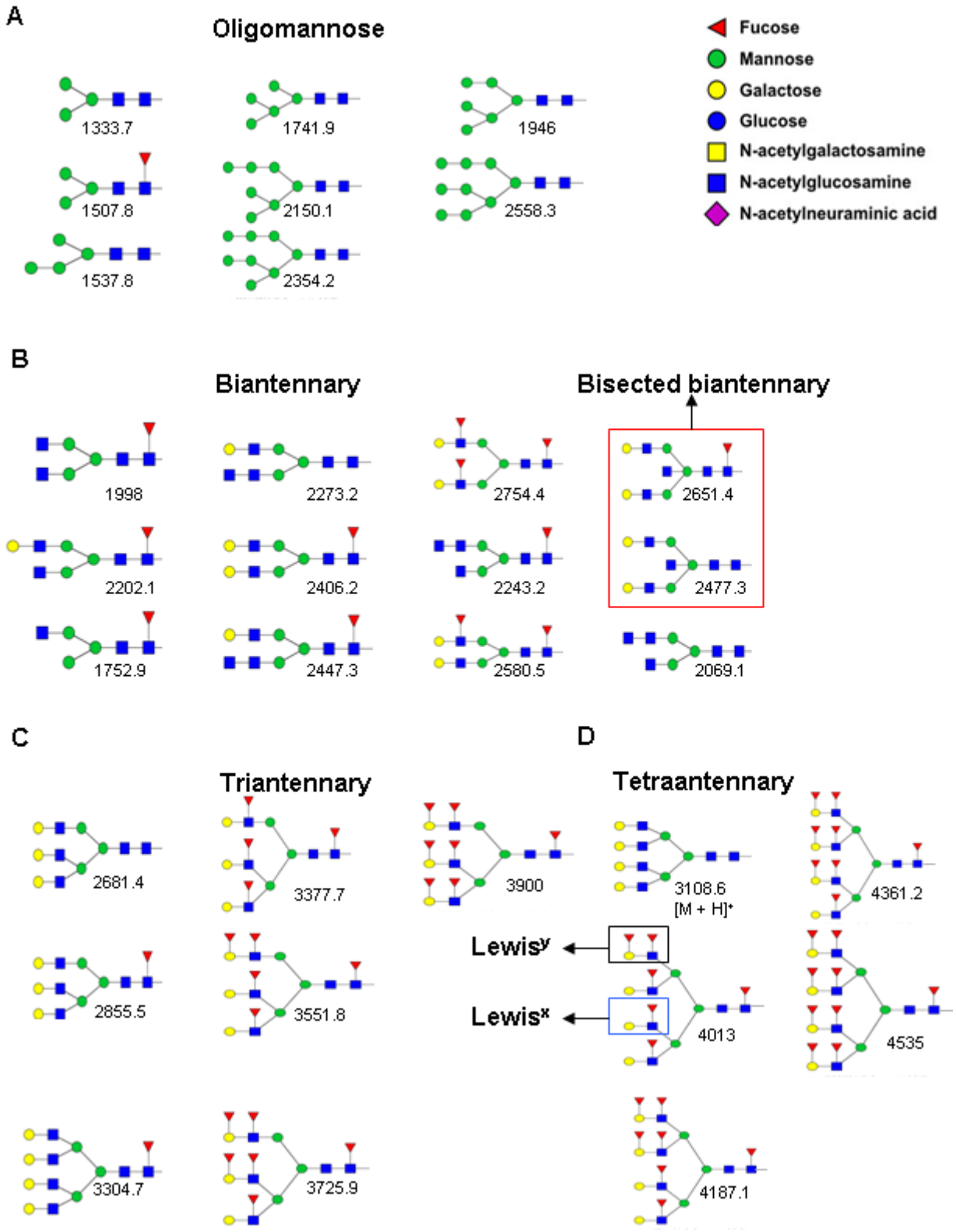

Figure 32. Characterization of non-sialylated N-glycans in human sperm. Non-sialylated N-glycans in human sperm were characterized and divided into four classes. Interpretation of MS data from 2-AB-labeled, permethylated N-glycans of human sperm revealed the presence of (**A**) oligomannose structures bearing Fuc_{0-1}-Man_{3-9}-$GlcNAc_2$, (**B**) biantennary N-glycans carry a Fuc residue in most of the identified compositions, two bisected biantennary compositions (highlighted by a red box), (**C**) triantennary, and (**D**) tetraantennary N-glycans, which were found mainly core-fucosylated. A sequence of $Lewis^x$ (highlighted by blue box) and $Lewis^y$ (black box) capped most of the tri- and tetraantennary compositions of human sperm.

3.16 Alterations of sperm N-glycans as a consequence of the acrosome reaction

To investigate whether the acrosome reaction coincides with alterations of sperm N-glycans, human spermatozoa were incubated with a calcium ionophore, as a common inducer of the acrosome reaction. Afterwards, N-glycans were isolated, labeled with 2-AB, and then separated and analyzed using HPLC (Figure 33A, B). Quantification of 16 obtained N-glycan fractions showed alterations in all of the N-glycan structures after ionophore treatment. These observed differences in the amounts of all N-glycans may suggest that a massive recordation in N-glycan compositions occurs as a consequence of acrosomal exocytosis (Figure 33C).

First eluted fractions (Peak No. 1 to 7) contained hyposialylated N-glycan structures due to their higher intensities in ionophore treated sample. On the other hand, obtained fractions at the end of HPLC separation (Peak No. 10 to 16) carried sialylated N-glycans as their intensities in untreated spermatozoa were substantially higher compared with ionophore treated samples (Figure 33C). Thus, this comparative analysis in the quantity of N-glycan fractions between acrosome intact and reacted samples demonstrated that the acrosome reaction could manipulate sperm N-glycans, because of the massive shedding of sialic acids from the sialylated N-linked glycans.

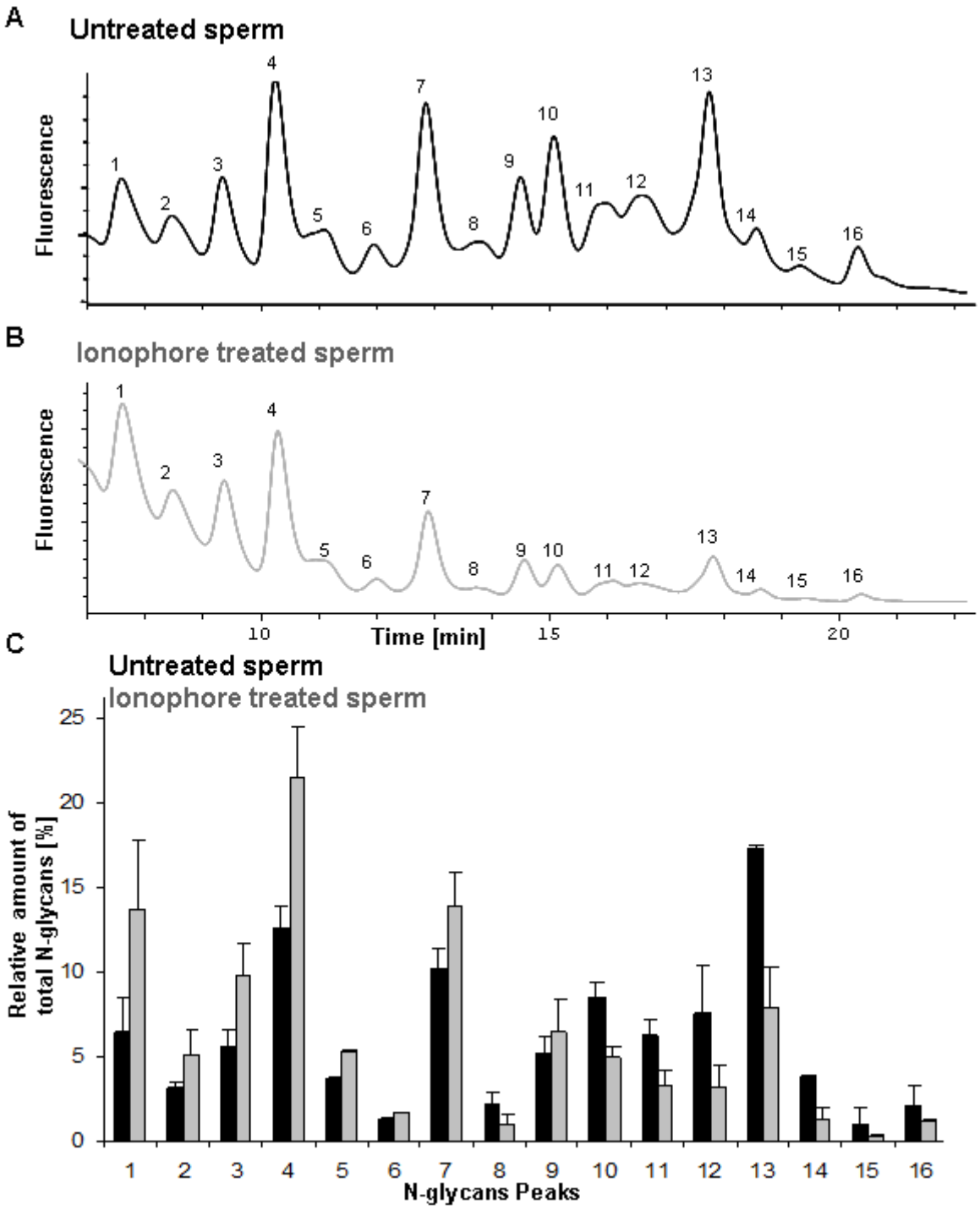

Figure 33. Modifications of N-glycan after induction of acrosome reaction. N-glycans of untreated (**A**) and ionophore-treated (**B**) human spermatozoa were isolated, fluorescently labeled with 2-AB and then separated and quantified by HPLC. (**C**) the relative amount of each N-glycan was calculated from the intensity measurement of corresponding HPLC fraction, suggesting a substantial alteration in N-glycans structures due to the acrosome reaction (n=3).

3.17 Differential expression of O-glycan transferases in the epididymis

As a first step for future studies on possible O-glycan alterations in the epididymis after UPEC infection, we investigated if enzymes related to the biosynthesis of O-glycans are expressed in the epididymis. In this regard, in the mouse epididymis we profiled the expression levels of 21 different O-glycan transferases from four main types of responsible enzymes for initiation of O-glycan synthesis, i.e. Galt, Galtl, Pofut, and Pomt (Figure 34).

In this regard, a differential expression of O-glycan transferases in the mouse epididymis was observed from highly expressed (*Galnt12*, *Galnt14*, *Galnt10*, *pofut2*, *Galntl4*) to lowly expressed (*Galnt1*, *Galnt13*, *Galnt3*, *Galnt11*, *Galntl2*, *Galntl5*, *Galntl3*, *Pomt1*, *Pomt2*, *Pofut1*, *Galntl1*) genes. Some genes could not be amplified (*Galnt4*, *Galnt5*, *Pofut1*, *Galnt7*, *Galnt6*) (Figure 34). Thus, the expression of O-glycan transferase genes may indicate that the epididymis plays an active role in the biosynthesis of O-glycans. However, for a precise interpretation about the different expression levels of these genes in the epididymis a quantitative real-time PCR would be necessary.

O-glycan transferases		Expression in mouse epididymis
N-acetyl-galactos-aminyl-transferase	GalNt1	+
	GalNt13	+
	GalNt7	-
	GalNt3	+
	GalNt11	+
	GalNt10	++
	GalNt5	-
	GalNt2	+
	GalNt6	-
	GalNt14	++
	GalNt12	++
	GalNtl2	+
	GalNt4	-
	GalNtl4	++
	GalNtl5	+
	GalNtl1	+
	Wbscr17	+
O-mannosyl transferase	Pomt1	+
	Pomt2	+
O-fucosyl transferase	Pofut1	-
	Pofut2	++

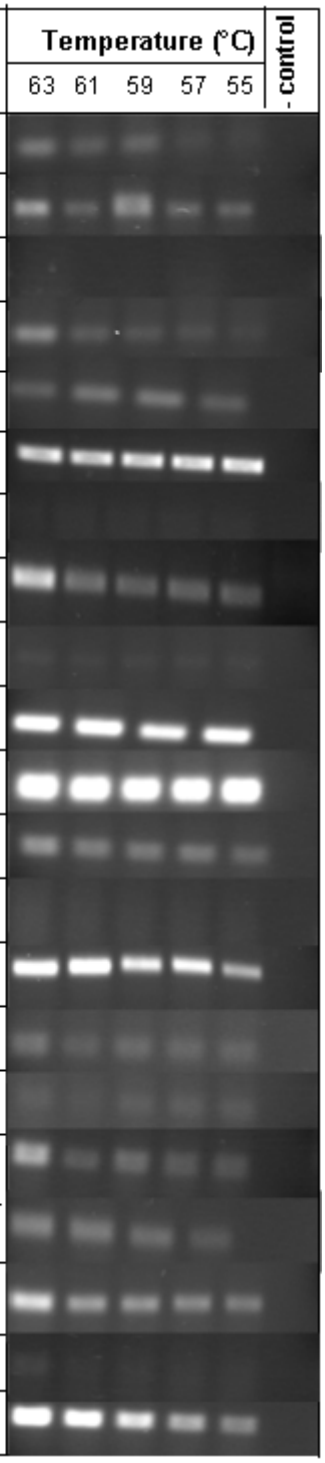

Figure 34. Different levels of expression of O-glycan transferases in the epididymis. The extent of mRNA presence in the epididymis of wild type mouse was investigated among these genes. The bands represent the amplification products of a temperature gradient RT-PCR (55-63°C) on 21 primer sets specific for O-glycan synthesis genes that were subjected to agarose gel electrophoresis. The negative (-) control reaction mixture lacked the template cDNA. According to the intensity of PCR bands under the same condition, these genes were divided into highly expressed (++), low expressed (+) and not amplified (-).

4 DISCUSSION

From insemination to fertilization, spermatozoa are protected by their glycocalyx against female cellular (macrophages, neutrophils) and humoral (complements, antibodies) immunity which principally could be triggered by spermatozoa as antigens [139, 140]. In addition to resisting female immunity, every single sperm carries a unique glycocalyx, due to several post-meiotic modifications during the transition from the testis to the epididymis and then by secretions of the accessory glands, denoting a sperm's individuality. This individuality is postulated to be a selection characteristic in the female reproductive tract [7, 141]. In close proximity to the egg, capacitation induces the release of glycoproteins such as DEFB126 from the sperm surface. This capacitation-mediated release of these immunosuppressive glycoproteins from the sperm surface exposes underlying moieties which are necessary for sperm-egg binding [16, 141, 142].

Following an inter-species insemination sperm trigger the production of antibodies in the female genital tract directed against non-self glycans, pointing to the species-specific characteristic of the sperm glycocalyx. In this regard, sialic acid types play an important role in inter-species incompatibility. Humans unlike other mammals are genetically unable to the synthesis of Neu5Gc and therefore are equipped with antibodies raised against Neu5Gc [143-145].

Two controversial findings were reported about the role of glycan moieties in the attachment of sperm to the zona pellucida. On one hand, studies based on a transgenic mouse model and MS analysis of ZP3 underestimated the importance of O-glycans in the zona pellucida [146, 147]. Instead, an N-terminal amino acid sequence of ZP2 was proposed to be necessary in the sperm-zona pellucida binding site [148]. On the other hand, many studies propose an essential role for glycans in fertilization particularly in mediating the specific interaction between spermatozoa and the zona pellucida of the egg [7, 49]. Binding of spermatozoa to the zona pellucida is thereby strongly induced by terminal Neu5Ac residues of SLe^x oligosaccharides on the surface of the zona pellucida. In addition, successful interaction of both gametes requires previous desialylation of the spermatozoal surface (Figure 35) [16]. For this purpose, spermatozoa are equipped with sialidases [16, 149-151]. Under normal conditions, neuraminidases are only activated in the female reproductive tract as a consequence of capacitation and/or the acrosome reaction [16, 149-151]. Two activated neuraminidases (NEU1, NEU3) on sperm mediate the removal of sialic acid moieties during

capacitation [16]. Different localization of detected neuraminidases (i.e. NEU1 in the oviduct, NEU3 in the oviduct and the uterus) may refer to a ligand-specific desialylation function of neuraminidases on glycoproteins and gangliosides, however, little detail is known [16]. According to a study by Ma et al. on the capacitation of sperm under a mimicry condition (*in vitro*), sialidase activity was abated in the presence of protease inhibitors. Thus, the release and activation of sperm sialidases during capacitation seems to be protease-dependent [16]. The treatment of sperm with a neuraminidase inhibitor (DANA) during the *in vitro* capacitation attenuated the phosphorylation of ERK and tyrosine, indicating a putative involvement of downstream signaling pathways (e.g. MAPK/ERK) in the function of neuraminidases [16]. Defects in the detachment of sialic acids from the surface of sperm play a negative role in sperm-zona pellucida interaction. For instance, the presence of a neuraminidase inhibitor (DANA) decreases the rate of *in vitro* fertilization, and the lack or lower expression level of neuraminidases are found in idiopathic infertile males. These findings emphasize the vital importance of a timely activation of sperm neuraminidases for fertilization [16]. In this study, the active role of neuraminidases in sperm hyposialylation is further confirmed by the observation of a higher level of sialic acid loss in the presence of neuraminidase (Figure 23). A process that was counteracted using a neuraminidase inhibitor (Figure 24). The glycocalyx on the spermatozoal surface undergoes massive redecoration after capacitation [16] and the acrosome reaction (Figure 35). Premature release of neuraminidases prior to ejaculation is usually avoided as untimely desialylation could result in elimination of spermatozoa by phagocytic cells [152]. In pathophysiological conditions such as bacterial epididymitis, considerable premature exocytosis of the acrosome has been observed *in vivo* and *in vitro*, which contributes substantially to the loss of fertilizing capacity as shown by subsequent *in vitro* fertilization (IVF) experiments in mouse [24].

This prompted us to examine if undue acrosome reactions could affect the sialome of epididymal spermatozoa and surrounding epithelial cells. To study this, we used an established acute mouse bacterial epididymitis model and ejaculates of men with a recent history of the disease.

Induction of the acrosome reaction causes sperm hyposialylation (Figure 21). UPEC also induces the acrosome reaction (Figure 22) and loss of sialic acids (Figure 23). Similarly, in murine epididymitis as well as in *in vitro* treated human spermatozoa, UPEC caused a premature acrosome reaction leading to a significant desialylation of spermatozoa as well as adjacent epithelial cells (illustrated in Figure 35). Surprisingly, the investigated desialylation

was much more pronounced in epididymitis patients, whose samples were collected 14 days after antibiotic therapy, than in mouse sperm (Figure 26). In patients the sperm hyposialylation coincided with undue acrosome reactions (Figure 25). The desialylation could be efficiently blocked with a neuraminidase inhibitor (DANA) *in vitro* (Figure 24), indicating that the loss of sialic acid residues is particularly a consequence of endogenous neuraminidases along with activation of the acrosome reaction (Figure 35). Hence, regarding the lower amount of Neu5Ac in UPEC treated sperm (+) compared to DANA+UPEC treated conditions (Figure 24), a release of sialic acid could be proposed due to activation of sperm neuraminidases during UPEC infection.

A limitation in the analysis of human samples in this study is the relatively small number of semen samples from patients/controls suitable for glycoanalysis due to the need to clean ejaculates by the swim-up method. Since semen samples of patients with acute epididymitis are usually characterized by a largely reduced semen quality and leukocytospermia, the swim-up technique was necessary to select the viable and motile sperm, thereby removing contaminating non-sperm cells (e.g. leukocytes), and thus, to avoid bias between patient and control samples.

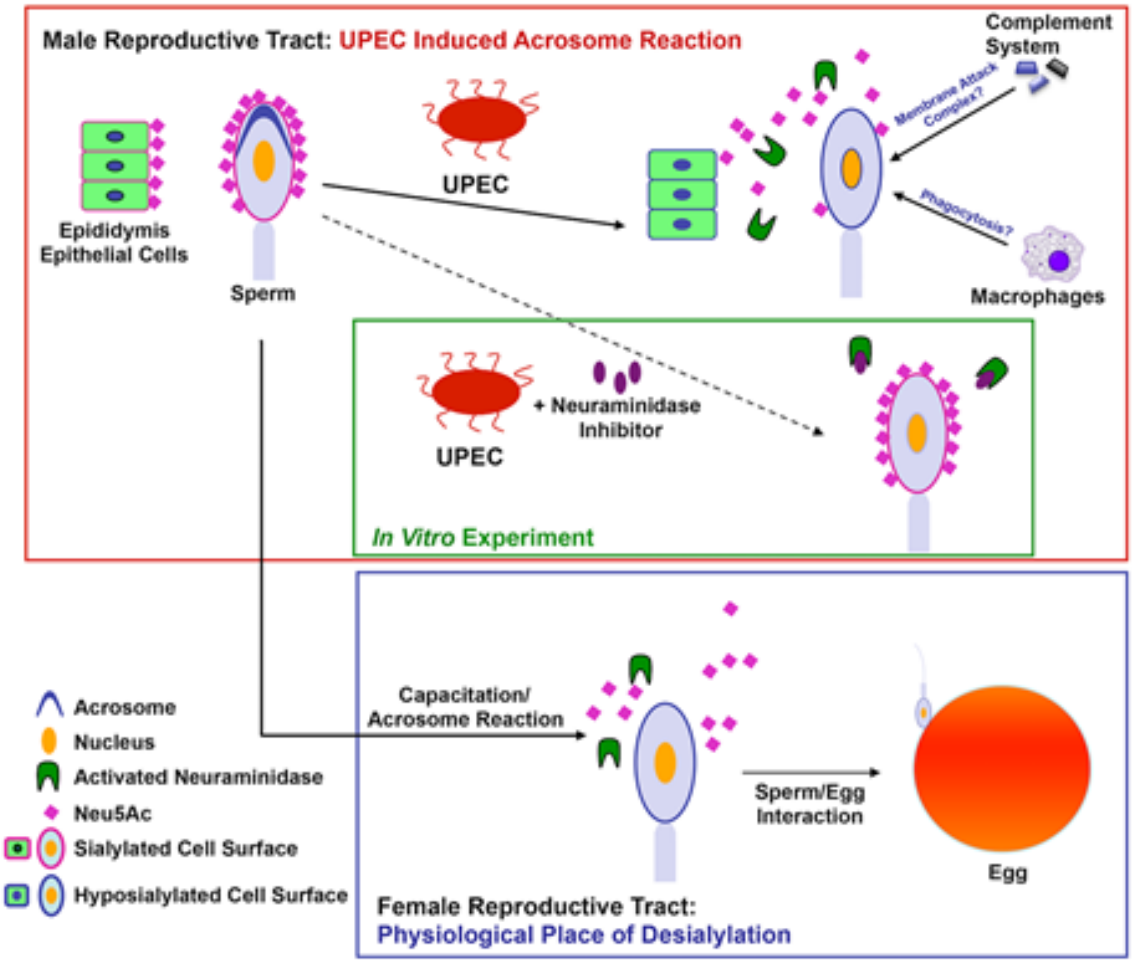

Figure 35. Summary and working model. Blue box; In the female reproductive tract capacitation/acrosome reaction leads to a proteolytic activation and release of neuraminidases, resulting in a desialylation of spermatozoa required for sperm/egg interaction. Red box; UPEC induced acrosome reaction triggers a premature desialylation of spermatozoa and the release of sialic acid residues from adjacent cells in the male reproductive tract. Consequently, pathological hyposialylation may negatively influence the protection of host cells against phagocytosis and complement system. Green box; *In vitro* UPEC induced hyposialylation of spermatozoa could be counteracted using neuraminidase inhibitors [28]. (Copyright © 2016, by the American Society for Biochemistry and Molecular Biology)

Sialic acids play multifactorial, mainly defensive, roles in the host response to infection. Thus, premature activation of sperm neuraminidases during epididymitis may endanger sperm via modulation of the immune response due to the lack of immune suppression by sialic acids after infection. However, the putative underlying immune mechanisms still need to be comprehensively addressed.

Sialic acids in host-pathogen interactions mediate an anti-bacterial function through electrostatic repulsion characteristic of negative charged sialic acids on the surface of cells [153]. In this regard, the UPEC infection-associated desialylation of sperm may impair this defense barrier of the male gamete against pathogens. In contrast to the defensive role of sialylated glycans, some glycoconjugates on the host surface are used as receptors for a variety of pathogens [77, 89]. For instance, glycosylated mucus secretions are involved in penetration of some pathogens into the cell membrane of the host [154-156]. The attachment of pathogenic *E. coli* to glycoconjugates of human cells are mediated by lectin-like adhesins on FimH [157, 158]. Due to the desialylation and the resulting loss of negatively charged sialic acid residues, type-1 fimbriae like FimH may better reach potential binding partners such as Manα1-3Man or Manα1-3Manβ1-4GlcNAc [159]. Therefore, an altered and hyposialylated glycocalyx may predispose sperm as a potential target for pathogens such as UPEC. In contrast, a sialic acid dependent UPEC binding to epithelial cells was described [160]. Accordingly, the adhesion of UPEC to epididymal epithelial cells would be inhibited by epithelial desialylation.

4.1 Possible effects of hyposialylation of sperm on the immune response

Innate and adaptive immune responses are to a large extent modulated by the contribution of sialylated carbohydrates. Innate immune reactions (e.g. complement reaction) is suppressed by sialylated moieties present on the cell surface. Complement C1q initiates the classical complement pathway, resulting in phagocytic removal of targeted cells [161, 162]. Terminal

sugar residues are decisive for attachment of C1q to their receptor structures [163]. For instance, microglia (as the resident macrophages of the central nervous system), which are involved in neuritis, require the binding of C1q to the complement receptor 3, a reaction which occurs only if the neuronal glycocalyx is desialylated [164]. This reflects the preventive effect of sialic acids on complement opsonization and microglial/macrophage phagocytosis [165, 166].

Massive release of sialic acid residues from the cell surface of epididymal epithelial cells and spermatozoa may contribute to the observed tissue damage in epididymitis (Figure 35). This view is supported by the fact that bacterial LPS triggers complement activation and that hyposialylation promotes the perforation of host cell membranes by the membrane attack complex counteracting a protective mechanism conveyed by complement factor H [144]. In this regard, complement factor H exhibits sialic acid specific binding domains, which are necessary for an efficient cell surface-binding [145]. As binding of sialic acids to factor H perturbs activation of complements, the alternative pathway of complement activation is also triggered in the absence of sialic acids [24]. Factor H on cell membranes is essential to remove activated complement factor 3b from cellular surfaces to prevent perforation of host cell membranes and limit tissue damage. As recently shown, complement factor H is an important component of seminal plasma as it protects spermatozoa against such a complement attack in the female reproductive tract [146]. Thus, hyposialylation of spermatozoa and other epididymal host cells may result in a deficit of sialic acid-dependent factor H binding and thus, less protection against the activated complement system. It seems that factor H attachment to surface sialic acids may play an important role in sperm survival which could be impaired by sialic acid loss caused by UPEC epididymitis.

Inflammation substantially alters the decoration of oligosaccharides in acute phase proteins such as pentraxin-related protein 3 (PTX3) [167, 168]. In UPEC-associated epididymitis, higher levels of proinflammatory cytokines (such as IL1, IL6, and TNF-α) are present [126]. Innate immune cells and several non-immune cell types secrete PTX3, a long pentraxin glycoprotein in the inflammatory response to TNF-α and IL-1ß [169-172]. The affinity of PTX3 to C1q is increased after enzymatic cleavage of the sialic acids in the N-glycosylation binding site of PTX3, suggesting that PTX3 modulates the activity of complements by binding to C1q [163, 173-175].

As a further point, CD52 modulates the classical complement pathway. The epididymis incorporates CD52 in the sperm plasma membrane [176, 177]. N- and O-glycans are associated with epididymal secreted CD52, which are different to those from lymphocyte type CD52 [176, 177]. Highly sialylated N-glycans of CD52 (consisting of N-acetyllactosamine repeats) suppress complements by interacting with C1q [178-180].

Moreover, many sialylated and polysialylated glycoproteins are integrated into the plasma membrane of spermatozoa during epididymal transit [119, 181]. These glycoproteins inhibit *inter alia* in a sialic acid-dependent way the phagocytosis by leukocytes as seen in murine spermatozoa [152, 182]. In this regard, the substantial loss of sialic acid residues during epididymitis could prompt phagocytosis of spermatozoa during transit through the epididymis and/or the female reproductive tract, as already indicated [152, 183].

The presence of leukocytes (mainly macrophages) is a frequent observation in the lumen of the epididymal duct of healthy men and rodents. Together with neutrophils and T cells their numbers increase strongly in infection as a consequence of immune cell infiltration during epididymitis [11, 126, 184, 185]. In addition, phagocytic cells in semen are able to engulf abnormal sperm. Sialoglycoproteins, which are secreted by the epididymis and are bound to the sperm surface, inhibit phagocytosis by macrophages [152, 186]. Taken together, the substantial sialic acid deficiency caused by UPEC infection may enhance sperm vulnerability to phagocytosis during transit through the epididymis and/or possibly in the female genital tract [139].

The adaptive immune response is also modulated by sialic acids. The monocyte-derived dendritic cell surface is highly sialylated [187]. *In vitro* α2,6 desialylation of dendritic cells (DCs) enhances the phagocytic capacity of *E. coli* pathovars, followed by an increase in the expression level of MHC molecules and cytokines (such as IL-12, IL-6, IL-10, and TNF-α) through activation of NF-κB and other signaling pathways [188]. Moreover, an increased number of some subpopulations of DC (e.g. $CD11c^+$ $IL\text{-}23^+$ myeloid DC, $CD123^+$ plasmacytoid DC) in chronic epididymitis can be modulated in the same manner using sialic acids [189]. Therefore, it appears likely that soluble neuraminidase may also detach sialic acid residues from the cell surface of luminal immune cells in the epididymis during infection.

Sialic acids in the form of polySia play a shielding role against neutrophils, which are major attacking immune cells to sperm following insemination. Neutrophils form a NET

(made of DNA, histones, anti-microbial peptides, proteins, and enzymes) to entrap foreigners (i.e. pathogens, spermatozoa) [190-192]. To evade this trap, NET is cleaved by the DNase of semen [191, 192]. After enzymatic degradation of NET, released histones are cytotoxic [193]. However, available polySias in glycoconjugates (i.e. neural cell adhesion molecule (NCAM) and polysialylated polysialyltransferase ST8SiaII), which are incorporated into sperm and epididymosomes, abolish the cytotoxicity of nucleosomes in the female innate immunity [119, 194].

4.2 Activation of siglecs as a putative consequence of sperm desialylation

A large number of siglecs expressed in leukocytes interact with their ligands through sialic acids, leading to an immune discrimination between self and non-self [153, 195, 196]. Siglecs modulate both innate and adaptive immune responses [153]. For instance, the siglec CD22 acts as a key regulator of B-cells, and modulates B-cell signaling function by recognition of α2,6-linked sialic acids [197]. Thus, terminal sialic acids of leukocytes play an important role in counteracting excessive immune response via an interaction with siglecs in *cis* [198]. The majority of siglecs (e.g. siglec G/10) dampens cell signaling activation by employing a tyrosine domain in the cytoplasmic tail [153, 199, 200]. Siglec G/10 is located on B-cells, macrophages, and DC. As an example, the anti-inflammatory signaling of siglec G/10 is activated by the interaction with sialic acid residues on CD24 in *cis* [198]. During sepsis, generation of inflammatory cytokines such as IL-6 and TNF, in response to binding of pathogen-associated molecular patterns and/or damage-associated molecular patterns to toll-like receptors, is known to be repressed by sialylated glycans of CD24-bound siglec G/10 [198, 201]. Thus, this complex represses tissue damage-induced immune responses [199], similar to those seen in infected epididymis [8]. Some bacteria like *Clostridium perfringens* secrete microbial sialidases targeting the described sialic acid mediated CD24-siglec G/10 complex. As a consequence, mice have an increased risk of septicemia, as previously shown [198, 202]. Sialidase treatment aggravates pathogenicity, and conversely, sialidase inhibitors suppress the inflammatory response and septic symptoms [198]. Moreover, in natural killer (NK) cells, siglec-7 plays an inhibitory role when these cells are covered by (Neu5Acα2-8Neu5Ac)-containing glycans. Sialidase treatment of NK cells enhances cytotoxicity in highly sialylated tissues [203-206]. In addition, sialic acid mediated functions of siglecs in sepsis were observed not only in white blood cells, but also in platelets. Sialic acid deficient platelets in infection are vulnerable to clearance by asialoglycoprotein receptors of hepatocytes, resulting in coagulopathy [207]. Thus, in epididymitis patients, activated endogenous

sialidases may act as an indirect virulence factor similar to microbial sialidases of *Clostridium perfringens*, *Vibrio cholerae* and *Streptococcus pneumoniae* [208].

4.3 Alterations of sperm glycocalyx in diagnosis and therapy of epididymitis patients

Alterations in the glycosylation pattern of proteins are considered a diagnostic marker of some diseases [209, 210]. Based on our study, sperm desialylation during infectious epididymitis would be worth investigating as a diagnostic marker in subsequent male infertility. In addition, the putative consequences of antibiotic therapies on the status of sperm sialic acids should be further investigated. Sialidase inhibitor-based drugs (i.e. zanamivir, oseltamivir, peramivir, and laninamivir octanoate) are successfully used in the treatment of influenza [211]. Moreover, an administration of sialidase inhibitor *in vivo* decreased the damage of sepsis in a mouse model [212]. During UPEC infection of sperm *in vitro*, desialylation was inhibited using a neuraminidase inhibitor (Figures 24, 35). Thus, our study may also suggest a potential therapeutic application for neuraminidase inhibitors to preserve fertility of epididymitis patients.

Putatively, a further level of intervention also could be upstream by blocking the proteolytic activation and release of neuraminidases using suitable protease inhibitors according to Ma et al. [79].

4.4 Sperm glycans and their putative immunomodulatory roles during infection

N-glycan analysis of human sperm revealed an association of three main classes of N-glycans: oligomannose, complex, and hybrid (Figures 29, 31, 32). Intriguingly, detected oligomannose (carrying 3-9 Man in branches) and complex (forming bi-, tri-, tetraantennary and bisected biantennary structures, and bearing a core Fuc in the majority of them) types confirmed the MS profiling results of Pang et al. [105, 213].

Previously analyzed MALDI-TOF MS data failed to identify varieties of sialylated N-glycans in human spermatozoa [105]. In spite of these analyses, interestingly, obtained MS and MS/MS data (Figures 29-31) revealed ten sialylated compositions from complex and hybrid types of N-glycans. However, a comprehensive MS/MS is still required to further validate the association of these novel sialylated compositions with sperm, especially the hybrid types (Figure 31).

In addition to alterations in sialic acid moieties of spermatozoa following acrosome reaction (Figures 21, 35), an alteration in N-glycan compositions of sperm occurred following the induction of acrosome exocytosis (Figure 33). This massive redecoration in the sperm glycocalyx along with capacitation and the acrosome reaction may denote the loss of glycoconjugates (such as β-defensins and GPI-anchored proteins) together with the realignment of glycosylated structures (e.g. gangliosides) and glycan-altering enzymes (such as PH20) [7].

Clark et al. characterized sialylated bisecting biantennary compositions in sperm and the zona pellucida, hampering immune attacks of NK cells [214]. Additionally, these glycostructures are also applied in tumor cells, *HIV*, and *Helicobacter pylori* to mislead immune defense. During development, this bisecting biantennary structure is also present in α-fetoprotein found in the yolk sac and fetal liver [214] According to the hypothesis of the "eutherian fetoembryonic defense system", this bisecting biantennary composition and other glycoproteins such as glycodelins present in the seminal plasma and amniotic fluid play an immunosuppressive role for gametes and developing embryos in the female reproductive tract [214]. In our study similar bisected biantennary compositions were identified in association with the glycocalyx of human spermatozoa. However, these bisected biantennary compositions were non-sialylated (Figure 32).

The contribution of Fuc to the structure of Lewis^x (either sialylated or non-sialylated types) and Lewis^y was largely identified in complex structures of the human sperm N-glycome (Figures 31, 32). This finding is consistent with MS analysis of Pang et al., who also demonstrated the localization of Lewis^y to the acrosome [105]. Regarding the outlined roles of Lewis^x and Lewis^y in tolerance to host adaptive immune reactions, these motifs attenuate antigen-driven responses upon some pathogens (e.g. *Helicobacter pylori*, *Schistosoma* as parasitic helminths), and *HIV*-infected T cells [215-219]. In non-pathogenic variants of *Helicobacter pylori*, the Lewis^x and Lewis^y in LPS structures interact with DC through dendritic cell-specific intercellular adhesion molecule-3-grabbing non-integrin (DC-SIGN), and consequently, modulate the balance of Th1-Th2 [216]. A higher contribution of Lewis^x compositions to the antennae of glycans enhances the affinity of glycans to DC-SIGN [220]. Conversely, the pathogenic variants of *Helicobacter pylori* that are devoid of Lewis compositions trigger an immense immune response [215]. Moreover, DC-SIGN strongly attaches to oligomannose structures [220, 221]. Therefore, the presence of several N-glycan compositions carrying high mannose, Lewis^x, and Lewis^y (Figure 32) together with sialylated

N-glycans in the sperm glycocalyx (Figure 31) may provide an immune privileged environment for sperm to suppress the immune response. Consequently, sperm can survive in the male and female reproductive organs, which are equipped with a physiological defense mechanism to abolish sexually transmitted pathogens and impaired spermatozoa [105, 213]. The detection of SLe^x in our study (Figure 31), however, is in contrast with the MS findings of Pang et al. that suggested the absence of SLe^x in the structure of N- and O-glycans of human seminal plasma [213]. Nevertheless, they did show, similar to our MS data in sperm, the substantial presence of $Lewis^x$ and $Lewis^y$ in seminal plasma [213].

In addition to the structural analysis of the sperm and seminal plasma glycocalyx [213, 222], future studies should address the putative correlation of UPEC infections and possible N-glycan alterations in sialylated and non-sialylated compositions, especially in the functional Lewis structures together with their immunomodulatory functions during epididymitis.

Besides N-glycans, $Lewis^x$ and $Lewis^y$ compositions occur in O-glycans (e.g. mucins) of seminal plasma [223]. O-glycans were specifically detected in the acrosome of spermatid and spermatozoa (Figure 12) [224]. Functional core 1 and 2 structures of O-glycans, bearing sialic acid and/or Fuc in antennae (e.g. $Lewis^y$), are present in the male reproductive tract on CD52. In addition, in infertile women, these O-glycan cores are also found in antisperm antibodies (i.e. sperm mobilizing and agglutinating antibodies) directed against CD52 [176, 177, 225].

DEFB126 (as a sialoglycoprotein) plays an important protective role and enables sperm to resist female immune attacks [7, 113]. The presence of sialic acids in DEFB126 is known to be essential for the migration of sperm through the cervical mucus since the enzymatic desialylation of DEFB126 from spermatozoa *in vitro* diminishes successful transit in the cervical mucus [116]. Moreover, a deletion in *DEFB126* abates the association of sperm coated O-glycans, leading to male subfertility, which is characterized by a defective competence of sperm to traverse the cervical mucus [226]. Detachment of DEFB126 from sperm causes a substantial increase against sperm immunogenic proteins in the immune response, including a remarkable elevation in affinity to antisperm antibodies (ADAM30, PH20) in the absence of DEFB126 or its sialic acid moieties [142]. Furthermore, DEFB126 contributes to a temporary binding of sperm to epithelial cells of the oviduct, preserving the competent spermatozoa for subsequent fertilization [227]. However, around the time of ovulation and as a consequence of capacitation, DEFB126 is released from the sperm surface and the sperm-epithelium attachment dissociates [227, 228]. Additionally, this essential step,

which arises prior to the progress of sperm towards the egg, is impaired after neuraminidase treatment, denoting the functional role of sialic acids in DEFB126 [227]. However, a study of an array of twelve epididymal β-defensins in a LPS-caused epididymitis animal model demonstrated that the expression levels of these β-defensins are mainly attenuated, and the reduced expression of SPAG11E (as a caput secreted β-defensin) causes a motility failure of sperm [229]. Nevertheless, alterations of β-defensins against UPEC infection in the male reproductive tract are largely unknown.

The initiating enzymes for synthesis of O-glycans show a different expression pattern in the epididymis (Figure 34). According to the study of Pang et al. only core 1 and core 2 are associated with seminal plasma and they are capped with sialic acid and/or Fuc [213]. Infertility, azoospermia, sperm malfunction, and malformation were reported along with the deletion of *GalNAc-T3* as an initiating enzyme in the synthesis of O-glycans [230]. By contrast, normal spermatogenesis and fertility were indicated in *GAL transferase 1* deficient mice whose core 2 was abrogated [231]. Moreover, other studies also provided no concrete evidence of sperm impairment following the deletion of O-glycan transferases in core 1 and 2 mucins as well as in O-fucosylated glycans [65, 232].

On the other hand, a deletion in a complex N-glycan synthesis gene (*Mgat 1*) coincides with a defect in spermatogenesis and apoptosis in spermatogenic cells [65] with multinucleated cells (MNC), instead of spermatozoa, visible in the lumen of the testis and occasionally in the epididymis [65]. The MNC appear alongside a disruption in the differentiation of spermatid into sperm [65]. MNC formation occurs as a consequence of the absence of complex N-glycan structures in gangliosides, which are sialylated glycosphingolipids, in Sertoli and germ cells, thereby causing a failure in the connection of spermatids to supporting cells [233-235]. In addition to gangliosides, complex N-glycans of cell adhesion molecules are involved in the attachment of spermatogonia to Sertoli cells, and their deficiency leads to MNC formation in the testis, and thus to male sterility [236-238]. Every spermatogenic cell contains various N-glycan types. For instance, in spermatocytes higher levels of oligomannose compared to complex N-glycans are present due to the inhibition of the synthesis of complex N-glycans by means of a specific upregulation of a Mgat1 inhibitor (i.e. GlcNAcT-I inhibitory protein (GnT1IP)) [239].

In comparison to N-glycans, the essential effects of O-glycans in spermatogenesis and sperm functions appear underestimated. To alleviate this gap in knowledge, other O-glycan

types including other putative mucin cores (i.e. core 3-8) and O-mannosyl glycans need to be investigated.

4.5 Massive alteration of sperm glycocalyx caused by UPEC infection

In conclusion, the present study shows that UPEC-induced epididymitis is associated with the massive alteration in the glycocalyx of sperm and surrounding epithelial cells in the epididymis (Figure 35). Intriguingly, UPEC infection causes hyposialylation in mouse epididymal spermatozoa and epithelial cells as well as in ejaculated spermatozoa of men with past history of epididymitis. Likely this happens mechanistically through activation of endogenous sialidases. Hyposialylation has the potential to negatively impact on course and magnitude of infection in patients suffering from UPEC elicited epididymitis providing a possible explanation for the characteristic long-term impairment of fertility associated with this pathovar [53, 95]. However, the precise consequences of the examined hyposialylation and the potential of sialidase inhibitors as therapeutic agent during UPEC infection need to be further investigated. Moreover, the current study demonstrates a massive redistribution in N-glycans (Figure 33) of human sperm as a consequence of the acrosome reaction, the exocytotic process which occurs untimely during UPEC infection (Figure 35). In spite of the mentioned papers, a better understanding is still needed in the comparative glycome analysis of human and mouse epididymal epithelial cells and spermatozoa to better judge how well the animal model reflects the situation in men. Furthermore, since O-glycans are expressed in the epididymis (Figure 34) and they contribute to sperm-associated glycoproteins (e.g. DEFB126) in protection against the immune response in the female genital tract [7], a comprehensive analysis of putative O-glycan alterations during UPEC infection in men and mice is warranted. Taken together, UPEC substantially manipulate the sophisticated decoration of the glycocalyx in sperm and epididymal epithelial cells, which predominately includes the remodeling of the sialome. Accordingly, these UPEC-caused alterations of the sperm glycocalyx may be implicated in male fecundity as sperm become vulnerable to the immunorecognition in the female reproductive tract.

5 SUMMARY

In mammals, glycoconjugates (e.g. O-glycans, three major classes of N-glycans) coat the surface of sperm. Terminal sialic acid residues and/or fucose act immunosuppressive and facilitate the survival in the female reproductive organs. Urinary tract infections caused by uropathogenic *Escherichia coli* (UPEC) pathovars belong to the most frequent infections in human. In men, pathogens can also spread to the genital tract via the continuous ductal system eliciting bacterial prostatitis and/or epididymo-orchitis. Antibiotic treatment usually clears pathogens in acute epididymitis, however, fertility of patients can be permanently impaired. Since premature acrosome reaction was observed in an UPEC epididymitis mouse model and sialidases on the sperm surface are considered to be activated via proteases of the acrosome, we aimed to investigate whether alterations of the sialome of epididymal spermatozoa and surrounding epithelial cells occur during UPEC infection. We found a massive redecoration of sperm N-glycans, especially hyposialylation, along with an acrosome reaction induced *in vitro*. In UPEC elicited acute epididymitis in mouse, a substantial loss of N-acetylneuraminic acid (Neu5Ac) residues was detected in epididymal spermatozoa and epithelial cells using combined laser microdissection/HPLC-ESI-MS analysis. Lectin staining suggested that infection reduced substantially α2,6-linked Neu5AC in mouse epididymis and sperm. In support, a substantial reduction of sialic acid residues bound to the surface of spermatozoa was documented in men with a recent history of *E. coli* associated epididymitis concurrent with premature acrosome reaction. *In vitro*, such an UPEC induced Neu5Ac release from human spermatozoa was effectively counteracted by a sialidase inhibitor. These findings strongly suggest a substantial remodeling of the glycocalyx of spermatozoa and epididymal epithelial cells by endogenous sialidases after premature acrosome reaction during acute epididymitis.

6 ZUSAMMENFASSUNG

Bei Säugetieren sind Spermatozoen mit Glycokonjugaten (z. B. O-Glykane, drei Hauptklassen von N-Glykanen) dekoriert. Diese besitzen immunsuppressive Eigenschaften. Vor allem N-terminale Neuraminsäuren und/oder Fucose schützen die Spermien vor Immunangriffen in weiblichen Reproduktionstrakt. Durch uropathogene *Escherichia coli* (UPEC) hervorgerufene Harnwegsinfektionen gehören zu den häufigsten Infektionen des Menschen. Bei Männern können sich Krankheitserreger auch kanalikulär in den Genitaltrakt ausbreiten und eine bakterielle Prostatitis und/oder Epididymo-Orchitis hervorrufen. Eine Antibiotika-Behandlung eradiziert in der Regel die Krankheitserreger bei akuter Epididymitis, dennoch kann es zu einer dauerhaften Beeinträchtigung der Fruchtbarkeit der betroffenen Männer kommen. Eine massive Redekoration der N-Glycane auf Spermien, insbesondere ein starker Verlust an Sialinsäure (Hyposialylation), ist mit einer experimenell-induzierten acrosomalen Reaktion assoziiert. Da bereits eine vorzeitige acrosomale Reaktion in einem UPEC-induzierten Epididymitis-Mausmodell beobachtet wurde, und zudem Sialidasen auf der Spermienoberfläche vermutlich durch Proteasen des Akrosoms aktiviert werden können, war es das Ziel dieser Arbeit zu untersuchen, ob Veränderungen des Sialoms im Nebenhoden bei der Epididymitis auftreten. Ein substantieller Verlust an N-Acetylneuraminsäure (Neu5Ac)-Resten wurde in epididymalen Spermatozoen und Epithelzellen der UPEC-induzierten akuten Epididymitis der Maus mittels kombinierter Laser-Mikrodissektion/HPLC-ESI-MS-Analyse nachgewiesen. Lektin-Färbungen lassen vermuten, dass die Infektion zu einer deutlichen Verminderung der α2,6-verknüpften Neu5Ac im Nebenhoden und in den luminalen Spermien führt. Unterstützend wurde bei Männern mit einer kürzlich diagnostizierten *E. coli*-assoziierten Epididymitis eine deutliche Verringerung der gebundenen Sialinsäurereste an der Oberfläche der Spermien zusammen mit einer vorzeitigen acrosomalen Reaktion dokumentiert. Die UPEC-induzierte Neu5Ac-Freisetzung aus menschlichen Spermien konnte *in vitro* wirksam durch einen Sialidase-Inhibitor gehemmt werden. Diese Ergebnisse legen eine wesentliche Umgestaltung der Glykokalyx von Spermatozoen und epididymalen Epithelzellen durch endogene Sialidasen nach vorzeitiger Akrosomenreaktion während der akuten Epididymitis nahe.

7 REFERENCES

1. Staack, A., et al., *Mouse urogenital development: a practical approach.* Differentiation, 2003. **71**(7): p. 402-13.
2. Li, N., T. Wang, and D. Han, *Structural, cellular and molecular aspects of immune privilege in the testis.* Front Immunol, 2012. **3**: p. 152.
3. Cobb, J. and M.A. Handel, *Dynamics of meiotic prophase I during spermatogenesis: from pairing to division.* Semin Cell Dev Biol, 1998. **9**(4): p. 445-50.
4. Schultz, N., F.K. Hamra, and D.L. Garbers, *A multitude of genes expressed solely in meiotic or postmeiotic spermatogenic cells offers a myriad of contraceptive targets.* Proc Natl Acad Sci U S A, 2003. **100**(21): p. 12201-6.
5. Guyonnet, B., et al., *The epididymal transcriptome and proteome provide some insights into new epididymal regulations.* J Androl, 2011. **32**(6): p. 651-64.
6. Yasuzumi, F., *Need based structural changes in the ductulus efferentis during sperm movements in the human epididymis.* Okajimas Folia Anat Jpn, 2007. **84**(1): p. 25-34.
7. Tecle, E. and P. Gagneux, *Sugar-coated sperm: Unraveling the functions of the mammalian sperm glycocalyx.* Mol Reprod Dev, 2015. **82**(9): p. 635-50.
8. Stammler, A., et al., *Epididymitis: ascending infection restricted by segmental boundaries.* Hum Reprod, 2015. **30**(7): p. 1557-65.
9. Joseph, A., H. Yao, and B.T. Hinton, *Development and morphogenesis of the Wolffian/epididymal duct, more twists and turns.* Dev Biol, 2009. **325**(1): p. 6-14.
10. Hinton, B.T., et al., *How do you get six meters of epididymis inside a human scrotum?* J Androl, 2011. **32**(6): p. 558-64.
11. Michel, V., et al., *Epididymitis: revelations at the convergence of clinical and basic sciences.* Asian J Androl, 2015. **17**(5): p. 756-63.
12. De Grava Kempinas, W. and G.R. Klinefelter, *Interpreting histopathology in the epididymis.* Spermatogenesis, 2014. **4**(2): p. e979114.
13. Knorr, D.W., T. Vanha-Perittula, and M.B. Lipsett, *Structure and function of rat testis through pubescence.* Endocrinology, 1970. **86**(6): p. 1298-304.
14. Zaneveld, L.J., et al., *Human sperm capacitation and the acrosome reaction.* Hum Reprod, 1991. **6**(9): p. 1265-74.
15. Sharon, A.V.a.N., *Historical Background and Overview*, in *Essentials of Glycobiology*, R.D.C. Ajit Varki, Jeffrey D Esko, Hudson H Freeze, Pamela Stanley, Carolyn R Bertozzi, Gerald W Hart, and Marilynn E Etzler, Editor. 2009.
16. Ma, F., et al., *Sialidases on mammalian sperm mediate deciduous sialylation during capacitation.* J Biol Chem, 2012. **287**(45): p. 38073-9.
17. Blackmore, P.F., et al., *Progesterone and 17 alpha-hydroxyprogesterone. Novel stimulators of calcium influx in human sperm.* J Biol Chem, 1990. **265**(3): p. 1376-80.
18. Mengerink, K.J. and V.D. Vacquier, *Glycobiology of sperm-egg interactions in deuterostomes.* Glycobiology, 2001. **11**(4): p. 37R-43R.

19. Berger, R.E., D. Kessler, and K.K. Holmes, *Etiology and manifestations of epididymitis in young men: correlations with sexual orientation.* J Infect Dis, 1987. **155**(6): p. 1341-3.

20. Rusz, A., et al., *Influence of urogenital infections and inflammation on semen quality and male fertility.* World J Urol, 2012. **30**(1): p. 23-30.

21. Wiles, T.J., R.R. Kulesus, and M.A. Mulvey, *Origins and virulence mechanisms of uropathogenic Escherichia coli.* Exp Mol Pathol, 2008. **85**(1): p. 11-9.

22. Berger, R.E., et al., *Etiology, manifestations and therapy of acute epididymitis: prospective study of 50 cases.* J Urol, 1979. **121**(6): p. 750-4.

23. Berger, R.E., et al., *Chlamydia trachomatis as a cause of acute "idiopathic" epididymitis.* N Engl J Med, 1978. **298**(6): p. 301-4.

24. Lang, T., et al., *Structural and functional integrity of spermatozoa is compromised as a consequence of acute uropathogenic E. coli-associated epididymitis.* Biol Reprod, 2013. **89**(3): p. 59.

25. Brecchia, G., et al., *Short- and long-term effects of lipopolysaccharide-induced inflammation on rabbit sperm quality.* Anim Reprod Sci, 2010. **118**(2-4): p. 310-6.

26. Pilatz, A., et al., *Acute epididymitis in ultrasound: results of a prospective study with baseline and follow-up investigations in 134 patients.* Eur J Radiol, 2012. **82**(12): p. e762-8.

27. Lotti, F., et al., *Ultrasonographic and clinical correlates of seminal plasma interleukin-8 levels in patients attending an andrology clinic for infertility.* Int J Androl, 2011. **34**(6 Pt 1): p. 600-13.

28. Khosravi, F., et al., *Desialylation of Spermatozoa and Epithelial Cell Glycocalyx Is a Consequence of Bacterial Infection of the Epididymis.* J Biol Chem, 2016. **291**(34): p. 17717-26.

29. Haugen, B.J., et al., *In vivo gene expression analysis identifies genes required for enhanced colonization of the mouse urinary tract by uropathogenic Escherichia coli strain CFT073 dsdA.* Infect Immun, 2007. **75**(1): p. 278-89.

30. Dohle, G.R., et al., *EAU guidelines on male infertility.* Eur Urol, 2005. **48**(5): p. 703-11.

31. Mulvey, M.A., et al., *Bad bugs and beleaguered bladders: interplay between uropathogenic Escherichia coli and innate host defenses.* Proc Natl Acad Sci U S A, 2000. **97**(16): p. 8829-35.

32. Bower, J.M., D.S. Eto, and M.A. Mulvey, *Covert operations of uropathogenic Escherichia coli within the urinary tract.* Traffic, 2005. **6**(1): p. 18-31.

33. Tanaka, K., et al., *Local expression of cytokine messenger RNA in rat model of Escherichia coli epididymitis.* J Urol, 1995. **154**(6): p. 2179-84.

34. Turner, T.T., et al., *Cytokine responses to E. coli-induced epididymitis in the rat: blockade by vasectomy.* Urology, 2011. **77**(6): p. 1507 e9-14.

35. Bhushan, S., et al., *Uropathogenic E. coli induce different immune response in testicular and peritoneal macrophages: implications for testicular immune privilege.* PLoS One, 2011. **6**(12): p. e28452.

36. Hilbert, D.W., et al., *Clinical Escherichia coli isolates utilize alpha-hemolysin to inhibit in vitro epithelial cytokine production.* Microbes Infect, 2012. **14**(7-8): p. 628-38.

37. Dhakal, B.K. and M.A. Mulvey, *The UPEC pore-forming toxin alpha-hemolysin triggers proteolysis of host proteins to disrupt cell adhesion, inflammatory, and survival pathways.* Cell Host Microbe, 2012. **11**(1): p. 58-69.

38. Cocuzza, M., et al., *Clinical relevance of oxidative stress and sperm chromatin damage in male infertility: an evidence based analysis.* Int Braz J Urol, 2007. **33**(5): p. 603-21.

39. Kao, S.H., et al., *Increase of oxidative stress in human sperm with lower motility.* Fertil Steril, 2008. **89**(5): p. 1183-90.

40. Aitken, R.J., *Molecular mechanisms regulating human sperm function.* Mol Hum Reprod, 1997. **3**(3): p. 169-73.

41. Griveau, J.F. and D. Le Lannou, *Reactive oxygen species and human spermatozoa: physiology and pathology.* Int J Androl, 1997. **20**(2): p. 61-9.

42. Hung, C.S., et al., *Structural basis of tropism of Escherichia coli to the bladder during urinary tract infection.* Mol Microbiol, 2002. **44**(4): p. 903-15.

43. Wright, K.J., P.C. Seed, and S.J. Hultgren, *Development of intracellular bacterial communities of uropathogenic Escherichia coli depends on type 1 pili.* Cell Microbiol, 2007. **9**(9): p. 2230-41.

44. Johnson, J.R., *Virulence factors in Escherichia coli urinary tract infection.* Clin Microbiol Rev, 1991. **4**(1): p. 80-128.

45. Stanley, P., V. Koronakis, and C. Hughes, *Acylation of Escherichia coli hemolysin: a unique protein lipidation mechanism underlying toxin function.* Microbiol Mol Biol Rev, 1998. **62**(2): p. 309-33.

46. Wiles, T.J., et al., *Inactivation of host Akt/protein kinase B signaling by bacterial pore-forming toxins.* Mol Biol Cell, 2008. **19**(4): p. 1427-38.

47. Fuster, M.M. and J.D. Esko, *The sweet and sour of cancer: glycans as novel therapeutic targets.* Nat Rev Cancer, 2005. **5**(7): p. 526-42.

48. Gupta, S.K. and B. Bhandari, *Acrosome reaction: relevance of zona pellucida glycoproteins.* Asian J Androl, 2011. **13**(1): p. 97-105.

49. Pang, P.C., et al., *Human sperm binding is mediated by the sialyl-Lewis(x) oligosaccharide on the zona pellucida.* Science, 2011. **333**(6050): p. 1761-4.

50. Freeze, H.H. and A.D. Elbein, *Glycosylation Precursors*, in *Essentials of Glycobiology*, C.R. Varki A, Esko JD, Freeze HH, Stanley P, Bertozzi CR, Hart GW, Etzler ME Editor. 2009, Cold Spring Harbor (NY): Cold Spring Harbor Laboratory Press.

51. Paulson, J.C. and K.J. Colley, *Glycosyltransferases. Structure, localization, and control of cell type-specific glycosylation.* J Biol Chem, 1989. **264**(30): p. 17615-8.

52. Colley, K.J., *Golgi localization of glycosyltransferases: more questions than answers.* Glycobiology, 1997. **7**(1): p. 1-13.

53. Varki, A., J.D. Esko, and K.J. Colley, *Cellular Organization of Glycosylation*, in *Essentials of Glycobiology*, C.R. Varki A, Esko JD, Freeze HH, Stanley P, Bertozzi

CR, Hart GW, Etzler ME, Editor. 2009, Cold Spring Harbor (NY): Cold Spring Harbor Laboratory Press.

54. Varki, A., *Nothing in glycobiology makes sense, except in the light of evolution.* Cell, 2006. **126**(5): p. 841-5.

55. Schenk, B., F. Fernandez, and C.J. Waechter, *The ins(ide) and out(side) of dolichyl phosphate biosynthesis and recycling in the endoplasmic reticulum.* Glycobiology, 2001. **11**(5): p. 61R-70R.

56. Stanley, P., H. Schachter, and N. Taniguchi, *N-Glycans*, in *Essentials of Glycobiology*, C.R. Varki A, Esko JD, Freeze HH, Stanley P, Bertozzi CR, Hart GW, Etzler ME, Editor. 2009, Cold Spring Harbor (NY): Cold Spring Harbor Laboratory Press.

57. Ioffe, E. and P. Stanley, *Mice lacking N-acetylglucosaminyltransferase I activity die at mid-gestation, revealing an essential role for complex or hybrid N-linked carbohydrates.* Proc Natl Acad Sci U S A, 1994. **91**(2): p. 728-32.

58. Campbell, R.M., et al., *Complex asparagine-linked oligosaccharides in Mgat1-null embryos.* Glycobiology, 1995. **5**(5): p. 535-43.

59. Freeze, H.H. and M. Aebi, *Altered glycan structures: the molecular basis of congenital disorders of glycosylation.* Curr Opin Struct Biol, 2005. **15**(5): p. 490-8.

60. Brockhausen, I., H. Schachter, and P. Stanley, *O-GalNAc Glycans*, in *Essentials of Glycobiology*, C.R. Varki A, Esko JD, Freeze HH, Stanley P, Bertozzi CR, Hart GW, Etzler ME, Editor. 2009, Cold Spring Harbor (NY): Cold Spring Harbor Laboratory Press.

61. Freeze, H.H. and R.S. Haltiwanger, *Other Classes of ER/Golgi-derived Glycans*, in *Essentials of Glycobiology*, C.R. Varki A, Esko JD, Freeze HH, Stanley P, Bertozzi CR, Hart GW, Etzler ME, Editor. 2009, Cold Spring Harbor (NY): Cold Spring Harbor Laboratory Press.

62. Moloney, D.J., et al., *Fringe is a glycosyltransferase that modifies Notch.* Nature, 2000. **406**(6794): p. 369-75.

63. von Schonfeldt, V., J. Wistuba, and S. Schlatt, *Notch-1, c-kit and GFRalpha-1 are developmentally regulated markers for premeiotic germ cells.* Cytogenet Genome Res, 2004. **105**(2-4): p. 235-9.

64. Tang, H., et al., *Notch signaling maintains Leydig progenitor cells in the mouse testis.* Development, 2008. **135**(22): p. 3745-53.

65. Batista, F., et al., *Complex N-glycans are essential, but core 1 and 2 mucin O-glycans, O-fucose glycans, and NOTCH1 are dispensable, for mammalian spermatogenesis.* Biol Reprod, 2012. **86**(6): p. 179.

66. Martin, P.T., *Dystroglycan glycosylation and its role in matrix binding in skeletal muscle.* Glycobiology, 2003. **13**(8): p. 55R-66R.

67. Florman, H.M. and P.M. Wassarman, *O-linked oligosaccharides of mouse egg ZP3 account for its sperm receptor activity.* Cell, 1985. **41**(1): p. 313-24.

68. Wassarman, P.M., *Mammalian fertilization: molecular aspects of gamete adhesion, exocytosis, and fusion.* Cell, 1999. **96**(2): p. 175-83.

69. Kan, F.W., *High-resolution localization of hyaluronic acid in the golden hamster oocyte-cumulus complex by use of a hyaluronidase-gold complex.* Anat Rec, 1990. **228**(4): p. 370-82.

70. Dandekar, P., J. Aggeler, and P. Talbot, *Structure, distribution and composition of the extracellular matrix of human oocytes and cumulus masses.* Hum Reprod, 1992. **7**(3): p. 391-8.

71. Camaioni, A., et al., *Proteoglycans and proteins in the extracellular matrix of mouse cumulus cell-oocyte complexes.* Arch Biochem Biophys, 1996. **325**(2): p. 190-8.

72. Hunnicutt, G.R., P. Primakoff, and D.G. Myles, *Sperm surface protein PH-20 is bifunctional: one activity is a hyaluronidase and a second, distinct activity is required in secondary sperm-zona binding.* Biol Reprod, 1996. **55**(1): p. 80-6.

73. Martinez, M.L., L. Martelotto, and M.O. Cabada, *Purification and biological characterization of N-acetyl beta-D glucosaminidase from Bufo arenarum spermatozoa.* Mol Reprod Dev, 2000. **57**(2): p. 194-203.

74. Schauer, R., *Sialic acids: fascinating sugars in higher animals and man.* Zoology (Jena), 2004. **107**(1): p. 49-64.

75. Schauer, R., *Sialic acids as regulators of molecular and cellular interactions.* Curr Opin Struct Biol, 2009. **19**(5): p. 507-14.

76. Varki, A. and P. Gagneux, *Multifarious roles of sialic acids in immunity.* Ann N Y Acad Sci, 2012. **1253**: p. 16-36.

77. Angata, T. and A. Varki, *Chemical diversity in the sialic acids and related alpha-keto acids: an evolutionary perspective.* Chem Rev, 2002. **102**(2): p. 439-69.

78. Varki, A. and R. Schauer, *Sialic Acids*, in *Essentials of Glycobiology*. 2009, Cold Spring Harbor Laboratory Press: NY. p. 199-218.

79. Hayakawa, T., et al., *Fixation of the human-specific CMP-N-acetylneuraminic acid hydroxylase pseudogene and implications of haplotype diversity for human evolution.* Genetics, 2006. **172**(2): p. 1139-46.

80. Springer, S.A., S.L. Diaz, and P. Gagneux, *Parallel evolution of a self-signal: humans and new world monkeys independently lost the cell surface sugar Neu5Gc.* Immunogenetics, 2014. **66**(11): p. 671-4.

81. Varki, A. and R. Schauer, *Sialic Acids*, in *Essentials of Glycobiology*, C.R. Varki A, Esko JD, Freeze HH, Stanley P, Bertozzi CR, Hart GW, Etzler ME Editor. 2009, Cold Spring Harbor (NY): Cold Spring Harbor Laboratory Press.

82. Varki, A., *Glycan-based interactions involving vertebrate sialic-acid-recognizing proteins.* Nature, 2007. **446**(7139): p. 1023-9.

83. Rutishauser, U., *Polysialic acid at the cell surface: biophysics in service of cell interactions and tissue plasticity.* J Cell Biochem, 1998. **70**(3): p. 304-12.

84. Byrne, B., G.G. Donohoe, and R. O'Kennedy, *Sialic acids: carbohydrate moieties that influence the biological and physical properties of biopharmaceutical proteins and living cells.* Drug Discov Today, 2007. **12**(7-8): p. 319-26.

85. Varki, A., *Sialic acids in human health and disease.* Trends Mol Med, 2008. **14**(8): p. 351-60.

86. Schwarzkopf, M., et al., *Sialylation is essential for early development in mice.* Proc Natl Acad Sci U S A, 2002. **99**(8): p. 5267-70.

87. Schauer, R., *Achievements and challenges of sialic acid research.* Glycoconj J, 2000. **17**(7-9): p. 485-99.

88. Ilver, D., et al., *Bacterium-host protein-carbohydrate interactions.* Methods Enzymol, 2003. **363**: p. 134-57.

89. Lehmann, F., E. Tiralongo, and J. Tiralongo, *Sialic acid-specific lectins: occurrence, specificity and function.* Cell Mol Life Sci, 2006. **63**(12): p. 1331-54.

90. Vimr, E.R., et al., *Diversity of microbial sialic acid metabolism.* Microbiol Mol Biol Rev, 2004. **68**(1): p. 132-53.

91. Bleil, J.D. and P.M. Wassarman, *Structure and function of the zona pellucida: identification and characterization of the proteins of the mouse oocyte's zona pellucida.* Dev Biol, 1980. **76**(1): p. 185-202.

92. Gupta, S.K., et al., *Mammalian zona pellucida glycoproteins: structure and function during fertilization.* Cell Tissue Res, 2012. **349**(3): p. 665-78.

93. Wassarman, P.M., *The Parkes Lecture. Zona pellucida glycoprotein mZP3: a versatile player during mammalian fertilization.* J Reprod Fertil, 1999. **116**(2): p. 211-6.

94. Wassarman, P.M., *Development. The sperm's sweet tooth.* Science, 2011. **333**(6050): p. 1708-9.

95. Taga, M., et al., *A potential role for 6-sulfo sialyl Lewis X in metastasis of bladder urothelial carcinoma.* Urol Oncol, 2015. **33**(11): p. 496 e1-9.

96. Cummings, R.D. and R.P. McEver, *C-type Lectins*, in *Essentials of Glycobiology*, C.R. Varki A, Esko JD, Freeze HH, Stanley P, Bertozzi CR, Hart GW, Etzler ME, Editor. 2009, Cold Spring Harbor (NY): Cold Spring Harbor Laboratory Press.

97. Benoff, S., *Carbohydrates and fertilization: an overview.* Mol Hum Reprod, 1997. **3**(7): p. 599-637.

98. Schroter, S., et al., *The glycocalyx of the sperm surface.* Hum Reprod Update, 1999. **5**(4): p. 302-13.

99. Bernal, A., et al., *Presence and regional distribution of sialyl transferase in the epididymis of the rat.* Biol Reprod, 1980. **23**(2): p. 290-3.

100. Tulsiani, D.R., *Glycan-modifying enzymes in luminal fluid of the mammalian epididymis: an overview of their potential role in sperm maturation.* Mol Cell Endocrinol, 2006. **250**(1-2): p. 58-65.

101. Deng, X., K. Czymmek, and P.A. Martin-DeLeon, *Biochemical maturation of Spam1 (PH-20) during epididymal transit of mouse sperm involves modifications of N-linked oligosaccharides.* Mol Reprod Dev, 1999. **52**(2): p. 196-206.

102. Nicolson, G.L., et al., *Lectin-binding sites on the plasma membranes of rabbit spermatozoa. Changes in surface receptors during epididymal Maturation and after ejaculation.* J Cell Biol, 1977. **74**(3): p. 950-62.

103. Purohit, S., M. Laloraya, and P.G. Kumar, *Distribution of N- and O-linked oligosaccharides on surface of spermatozoa from normal and infertile subjects.* Andrologia, 2008. **40**(1): p. 7-12.

104. Kohn, F.M., et al., *Detection of human sperm acrosome reaction: comparison between methods using double staining, Pisum sativum agglutinin, concanavalin A and transmission electron microscopy.* Hum Reprod, 1997. **12**(4): p. 714-21.

105. Pang, P.C., et al., *Expression of bisecting type and Lewisx/Lewisy terminated N-glycans on human sperm.* J Biol Chem, 2007. **282**(50): p. 36593-602.

106. Lis, H. and N. Sharon, *Lectins as molecules and as tools.* Annu Rev Biochem, 1986. **55**: p. 35-67.

107. Weis, W.I. and K. Drickamer, *Structural basis of lectin-carbohydrate recognition.* Annu Rev Biochem, 1996. **65**: p. 441-73.

108. Haas, G.G., Jr., et al., *The effect of fixatives and/or air-drying on the plasma and acrosomal membranes of human sperm.* Fertil Steril, 1988. **50**(3): p. 487-92.

109. Zeng, F.Y. and H.J. Gabius, *Sialic acid-binding proteins: characterization, biological function and application.* Z Naturforsch C, 1992. **47**(9-10): p. 641-53.

110. Gabriel, L.K., et al., *Localization of wheat germ agglutinin lectin receptors on human sperm by fluorescence microscopy: utilization of different fixatives.* Arch Androl, 1994. **33**(2): p. 77-85.

111. Runnebaum, I.B., W.B. Schill, and E. Topfer-Petersen, *ConA-binding proteins of the sperm surface are conserved through evolution and in sperm maturation.* Andrologia, 1995. **27**(2): p. 81-90.

112. D'Cruz, O.J. and G.G. Haas, Jr., *Fluorescence-labeled fucolectins are superior markers for flow cytometric quantitation of the human sperm acrosome reaction.* Fertil Steril, 1996. **65**(4): p. 843-51.

113. Tollner, T.L., C.L. Bevins, and G.N. Cherr, *Multifunctional glycoprotein DEFB126--a curious story of defensin-clad spermatozoa.* Nat Rev Urol, 2012. **9**(7): p. 365-75.

114. Belleannee, C., V. Thimon, and R. Sullivan, *Region-specific gene expression in the epididymis.* Cell Tissue Res, 2012. **349**(3): p. 717-31.

115. Rao, J., et al., *Cloning and characterization of a novel sperm-associated isoantigen (E-3) with defensin- and lectin-like motifs expressed in rat epididymis.* Biol Reprod, 2003. **68**(1): p. 290-301.

116. Tollner, T.L., et al., *Macaque sperm coating protein DEFB126 facilitates sperm penetration of cervical mucus.* Hum Reprod, 2008. **23**(11): p. 2523-34.

117. Drake, P.M., et al., *Polysialic acid, a glycan with highly restricted expression, is found on human and murine leukocytes and modulates immune responses.* J Immunol, 2008. **181**(10): p. 6850-8.

118. Watanabe, M., M. Timm, and H. Fallah-Najmabadi, *Cardiac expression of polysialylated NCAM in the chicken embryo: correlation with the ventricular conduction system.* Dev Dyn, 1992. **194**(2): p. 128-41.

119. Simon, P., et al., *Polysialic acid is present in mammalian semen as a post-translational modification of the neural cell adhesion molecule NCAM and the polysialyltransferase ST8SiaII.* J Biol Chem, 2013. **288**(26): p. 18825-33.

120. Yeung, W.S., et al., *Roles of glycodelin in modulating sperm function.* Mol Cell Endocrinol, 2006. **250**(1-2): p. 149-56.

121. Pilatz, A., et al., *Acute epididymitis revisited: impact of molecular diagnostics on etiology and contemporary guideline recommendations.* Eur Urol, 2015. **68**(3): p. 428-35.

122. World Health Organization, *WHO laboratory manual for the examination and processing of human semen*. 5th ed. 2010: WHO Press.

123. Younglai, E.V., et al., *Sperm swim-up techniques and DNA fragmentation.* Hum Reprod, 2001. **16**(9): p. 1950-3.

124. Bhushan, S., et al., *Uropathogenic Escherichia coli block MyD88-dependent and activate MyD88-independent signaling pathways in rat testicular cells.* J Immunol, 2008. **180**(8): p. 5537-47.

125. Ludwig, M., et al., *Tissue penetration of sparfloxacin in a rat model of experimental Escherichia coli epididymitis.* Infection, 1997. **25**(3): p. 178-84.

126. Lang, T., et al., *Uropathogenic Escherichia coli modulates innate immunity to suppress Th1-mediated inflammatory responses during infectious epididymitis.* Infect Immun, 2014. **82**(3): p. 1104-11.

127. Bartel, J., et al., *Laser microdissection of paraffin embedded tissue as a tool to estimate the sialylation status of selected cell populations.* Anal Chem, 2014. **86**(5): p. 2326-31.

128. Wisniewski, J.R., P. Ostasiewicz, and M. Mann, *High recovery FASP applied to the proteomic analysis of microdissected formalin fixed paraffin embedded cancer tissues retrieves known colon cancer markers.* J Proteome Res, 2011. **10**(7): p. 3040-9.

129. Hara, S., et al., *Fluorometric high-performance liquid chromatography of N-acetyl- and N-glycolylneuraminic acids and its application to their microdetermination in human and animal sera, glycoproteins, and glycolipids.* Anal Biochem, 1987. **164**(1): p. 138-45.

130. Hara, S., et al., *Determination of mono-O-acetylated N-acetylneuraminic acids in human and rat sera by fluorometric high-performance liquid chromatography.* Anal Biochem, 1989. **179**(1): p. 162-6.

131. Bayer, N.B., et al., *Artificial and natural sialic acid precursors influence the angiogenic capacity of human umbilical vein endothelial cells.* Molecules, 2013. **18**(3): p. 2571-86.

132. Galuska, S.P., et al., *Quantification of nucleotide-activated sialic acids by a combination of reduction and fluorescent labeling.* Anal Chem, 2010. **82**(11): p. 4591-8.

133. Galuska, S.P., et al., *Characterization of oligo- and polysialic acids by MALDI-TOF-MS.* Anal Chem, 2007. **79**(18): p. 7161-9.

134. Galuska, S.P., et al., *Glycomic strategy for efficient linkage analysis of di-, oligo- and polysialic acids.* J Proteomics, 2012. **75**(17): p. 5266-78.

135. Wearne, K.A., et al., *Use of lectins for probing differentiated human embryonic stem cells for carbohydrates.* Glycobiology, 2006. **16**(10): p. 981-90.

136. Bleckmann, C., H. Geyer, and R. Geyer, *Nanoelectrospray-MS(n) of native and permethylated glycans.* Methods Mol Biol, 2011. **790**: p. 71-85.

137. Tousi, F., et al., *Differential chemical derivatization integrated with chromatographic separation for analysis of isomeric sialylated N-glycans: a nano-hydrophilic interaction liquid chromatography-MS platform.* Anal Chem, 2013. **85**(17): p. 8421-8.

138. Galuska, S.P., et al., *Enzyme-dependent variations in the polysialylation of the neural cell adhesion molecule (NCAM) in vivo.* J Biol Chem, 2008. **283**(1): p. 17-28.

139. Pandya, I.J. and J. Cohen, *The leukocytic reaction of the human uterine cervix to spermatozoa.* Fertil Steril, 1985. **43**(3): p. 417-21.

140. Thompson, L.A., et al., *The leukocytic reaction of the human uterine cervix.* Am J Reprod Immunol, 1992. **28**(2): p. 85-9.

141. Springer, S.A. and P. Gagneux, *Glycan evolution in response to collaboration, conflict, and constraint.* J Biol Chem, 2013. **288**(10): p. 6904-11.

142. Yudin, A.I., et al., *Beta-defensin 126 on the cell surface protects sperm from immunorecognition and binding of anti-sperm antibodies.* Biol Reprod, 2005. **73**(6): p. 1243-52.

143. Taylor, R.E., et al., *Novel mechanism for the generation of human xeno-autoantibodies against the nonhuman sialic acid N-glycolylneuraminic acid.* J Exp Med, 2010. **207**(8): p. 1637-46.

144. Padler-Karavani, V., et al., *Diversity in specificity, abundance, and composition of anti-Neu5Gc antibodies in normal humans: potential implications for disease.* Glycobiology, 2008. **18**(10): p. 818-30.

145. Ghaderi, D., et al., *Sexual selection by female immunity against paternal antigens can fix loss of function alleles.* Proc Natl Acad Sci U S A, 2011. **108**(43): p. 17743-8.

146. Thall, A.D., P. Maly, and J.B. Lowe, *Oocyte Gal alpha 1,3Gal epitopes implicated in sperm adhesion to the zona pellucida glycoprotein ZP3 are not required for fertilization in the mouse.* J Biol Chem, 1995. **270**(37): p. 21437-40.

147. Williams, S.A., et al., *Fertilization in mouse does not require terminal galactose or N-acetylglucosamine on the zona pellucida glycans.* J Cell Sci, 2007. **120**(Pt 8): p. 1341-9.

148. Baibakov, B., et al., *Human sperm bind to the N-terminal domain of ZP2 in humanized zonae pellucidae in transgenic mice.* J Cell Biol, 2012. **197**(7): p. 897-905.

149. Srivastava, P.N., L.J. Zaneveld, and W.L. Williams, *Mammalian sperm acrosomal neuraminidases.* Biochem Biophys Res Commun, 1970. **39**(4): p. 575-82.

150. Srivastava, P.N. and H. Abou-Issa, *Purification and properties of rabbit spermatozoal acrosomal neuraminidase.* Biochem J, 1977. **161**(2): p. 193-200.

151. Srivastava, P.N., V.M. Kumar, and K.D. Arbtan, *Neuraminidase induces capacitation and acrosome reaction in mammalian spermatozoa.* J Exp Zool, 1988. **245**(1): p. 106-10.

152. Toshimori, K., et al., *Loss of sperm surface sialic acid induces phagocytosis: an assay with a monoclonal antibody T21, which recognizes a 54K sialoglycoprotein.* Arch Androl, 1991. **27**(2): p. 79-86.

153. Crocker, P.R., J.C. Paulson, and A. Varki, *Siglecs and their roles in the immune system.* Nat Rev Immunol, 2007. **7**(4): p. 255-66.

154. Cone, R.A., *Barrier properties of mucus.* Adv Drug Deliv Rev, 2009. **61**(2): p. 75-85.

155. Fahy, J.V. and B.F. Dickey, *Airway mucus function and dysfunction.* N Engl J Med, 2010. **363**(23): p. 2233-47.

156. Corfield, A.P., *Mucins: a biologically relevant glycan barrier in mucosal protection.* Biochim Biophys Acta, 2015. **1850**(1): p. 236-52.

157. Hultgren, S.J., et al., *Pilus and nonpilus bacterial adhesins: assembly and function in cell recognition.* Cell, 1993. **73**(5): p. 887-901.

158. Ozer, A., et al., *Advanced glycation end products facilitate bacterial adherence in urinary tract infection in diabetic mice.* Pathog Dis, 2015. **73**(5).

159. Bouckaert, J., et al., *The affinity of the FimH fimbrial adhesin is receptor-driven and quasi-independent of Escherichia coli pathotypes.* Mol Microbiol, 2006. **61**(6): p. 1556-68.

160. Sakarya, S., et al., *Escherichia coli bind to urinary bladder epithelium through nonspecific sialic acid mediated adherence.* FEMS Immunol Med Microbiol, 2003. **39**(1): p. 45-50.

161. Bobak, D.A., et al., *Modulation of FcR function by complement: subcomponent C1q enhances the phagocytosis of IgG-opsonized targets by human monocytes and culture-derived macrophages.* J Immunol, 1987. **138**(4): p. 1150-6.

162. Bohlson, S.S., D.A. Fraser, and A.J. Tenner, *Complement proteins C1q and MBL are pattern recognition molecules that signal immediate and long-term protective immune functions.* Mol Immunol, 2007. **44**(1-3): p. 33-43.

163. Inforzato, A., et al., *Structure and function of the long pentraxin PTX3 glycosidic moiety: fine-tuning of the interaction with C1q and complement activation.* Biochemistry, 2006. **45**(38): p. 11540-51.

164. Linnartz, B., et al., *Sialic acid on the neuronal glycocalyx prevents complement C1 binding and complement receptor-3-mediated removal by microglia.* J Neurosci, 2012. **32**(3): p. 946-52.

165. Linnartz, B. and H. Neumann, *Microglial activatory (immunoreceptor tyrosine-based activation motif)- and inhibitory (immunoreceptor tyrosine-based inhibition motif)-signaling receptors for recognition of the neuronal glycocalyx.* Glia, 2013. **61**(1): p. 37-46.

166. Linnartz-Gerlach, B., et al., *Sialylation of neurites inhibits complement-mediated macrophage removal in a human macrophage-neuron Co-Culture System.* Glia, 2015.

167. Shiyan, S.D. and N.V. Bovin, *Carbohydrate composition and immunomodulatory activity of different glycoforms of alpha1-acid glycoprotein.* Glycoconj J, 1997. **14**(5): p. 631-8.

168. Mackiewicz, A., et al., *Acute phase mediated change in glycosylation of rat alpha 1-acid glycoprotein in transgenic mice.* Glycobiology, 1991. **1**(3): p. 265-9.

169. Lee, G.W., T.H. Lee, and J. Vilcek, *TSG-14, a tumor necrosis factor- and IL-1-inducible protein, is a novel member of the pentaxin family of acute phase proteins.* J Immunol, 1993. **150**(5): p. 1804-12.

170. Breviario, F., et al., *Interleukin-1-inducible genes in endothelial cells. Cloning of a new gene related to C-reactive protein and serum amyloid P component.* J Biol Chem, 1992. **267**(31): p. 22190-7.

171. Bottazzi, B., et al., *Multimer formation and ligand recognition by the long pentraxin PTX3. Similarities and differences with the short pentraxins C-reactive protein and serum amyloid P component.* J Biol Chem, 1997. **272**(52): p. 32817-23.

172. Vouret-Craviari, V., et al., *Expression of a long pentraxin, PTX3, by monocytes exposed to the mycobacterial cell wall component lipoarabinomannan.* Infect Immun, 1997. **65**(4): p. 1345-50.

173. Rovere, P., et al., *The long pentraxin PTX3 binds to apoptotic cells and regulates their clearance by antigen-presenting dendritic cells.* Blood, 2000. **96**(13): p. 4300-6.

174. Nauta, A.J., et al., *Biochemical and functional characterization of the interaction between pentraxin 3 and C1q.* Eur J Immunol, 2003. **33**(2): p. 465-73.

175. Garlanda, C., et al., *Non-redundant role of the long pentraxin PTX3 in anti-fungal innate immune response.* Nature, 2002. **420**(6912): p. 182-6.

176. Diekman, A.B., et al., *Evidence for a unique N-linked glycan associated with human infertility on sperm CD52: a candidate contraceptive vaccinogen.* Immunol Rev, 1999. **171**: p. 203-11.

177. Parry, S., et al., *The sperm agglutination antigen-1 (SAGA-1) glycoforms of CD52 are O-glycosylated.* Glycobiology, 2007. **17**(10): p. 1120-6.

178. Hardiyanto, L., A. Hasegawa, and S. Komori, *The N-linked carbohydrate moiety of male reproductive tract CD52 (mrt-CD52) interferes with the complement system via binding to C1q.* J Reprod Immunol, 2012. **94**(2): p. 142-50.

179. Hasegawa, A. and K. Koyama, *Antigenic epitope for sperm-immobilizing antibody detected in infertile women.* J Reprod Immunol, 2005. **67**(1-2): p. 77-86.

180. Koyama, K., A. Hasegawa, and S. Komori, *Functional aspects of CD52 in reproduction.* J Reprod Immunol, 2009. **83**(1-2): p. 56-9.

181. Sullivan, R., G. Frenette, and J. Girouard, *Epididymosomes are involved in the acquisition of new sperm proteins during epididymal transit.* Asian J Androl, 2007. **9**(4): p. 483-91.

182. Shahraz, A., et al., *Anti-inflammatory activity of low molecular weight polysialic acid on human macrophages.* Sci Rep, 2015. **5**: p. 16800.

183. Ma, X., et al., *Sialylation Facilitates the Maturation of Mammalian Sperm and Affects Its Survival in Female Uterus.* Biol Reprod, 2016. **94**(6): p. 123.

184. Kang, T.W., et al., *Three cases of xanthogranulomatous epididymitis caused by E. coli.* J Infect, 2007. **54**(2): p. e69-73.

185. Jantos, C., et al., *Experimental epididymitis due to Chlamydia trachomatis in rats.* Infect Immun, 1992. **60**(6): p. 2324-8.

186. Tomlinson, M.J., et al., *The removal of morphologically abnormal sperm forms by phagocytes: a positive role for seminal leukocytes?* Hum Reprod, 1992. **7**(4): p. 517-22.

187. Videira, P.A., et al., *Surface alpha 2-3- and alpha 2-6-sialylation of human monocytes and derived dendritic cells and its influence on endocytosis.* Glycoconj J, 2008. **25**(3): p. 259-68.

188. Cabral, M.G., et al., *The phagocytic capacity and immunological potency of human dendritic cells is improved by alpha2,6-sialic acid deficiency.* Immunology, 2012. **138**(3): p. 235-45.

189. Duan, Y.G., et al., *Characterisation of dendritic cell subsets in chronically inflamed human epididymis.* Andrologia, 2015.

190. Brinkmann, V., et al., *Neutrophil extracellular traps kill bacteria.* Science, 2004. **303**(5663): p. 1532-5.

191. Brinkmann, V. and A. Zychlinsky, *Beneficial suicide: why neutrophils die to make NETs.* Nat Rev Microbiol, 2007. **5**(8): p. 577-82.

192. Alghamdi, A.S. and D.N. Foster, *Seminal DNase frees spermatozoa entangled in neutrophil extracellular traps.* Biol Reprod, 2005. **73**(6): p. 1174-81.

193. Saffarzadeh, M., et al., *Neutrophil extracellular traps directly induce epithelial and endothelial cell death: a predominant role of histones.* PLoS One, 2012. **7**(2): p. e32366.

194. Ulm, C., et al., *Soluble polysialylated NCAM: a novel player of the innate immune system in the lung.* Cell Mol Life Sci, 2013. **70**(19): p. 3695-708.

195. Carlin, A.F., et al., *Molecular mimicry of host sialylated glycans allows a bacterial pathogen to engage neutrophil Siglec-9 and dampen the innate immune response.* Blood, 2009. **113**(14): p. 3333-6.

196. Duong, B.H., et al., *Decoration of T-independent antigen with ligands for CD22 and Siglec-G can suppress immunity and induce B cell tolerance in vivo.* J Exp Med, 2010. **207**(1): p. 173-87.

197. Crocker, P.R., *Siglecs in innate immunity.* Curr Opin Pharmacol, 2005. **5**(4): p. 431-7.

198. Chen, G.Y., et al., *Amelioration of sepsis by inhibiting sialidase-mediated disruption of the CD24-SiglecG interaction.* Nat Biotechnol, 2011. **29**(5): p. 428-35.

199. Chen, G.Y., et al., *CD24 and Siglec-10 selectively repress tissue damage-induced immune responses.* Science, 2009. **323**(5922): p. 1722-5.

200. Jellusova, J., et al., *CD22 x Siglec-G double-deficient mice have massively increased B1 cell numbers and develop systemic autoimmunity.* J Immunol, 2010. **184**(7): p. 3618-27.

201. Rittirsch, D., M.A. Flierl, and P.A. Ward, *Harmful molecular mechanisms in sepsis.* Nat Rev Immunol, 2008. **8**(10): p. 776-87.

202. Macauley, M.S., P.R. Crocker, and J.C. Paulson, *Siglec-mediated regulation of immune cell function in disease.* Nat Rev Immunol, 2014. **14**(10): p. 653-66.

203. Avril, T., et al., *Probing the cis interactions of the inhibitory receptor Siglec-7 with alpha2,8-disialylated ligands on natural killer cells and other leukocytes using glycan-specific antibodies and by analysis of alpha2,8-sialyltransferase gene expression.* J Leukoc Biol, 2006. **80**(4): p. 787-96.

204. Falco, M., et al., *Identification and molecular cloning of p75/AIRM1, a novel member of the sialoadhesin family that functions as an inhibitory receptor in human natural killer cells.* J Exp Med, 1999. **190**(6): p. 793-802.

205. Nicoll, G., et al., *Ganglioside GD3 expression on target cells can modulate NK cell cytotoxicity via siglec-7-dependent and -independent mechanisms.* Eur J Immunol, 2003. **33**(6): p. 1642-8.

206. Nicoll, G., et al., *Identification and characterization of a novel siglec, siglec-7, expressed by human natural killer cells and monocytes.* J Biol Chem, 1999. **274**(48): p. 34089-95.

207. Grewal, P.K., et al., *The Ashwell receptor mitigates the lethal coagulopathy of sepsis.* Nat Med, 2008. **14**(6): p. 648-55.

208. Kim, S., et al., *Features and applications of bacterial sialidases.* Appl Microbiol Biotechnol, 2011. **91**(1): p. 1-15.

209. Chui, D., et al., *Genetic remodeling of protein glycosylation in vivo induces autoimmune disease.* Proc Natl Acad Sci U S A, 2001. **98**(3): p. 1142-7.

210. Parekh, R.B., et al., *Association of rheumatoid arthritis and primary osteoarthritis with changes in the glycosylation pattern of total serum IgG.* Nature, 1985. **316**(6027): p. 452-7.

211. De Clercq, E. and G. Li, *Approved Antiviral Drugs over the Past 50 Years.* Clin Microbiol Rev, 2016. **29**(3): p. 695-747.

212. Paulson, J.C. and N. Kawasaki, *Sialidase inhibitors DAMPen sepsis.* Nat Biotechnol, 2011. **29**(5): p. 406-7.

213. Pang, P.C., et al., *Analysis of the human seminal plasma glycome reveals the presence of immunomodulatory carbohydrate functional groups.* J Proteome Res, 2009. **8**(11): p. 4906-15.

214. Clark, G.F., et al., *Viewing AIDS from a glycobiological perspective: potential linkages to the human fetoembryonic defence system hypothesis.* Mol Hum Reprod, 1997. **3**(1): p. 5-13.

215. Bergman, M., et al., *Helicobacter pylori phase variation, immune modulation and gastric autoimmunity.* Nat Rev Microbiol, 2006. **4**(2): p. 151-9.

216. Bergman, M.P., et al., *Helicobacter pylori modulates the T helper cell 1/T helper cell 2 balance through phase-variable interaction between lipopolysaccharide and DC-SIGN.* J Exp Med, 2004. **200**(8): p. 979-90.

217. van Die, I., et al., *The dendritic cell-specific C-type lectin DC-SIGN is a receptor for Schistosoma mansoni egg antigens and recognizes the glycan antigen Lewis x.* Glycobiology, 2003. **13**(6): p. 471-8.

218. Meyer, S., et al., *DC-SIGN mediates binding of dendritic cells to authentic pseudo-LewisY glycolipids of Schistosoma mansoni cercariae, the first parasite-specific ligand of DC-SIGN.* J Biol Chem, 2005. **280**(45): p. 37349-59.

219. Kashiwagi, N., et al., *Lymphocyte membrane modifications induced by HIV infection.* Tohoku J Exp Med, 1994. **173**(1): p. 115-31.

220. van Liempt, E., et al., *Specificity of DC-SIGN for mannose- and fucose-containing glycans.* FEBS Lett, 2006. **580**(26): p. 6123-31.

221. Feinberg, H., et al., *Structural basis for selective recognition of oligosaccharides by DC-SIGN and DC-SIGNR.* Science, 2001. **294**(5549): p. 2163-6.

222. Saraswat, M., et al., *N-Glycoproteomics of Human Seminal Plasma Glycoproteins.* J Proteome Res, 2016. **15**(3): p. 991-1001.

223. Hanisch, F.G., et al., *Structure of neutral oligosaccharides derived from mucus glycoproteins of human seminal plasma.* Eur J Biochem, 1986. **155**(2): p. 239-47.

224. Agungpriyono, S., et al., *Distribution of lectin-bindings in the testis of the lesser mouse deer, Tragulus javanicus.* Anat Histol Embryol, 2009. **38**(3): p. 208-13.

225. Isojima, S., et al., *Establishment and characterization of a human hybridoma secreting monoclonal antibody with high titers of sperm immobilizing and agglutinating activities against human seminal plasma.* J Reprod Immunol, 1987. **10**(1): p. 67-78.

226. Tollner, T.L., et al., *A common mutation in the defensin DEFB126 causes impaired sperm function and subfertility.* Sci Transl Med, 2011. **3**(92): p. 92ra65.

227. Tollner, T.L., et al., *Beta-defensin 126 on the surface of macaque sperm mediates attachment of sperm to oviductal epithelia.* Biol Reprod, 2008. **78**(3): p. 400-12.

228. Suarez, S.S. and A.A. Pacey, *Sperm transport in the female reproductive tract.* Hum Reprod Update, 2006. **12**(1): p. 23-37.

229. Cao, D., et al., *Lipopolysaccharide-induced epididymitis disrupts epididymal beta-defensin expression and inhibits sperm motility in rats.* Biol Reprod, 2010. **83**(6): p. 1064-70.

230. Ichikawa, S., et al., *Ablation of the Galnt3 gene leads to low-circulating intact fibroblast growth factor 23 (Fgf23) concentrations and hyperphosphatemia despite increased Fgf23 expression.* Endocrinology, 2009. **150**(6): p. 2543-50.

231. Stone, E.L., et al., *Glycosyltransferase function in core 2-type protein O glycosylation.* Mol Cell Biol, 2009. **29**(13): p. 3770-82.

232. Hasegawa, K., Y. Okamura, and Y. Saga, *Notch signaling in Sertoli cells regulates cyclical gene expression of Hes1 but is dispensable for mouse spermatogenesis.* Mol Cell Biol, 2012. **32**(1): p. 206-15.

233. Takamiya, K., et al., *Complex gangliosides are essential in spermatogenesis of mice: possible roles in the transport of testosterone.* Proc Natl Acad Sci U S A, 1998. **95**(21): p. 12147-52.

234. Obholz, K.L., et al., *FNDC3A is required for adhesion between spermatids and Sertoli cells.* Dev Biol, 2006. **298**(2): p. 498-513.

235. Sandhoff, R., et al., *Novel class of glycosphingolipids involved in male fertility.* J Biol Chem, 2005. **280**(29): p. 27310-8.

236. van der Weyden, L., et al., *Loss of TSLC1 causes male infertility due to a defect at the spermatid stage of spermatogenesis.* Mol Cell Biol, 2006. **26**(9): p. 3595-609.

237. Wakayama, T., et al., *Heterophilic binding of the adhesion molecules poliovirus receptor and immunoglobulin superfamily 4A in the interaction between mouse spermatogenic and Sertoli cells.* Biol Reprod, 2007. **76**(6): p. 1081-90.

238. Yamada, D., et al., *Disruption of spermatogenic cell adhesion and male infertility in mice lacking TSLC1/IGSF4, an immunoglobulin superfamily cell adhesion molecule.* Mol Cell Biol, 2006. **26**(9): p. 3610-24.

239. Huang, H.H. and P. Stanley, *A testis-specific regulator of complex and hybrid N-glycan synthesis.* J Cell Biol, 2010. **190**(5): p. 893-910.

8 ACKNOWLEDGEMENTS

This study was performed under the supervision of Prof. Dr. Andreas Meinhardt (Institute of Anatomy and Cell Biology) and PD Dr. Sebastian Galuska (Institute of Biochemistry) at the Medical Faculty, Justus-Liebig University of Giessen. Foremost, I would like to deeply appreciate Prof. Meinhardt for accepting me as a Ph.D. student, leading the project, thoughtful guidance, critical comments, financial support, teaching writing skills and correction of this thesis. I would like to express my gratitude to PD Dr. Galuska for providing the opportunity of working as a permanent guest researcher in his lab and for leading the project. I thank him for introducing me to the world of glycobiology and sharing his office with me.

I would like to offer my special thanks to Dr. Vera Michel, who made an enormous contribution to my project, e.g. in the kind provision of LCMD material and by the correction of the German translation of the summary. Thanks, Vera, for great practical and intellectual help with a professional attitude.

I want to thank the present and past members of the Galuska lab especially Werner Mink and Siegfried Kühnhardt as my first mentors and technical assistance, Dr. Kai Maass (Institute of Inorganic and Analytical Chemistry) for teaching the GlycoWorkbench software, Dr. Peter Simon and Miriam Kaese for sharing materials and protocols as well as Dr. Christina Galuska and Philipp Christian for experimental help.

I wish to express my sincere thanks to Prof. Dr. Hans-Christian Schuppe, Mrs. Schuster and other colleagues from the Clinic of Urology, Pediatric Urology and Andrology (JLU Giessen). I should thank Prof. Schuppe who helped me kindly and taught me clinical aspects and gave me constructive comments and warm encouragement.

I would like to show my greatest appreciation to Dr. Adrian Pilatz and his team for the timely provision of valuable clinical samples and his contribution to the manuscript leading to publication in the Journal of Biological Chemistry.

I much appreciate my dear friend Dr. Ferial Aslani for introducing me to the lab facilities and her generous help in consulting and proofreading of this thesis.

I also want to acknowledge Mattew Jones (University of Giessen Lung Center, ECCPS) for proofreading of this thesis.

I want to thank Dr. Sudhanshu Bhushan and Dr. Zhang Zhengguo for generating the exquisite mouse model and providing UPEC.

I would like to extend my sincere thanks to Prof. Dr. Günter Lochnit (Institute of Biochemistry) for letting me work in his lab for MALDI-TOF analysis.

I also appreciate my other colleagues in the Institute of Anatomy and Cell Biology: Suada Fröhlich, Dr. Monika Fijak, Elke Stoschek, Dr. Magdalena Walecki, Ming Wang, Nour Nicolas, and Tao Lei for sharing materials and knowledge and Eva Wewel for kind administrative help. I wish you well-being and success.

This work was supported by a grant from the Deutsche Forschungsgemeinschaft (DFG). Therefore, I appreciate the DFG for financial support.

I want to express my gratitude to my parents and brother (Faramarz) who encouraged me and wished me luck. My biggest thank goes to Negah Ahmadvand who as a kind and patient wife supported me spiritually and scientifically. I owe my success in life to her unconditional help. Words cannot express how grateful I am.

I much appreciate Justus-Liebig-University of Giessen for provision of educational facilities and I thank the International Giessen Graduate Centre for the Life Sciences (GGL) for the training program.

Finally, I appreciate my home country (Iran) and Germany for providing excellent opportunity for education and research. I hope my study may help to the treatment of infertile couples, who wish to become parents.

9 OWN PUBLICATIONS

1- Publication originally from Ph.D.

- Desialylation of spermatozoa and epithelial cell glycocalyx is a consequence of bacterial infection of the epididymis.
  Khosravi F, Michel V, Galuska CE, Bhushan S, Christian P, Schuppe HC, Pilatz A, Galuska SP, Meinhardt A. Published in Journal of Biological Chemistry, 2016 Aug 19;291(34):17717-26

2- Other publications

- Association between plasminogen activator inhibitor 1 gene mutation and different subgroups of recurrent pregnancy loss and implantation failure.
  Khosravi F, Zarei S, Ahmadvand N, Akbarzadeh-Pasha Z, Savadi E, Zarnani AH, Sadeghi MR, Jeddi-Tehrani M. Published in the Journal of Assisted Reproduction and Genetics, 2014 Jan;31(1):121-4

3- Conference abstracts

- Epididymitis caused by infection with uropathogenic *Escherichia coli* results in desialylation of sperm glycocalyx and epithelial cells. **Farhad Khosravi**, Vera Michel, Hans-Christian Schuppe, Adrian Pilatz, Sudhanshu Bhushan, Andreas Meinhardt, Sebastian Galuska. 26th Joint Glycobiology meeting, Oct 2015, Lille, France (Oral presentation)
- Epididymitis caused by infection with uropathogenic *Escherichia coli* results in desialylation of sperm glycocalyx and epithelial cells. **Farhad Khosravi**, Vera Michel, Hans-Christian Schuppe, Adrian Pilatz, Sudhanshu Bhushan, Sebastian P. Galuska, Andreas Meinhardt. GGL Annual Congress, Sep 2015, University of Giessen, Germany (Poster presentation)
- The human sperm glycocalyx is altered by infection. **Farhad Khosravi**, Vera Michel, Hans-Christian Schuppe, Sebastian P. Galuska, Andreas Meinhardt. GGL Annual Congress, Sep 2014, University of Giessen, Germany (Poster presentation)
- The human sperm glycocalyx: alterations caused by acrosome reaction. **Farhad Khosravi**, Hans-Christian Schuppe, Sebastian P. Galuska, Andreas Meinhardt. DGA (26. Jahrestagung der Deutschen Gesellschaft für Andrology), Sep 2014, Giessen, Germany (Oral presentation)
- Identification of mouse sperm glycoprofile to evaluate possible alterations after urogenital tract infection. **Farhad Khosravi**, Tali Lang, Wernere Mink, Siegfried Kühnhardt, Sebastian P.Galuska, Andreas Meinhardt. GGL Annual Congress, Sep 2013, University of Giessen, Germany (Poster presentation)
- Methylenetetrahydrofolate Reductase, Plasminogen Activator Inibitor-1, Factor V Leiden polymorphism in 600 cases of Iranian women with recurrent pregnancy loss. Saeed Zarei, Farhad **Khosravi**, Zohreh Akbarzadeh, Fakhredin Reihani-Sabet, Elham Savadi Shiraz, Afsaneh Mohammadzadeh, Zhila Abedi, Hamid-Reza Khoram Khorshid, Amir-Hassan Zarnani, Banafsheh Tavangar, Negah Ahmadvand, Mahmood Jeddi-Tehrani. 4th International Congress of Molecular Medicine, Jun 2011, Istanbul, Turkey (Poster presentation)

- Y-chromosomal STR haplotypes in Tehran population. **Farhad Khosravi**, Negah Ahmadvand, Ali Farazmand, 10th Iranian Congress of Biochemistry & 3rd International Congress of Biochemistry and Molecular Biology. Nov 2009, Tehran, Iran (Poster presentation)
- Y-chromosomal STR Haplotypes in Iranian Torkaman population. Negah Ahmadvand, **Farhad Khosravi**, Ali Farazmand. 10th Iranian Congress of Biochemistry & 3rd International Congress of Biochemistry and Molecular Biology, Nov 2009, Tehran, Iran
- Analysis of Y-chromosome short tandem repeat (20 markers) polymorphism in a random population of Torkamans. Negah Ahmadvand, **Farhad Khosravi**, Ali Farazmand. 15th National & 3rd International Conference of Biology, Aug 2008, Tehran, Iran.
- Analysis of Y-chromosome short tandem repeat (20 markers) polymorphism in a random population of Tehran. **Farhad Khosravi**, Negah Ahmadvand, Ali Farazmand. 15th National & 3rd International Conference of Biology, Aug 2008, Tehran, Iran.

Desialylation of spermatozoa and epithelial cell glycocalyx is a consequence of bacterial infection of the epididymis

Farhad Khosravi[1,2], Vera Michel[1], Christina E. Galuska[2], Sudhanshu Bhushan[1], Philipp Christian[2], Hans-Christian Schuppe[3], Adrian Pilatz[3], Sebastian P. Galuska[2,4#], Andreas Meinhardt[1#]

[1]Institute of Anatomy and Cell Biology; [2]Institute of Biochemistry; [3]Department of Urology, Pediatric Urology and Andrology; Faculty of Medicine, Justus-Liebig-University, Giessen, Germany.
[4]Department of Reproductive Biology, Leibniz Institute for Farm Animal Biology (FBN), Germany

[#]These authors contributed equally to the work.

Running title: Desialylation of glycocalyx during epididymitis.

To whom correspondence should be addressed: Sebastian P. Galuska, Department of Reproductive Biology, Leibniz Institute for Farm Animal Biology (FBN), Germany, Tel. +49 (0) 38208-68-751; E-mail: galuska.sebastian@fbn-dummerstorf.de; Andreas Meinhardt, Institute of Anatomy and Cell Biology, Faculty of Medicine, University of Giessen, Germany, Tel. +49 (0) 641-99-47024; Fax. +49 (0) 641-99-47029; E-mail: andreas.meinhardt@anatomie.med.uni-giessen.de

Keywords: Uropathogenic *Escherichia coli*; epididymitis; neuraminidase; sialidase; sialic acids; glycocalyx

ABSTRACT

Urinary tract infections caused by uropathogenic *Escherichia coli* (UPEC) pathovars belong to the most frequent infections in human. In men, pathogens can also spread to the genital tract via the continuous ductal system eliciting bacterial prostatitis and/or epididymo-orchitis. Antibiotic treatment usually clears pathogens in acute epididymitis, however, patients' fertility can be permanently impaired. Since premature acrosome reaction was observed in an UPEC epididymitis mouse model and sialidases on the sperm surface are considered to be activated via proteases of the acrosome, we aimed to investigate whether alterations of the sialome of epididymal spermatozoa and surrounding epithelial cells occur during UPEC infection. In UPEC elicited acute epididymitis in mouse, a substantial loss of *N*-acetylneuraminic acid (Neu5Ac) residues was detected in epididymal spermatozoa and epithelial cells using combined laser microdissection/HPLC-ESI-MS analysis. In support, a substantial reduction of sialic acid residues bound to the surface of spermatozoa was documented in men with recent history of *E. coli* associated epididymitis. *In vitro*, such an UPEC induced Neu5Ac release from human spermatozoa was effectively counteracted by a sialidase inhibitor. These findings strongly suggest a substantial remodeling of the glycocalyx of spermatozoa and epididymal epithelial cells by endogenous sialidases after premature acrosome reaction during acute epididymitis.

Khosravi F et al., Published in Journal of Biological Chemistry, 2016 Aug 23

10 EHRENWÖRTLICHE ERKLÄRUNG

Ich erkläre: Ich habe die vorgelegte Dissertation selbständig und ohne unerlaubte fremde Hilfe und nur mit den Hilfen angefertigt, die ich in der Dissertation angegeben habe. Alle Textstellen, die wörtlich oder sinngemäß aus veröffentlichten oder nicht veröffentlichten Schriften entnommen sind, und alle Angaben, die auf mündlichen Auskünften beruhen, sind als solche kenntlich gemacht. Bei den von mir durchgeführten und in der Dissertation erwähnten Untersuchungen habe ich die Grundsätze guter wissenschaftlicher Praxis, wie sie in der „Satzung der Justus-Liebig-Universität Giessen zur Sicherung guter wissenschaftlicher Praxis“ niedergelegt sind, eingehalten.

I declare that I have completed this dissertation single-handedly without the unauthorized help of a second party and only with the assistance acknowledged therein. I have appropriately acknowledged and referenced all text passages that are derived literally from or are based on the content of published or unpublished work of others, and all information that relates to verbal communications. I have abided by the principles of good scientific conduct laid down in the charter of the Justus Liebig University of Giessen in carrying out the investigations described in the dissertation.

Giessen, den

_____

Farhad Khosravi